

Tactile Feedback for Robot Assisted Minimally
Invasive Surgery:
an Overview

Pauwel Goethals
Division PMA
Department of Mechanical Engineering
K.U.Leuven

July, 14, 2008

Contents

1	Minimally Invasive Surgery	2
1.1	Importance of touch	5
2	Psychophysics	7
2.1	Mechanoreceptors	8
2.2	What is perceivable by humans	11
2.3	Vibration	12
2.4	Simulation of sensation	13
3	Aim	15
3.1	Spatial resolution	15
3.2	Frequency range	16
3.3	Sensitivity, force and stroke	16
3.4	Other requirements	17
4	Sensors	19
4.1	Piezoresistance	22
4.1.1	Rigid Piezoresistance	22
4.1.2	Elastoresistance	23
4.1.3	Percolation theory	31
4.1.4	Dynamic Behaviour of (filled) Rubber	36
4.2	Piezoelectricity	37
4.3	Capacitive sensing (piezocapacitance)	38
4.4	Optics	40
4.5	Electromagnetic induction	42
4.6	Magnetoresistance	43
4.7	Ultrasound:	43
4.8	Electro-optical:	44
5	Displays	45
5.1	Electromagnetic	46
5.2	Electrostatic - Electrostrictive	47
5.3	Piezoelectric	47
5.4	Shape Memory Alloy (SMA)	49
5.5	Active fluids	49
5.6	Pneumatic	50
5.7	Acoustic	51
5.8	Photostrictive	52
5.9	Electrocutaneous	52
5.10	Conjugated polymers	52
5.11	Braille displays	53
6	Applications	54
6.1	Minimally invasive surgery	54
6.2	Robot manipulation	54
6.3	Other applications	55
	References	57

Preface

Designing a tactile feedback system is an ambitious goal, especially combined with the application of providing the sense of touch to surgeons during minimally invasive operations. Many different research groups around the world are working on this or related problems, including tactile sensors, tactile displays and robotic and minimally invasive surgery in general. This work is a collection of information about the subject.

The first Section hints at the evolutions in minimally invasive surgery, robotic surgery, and the importance of touch in surgery. The second Section discusses the psychophysics of touch. It is important to understand the biology behind the problem. This was not the focus of this document, and there is a lot more to learn about the subject that is not included, but some important references are there. The third section collects different requirements that are set for this goal. The next two sections describe a lot of tactile sensors and tactile displays designed and built using many different physical principles. The last Section covers a number of different applications for these sensors or displays.

Warning

This document is only superficially edited and contains a lot of references, but no selection process was used. This means not all references are equally valuable. Although the goal is to be as complete as possible, there is still a gargantuan amount of interesting related work that is not included. The main reason is that careful editing and going through everything is quite time consuming.

1 Minimally Invasive Surgery

In minimally invasive surgery (MIS) or medical endoscopy the patient is operated on via only a few small incisions, through which a camera (endoscope) and instruments are inserted. In laparoscopy or abdominal surgery the cavity is inflated with CO₂ to create a cavity. Other types of MIS include thoracoscopy or chest surgery and arthroscopy or orthopedic surgery. Many experts believe that minimally invasive techniques may eventually be used in as many as 75% of abdominal and thoracic operations [15]. It is for example often used for cholecystectomy (gall bladder removal) or the resection of colon cancer. By the early nineties, laparoscopic cholecystectomies in the USA outnumbered open surgery by a ratio of 65 to 35 [3]. The safety and advantages of laparoscopic cholecystectomy have been validated by controlled trials. The safety and efficacy of laparoscopic colectomy is yet to be proven by prospective randomised clinical trial, and a large multicentre study is (2003) underway in North America [4].

The success and popularity of laparoscopic cholecystectomy led the way to the development of the endoscopic resection of various intra-abdominal and intrathoracic tumours [4]. There have been many reports of laparoscopic colectomy for large bowel cancer. Many cases of video-assisted thoracotomy and lobectomy for lung cancers have also been carried out. Small numbers of laparoscopic hepatectomy and pancreatectomy have also been reported. This is obviously an ideal method for the removal of early cancers. Concerns were raised when reports of laparoscopic port-site recurrence of cancer appeared. There has also been doubt whether lymph node dissection can be carried out laparoscopically as adequately as by open surgery.

The range of minimally invasive interventions is currently quite wide and still extends, because the performed procedures may be often more potent and precise than the classical operations. These techniques, rounded out by improvements in the anaesthetic and analgesic field, have given us more possibilities, such as “minimally invasive surgery”, “major ambulatory surgery” and “day care surgery” or “minor ambulatory surgery” [3]. The treatment of cancer follows similar trends [4]. Procedures such as radiosurgery, radiofrequency ablation, and video-assisted endoscopic resections can achieve cancer control with minimised risk and morbidity.

The main advantages to minimally invasive surgery are lower risk and pain, shorter postoperative stay and thus an overall reduction of health-care costs, resulting in a speedy return to daily activities. The trauma to surrounding tissue is minimised, followed up with better cosmetics. [15] [16] [17] [3].

One of the main obstacles to the general and widespread adoption of these techniques is the difficulty of teaching them [3]. In the future, students will likely have to carry out simulated training before turning their hand to real operations, thus cutting down the number of surgical errors. The likely benefits of surgical simulation teaching are the following: operations carried out in a shorter time and with heightened safety. For this purpose, GMV developed a virtual medical trainer with two phantom omnis to provide haptic feedback [3].

To overcome some of the problems associated with conventional endoscopy, the system can be robot assisted. These systems are teleoperated with the

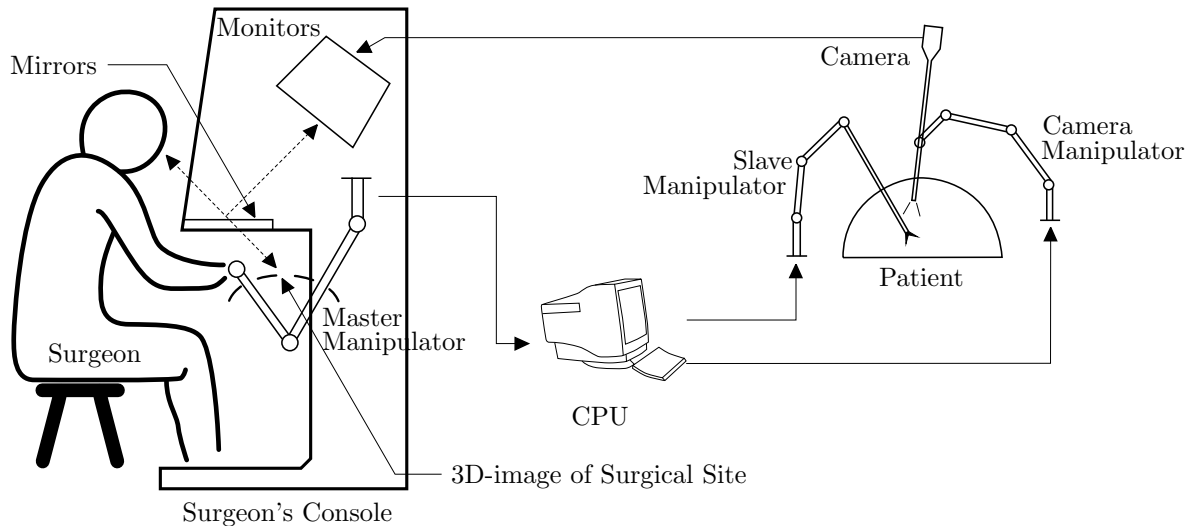


Figure 1: Schematic overview of a telesurgical system

surgeon at a console, controlling a ‘joystick’ and the instruments manipulated by robotic arms inside the patient (Figure 1). Rassweiler et al. [18] and Boehm et al. [19] discuss the development, advantages and disadvantages of telesurgery. In the future the need of cardiopulmonary bypass (CPB) will be avoided with virtual stabilising systems, which will have automatic safety margins. In the field of laserlaparoscopy, a more natural interface will be developed [20].

There are some advantages to robotic telemanipulation [17]. First, limited dexterity is restored as the surgeon no longer has to move the instruments in reverse direction. This can be done via a foot pedal to freeze the instruments, which allows repositioning the controllers and forearms to an ergonomically favourable position. Coupled with the fact that the surgeon can sit in a comfortable position makes robotic telemanipulation more ergonomic point. Visualisation is improved, and can even be threedimensional, with two different images displayed for each eye. Other key advantages are tremor eradication and scaling opportunities [21]. In robot assisted surgery, the surgeon can focus more on the medical aspect, without worrying about the technical skills required. Examples include the ‘da Vinci’-system produced by Intuitive Surgical and the ZEUS robot by Computer Motion. Computer Motion and Intuitive Surgical merged in 2003 and the ZEUS is no longer supported. Although the da Vinci robot is the only commercially available system for abdominal and thoracic surgery, there are plenty of experimental setups or systems for other types of surgery. Nouri [7] gives a thorough overview.

Because a robot assisted system is teleoperated, the surgeon can even be in a distant location. Faster intervention for astronauts in space, miners, fire fighters, and others working in hazardous environments is facilitated.

In 2001, Jacques Marescaux, a surgeon at the University of Strasbourg, in France, worked with Computer Motion to modify its system and perform the first remote surgery on a human patient, a gallbladder removal procedure called laparoscopic cholecystectomy [5]. Using a dedicated high-speed connection, Marescaux controlled the robot from New York City while the patient lay in an operating room in Strasbourg.

Remote operation is particularly desirable in a battlefield disaster zone and for

provision of rural health care [15]. Medical vehicles equipped with such remote-controlled robots could get surgical care to soldiers in a lot less time than it would take to evacuate them to the nearest base or hospital. Robotic surgery is possible from a distance with an unmanned aircraft (UAV) circling over the scene for communication [5]. There is a time delay of 20 ms for manipulation and 200 ms for video. The robot design should be as small as possible. The maximum time delay to successfully perform teleoperation or telesurgery is 200 ms. If tactile feedback is available, this increases to 400 ms [6].

Robot assistant surgery has some disadvantages as well. Because of the setup time the OR-time (Operation Room) it is still longer than conventional laparoscopic interventions like cholecystectomies, even if effective dissection time was shorter [17]. In heart surgery, there are more problems. The criticism in that case is that the duration is substantially longer, incomplete and the patient spent significantly longer on a heart pump than in open surgery [22]. Although 3D-vision is already a big improvement to 2D-vision, the operation times for robotic coronary surgery are still longer than conventional techniques [23].

The surgeons have to be convinced that MIS has an overall benefit for the patient. A lot of them consider robotic cardiac surgery as too daunting, too futuristic, or simply 'overkill' [24]. More recently, Robicsek [2] confirms that robotic cardiac surgery has not been as popular as some predicted. He calls it overkill, time-consuming and expensive, without real medical benefit. The same results can often be obtained with manual MIS.

Lack of tactile feedback is a limitation inherent in all surgical robotic systems. At present, robotic coronary surgery is not yet justified. Mechanical size, cavity access, tactile feedback, and visualisation still remain concerning issues and must be solved before these methods are established widely.

The main limitations of current technology for robot assisted surgery are [15] [17] [25] [26]:

- reduced number of degrees of freedom, resulting in low manipulability of the surgical instruments. Basic surgical manoeuvres like suturing demand highly developed technical skills
- no force or tactile feedback. In open surgery the surgeon controls his actions by visual and tactile feedback. Even in conventional endoscopy feedback of forces is reduced by friction
- absence of a natural interface. The techniques of MIS are hard to learn because the interface is too different from conventional surgery. Unnatural hand-eye co-ordination
- the robotic hardware is expensive

De Gerssem [21] already worked on the force feedback problem. Also a special force sensor was build for this purpose [9]. The forces measured during an operation on a rat stayed below 2.5 N. Tissue properties can also be estimated with active excitation of the instrument [8], but the possible effects of this on the tissue are unsure. Force feedback allows discrimination between tissues of different stiffness. Enhanced sensitivity makes it even possible to discriminate between smaller differences than would be possible without robotic system [27].

The usefulness of force feedback has been illustrated repeatedly. Performance increases significantly in a task where tubes have to be sorted by compliance with or without force feedback [14]. Another study shows that both surgeons and non surgeons exert lower forces during blunt dissection with force feedback [11]. This would result in lower tissue damage. Force feedback also helps to guide the instrument to the softest tissue. Okamura [12] gives a good discussion about the necessity of haptic feedback in robot assisted surgery. Forces and the variance of those forces decrease when force feedback is added in suturing tasks. Having only visual feedback also helps. A last experiment shows that the combination of force and visual feedback is better than either force or visual feedback alone [10]. This experiment, however, was less convincing due to the fact that the grasper was operated with the keyboard and could only be opened or closed completely. The grasping force was derived from motor current.

1.1 Importance of touch

Touch is very important for a lot of operations. As discussed above, the absence of tactile feedback is one of the main drawbacks of minimally invasive surgery. Especially in procedures demanding higher technical skills [17]. In laparoscopic colectomy, the absence of palpation is a major limitation [16]. The lack of tactile sensation during a laparoscopic colectomy greatly limits the surgeon's ability to stage the disease adequately. When tactile sensation is regained laparoscopic-assisted colectomy is safer and faster [28]. Palpation is also a standard screening procedure for the detection of breast, thyroid, prostate, and liver abnormalities. The pathological state of soft tissues is often correlated with changes in stiffness, which yields a qualitative estimation of the tissues Young's modulus [29].

Bholat et al. [30] investigate the importance of tactile feedback in surgery, comparing palpation, conventional instruments and laparoscopic (not robot assisted) instruments. Palpation is clearly faster and more accurate to detect shape or consistency in absence of visual feedback. Other studies compare palpation to other visualisation techniques like intraoperative ultrasound (IOUS), computed tomographic (CT) scans or magnetic resonance imaging (MRI). In a study of Norton et al. [31] all tumours in the palpable regions of the pancreas could be found by palpation; the others could be found with IOUS. Palpation is almost the best, second to IOUS [32], or the best [33] way to detect small liver tumours. Palpation can detect most (83%) and specify all liver metastases [33] [34]. Percutaneous ultrasound is the best noninvasive method of visualisation. Because of its poor sensitivity with respect to small and deeply located lesions, palpation is not always very accurate [29].

The above mentioned examples and studies show that a highly developed sense of touch is one of a surgeon's most important tools. The lack of tactile feedback can cause problems when visual feedback is not adequate. Surgeons can accidentally cut a blood vessel hidden underneath a layer of fat [26]. They rely on sensations from the finger tips to guide manipulation and to perceive a wide variety of anatomical structures and pathologies. There are different tactile feedback parameters to take into account: force reflection [35], vibration [36], small-scale shape (finding hidden anatomical features and locating tumours) [25].

The lack of tactile feedback during laparoscopic surgery can be overcome by the adoption of a 'hand-port', through which the surgeon inserts one hand into the operative field to aid dissection [4]. This necessitates a large cut, which makes the operation a lot less 'minimally invasive'. In video assisted thoracoscopic surgery (VATS), tumours found in peripheral lung zones are difficult to locate [13]. Accurate localisation of the imbedded tumour is critical to ensure that the entire nodule is removed and minimises the amount of healthy lung tissue resected. The tumours are often not visible from the lung surface. A frequently used method is sliding against the lung surface with a long metal rod inserted through the chest wall, to 'feel' the hard inclusion. This is difficult and time consuming. Miller et al. [13] propose a capacitive 12×3 tactile sensor probe from Pressure Profile Systems, Inc. With this probe, it is easier to locate inclusions. The instrument is located in the endoscopic image with leds and the tactile image is overlaid on the screen.

2 Psychophysics

In order to design a tactile feedback system that can produce a realistic feeling it is important to understand the psychophysics of touch. This section discusses the function of the different mechanoreceptors in the skin, the sensitivity of the human tactile sense and the reaction on different inputs like vibration or electricity. Lederman [37] gives a good overview of the psychology and the psychophysics of touch.

Perception of our environment through the sense of touch is described by haptics. Haptics has been around for about two decades, but progress has been hampered by its interdisciplinary nature [1] (announcement of IEEE transactions on haptics). It requires the cooperation of experts in such diverse areas as neurology, applied psychology, robotics, human-computer interaction, control systems engineering, and communications. The origin of the term haptics is found in the Greek word “haptesthai” which means the sense of touch with both tactile and kinaesthetic feedback [38]. Similar Greek words are “haptomai” or *ἅπτομαι*, which means touch and “haptikos” for to grasp, to touch. Haptics is usually subdivided in two modalities: kinaesthetic and tactile sense. Some more specific, less used terms are somesthesia (sense of the skin), statesthesia (sense of posture), kinaesthesia (sense of movement), and stereognosis (ability to determine shape and weight of an object) [39].

Kinaesthetic sensing or proprioception refers to the internal state of the limb through parameters such as joint angle and muscle effort, which allows us to feel large scale contour, shape, inertia and weight of object. Tactile or cutaneous sensing refers to distributed sensation from the skin [25] [40], which relates to sensations like textures, vibrations, and small scale shape. Proprioception is an unconscious sense: the sensory input from inside the muscles about length, tension, pressure, and noxious stimuli and tension between the muscles and the tendons, arrives in the unconscious part of the brain. We are not consciously aware of these stimuli so we can move around and use the information about where our limbs are without having to worry about it [41]. Other proprioceptors are located in the joints and ligaments or the sense of gravitation in the ear. Kinaesthetic information is insufficient where transmission dynamics (friction, backlash, compliance and inertia) tend to mask the desired signal [42].

In an experiment conducted by Srinivasan and LaMotte [43] the importance of both tactile and kinaesthetic information in softness discrimination was studied. When the objects had a deformable surface, the tactile sense is necessary and sufficient. When the surface is not deformable, both senses are needed. Bicchi et al. [44] have similar results. Mott and Sherrington [45] suggest that the kinaesthetic sense is less important in performing tasks than the tactile sense. They severed sensory roots in the spinal nerves of monkeys. When the upper limb, with the exception of most of the tactile sense in the hand was rendered insensible, they used their arm as normal; when the skin of the hand was rendered insensible, they didn't use their arm at all, even under strong incentive. They also note that when only the tactile sense of the thumb and part of the index finger is retained, movement is only slightly impaired.

However, a sense is never on its own. There is a connection between different senses, called multimodality [46]. We move our hand, see our finger feeling and feel the tactile input at the same time. For a surgeon it is important to

intuitively connect the sensation he feels on his finger with the movement he makes with the sensor and what he sees on the screen. Sight is the most important aid in manipulation and recognition tasks [47]. An elaborate discussion on multimodality can be found in [48], together with a proposal for a model of human perception (MHP). The performance of a simple task such as pushing a virtual button improves with simple tactile feedback [49]. This suggests that the improvement would be even larger in more complicated tasks.

An example of the high information possibilities of touch is *tadoma*. That is a technique for which one places a hand on the face and neck of a talker and monitors a variety of actions associated with speech. This way trained deaf and (almost) blind people can understand what is said [50] and learn how to speak [51]. Pasquero [52] gives an overview of the efforts made to create tactile languages.

2.1 Mechanoreceptors

Mechanoreceptors convert the mechanical deformations caused by force, vibration or slip of the skin into electrical nerve impulses. Apart from mechanoreceptors, the human skin also has thermoreceptors to sense temperature and nociceptors for pain. The human perception is the interpretation of these signals in the brain [26]. The four most important types of mechanoreceptor nerve endings in the glabrous skin can be categorised according to their temporal frequency response and size of their receptive fields [25] [53]. The hairy skin also has touch sensitive hair follicles. Figure 3 shows how they are located in the skin and Table 1 gives their properties. All receptors get much more information from pressing down than from releasing [54] [55] [56] (Figure 2).

Cutaneous mechanoreceptors are described as slowly adapting (SA) or fast adapting (FA or RA: rapidly adapting) according to their frequency response, particularly to static stimuli. The other criteria is receptive field size: Type I units have small receptive areas and well defined boundaries, while Type II units have large receptive areas with poorly defined boundaries. Type I receptors (both SA and FA) are located close to the surface of the skin where the deformations and induced stresses are more pronounced. Merkel disks are SAI receptors, Meissner’s corpuscles FAI, Ruffini endings SAII and Pacinian corpuscles FAII [42] [26]. Merkel disks (SAI) and Ruffini corpuscles (SAII) react to static pressure (P), Meissner cells (FAI) –and to a lesser degree Merkel disks– measure speed of skin indentation (dP/dt) and Pacini corpuscles (FAII) react on changes in indentation speed (d^2P/dt^2) [57]. There is an apparent trade-off between spatial and temporal resolving power [37]. SAI units are better than FAI capable of resolving the finest spatial details. FAI are somewhat better at resolving vibrotactile patterns. The FAII units cannot code spatial details at all, but are sensitive to the highest portion of the frequency spectrum. Pacini corpuscles have onion-like sheet, which effectively applies a mechanical high-pass filter to the indentation signal [57]. SAII often show selectivity to the direction of stretch.

Neurophysiological studies suggest that SAI mechanoreceptors are most important in small-scale shape perception [58], which suggests that a relatively low bandwidth display may suffice in many applications [25]. The ability to separately perceive two pointed indenters on the finger tip requires that the

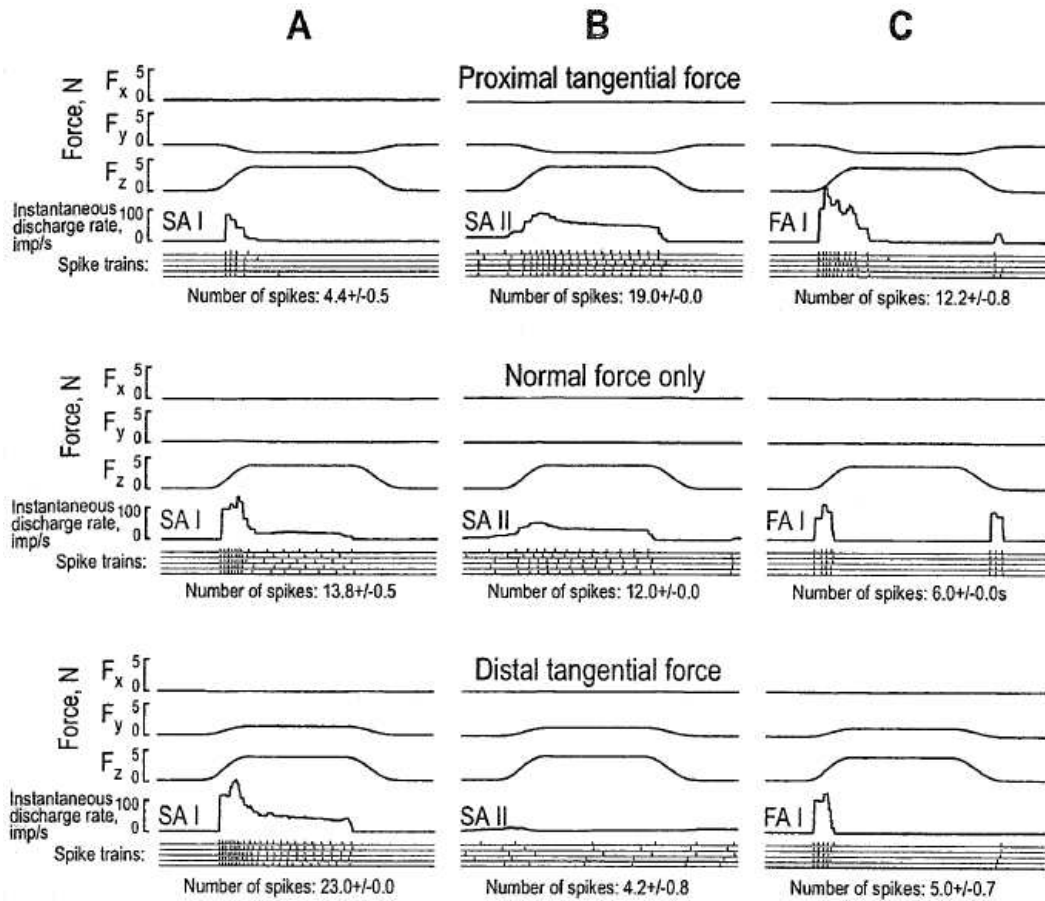


Figure 2: Response of mechanoreceptors to rising and dropping stimuli.

points be separated by 1–2 mm, and humans perceive a surface as textured rather than perceiving each small surface feature individually if the features are less than about 1 mm in extent.

Tactile units appear to vary in the number of specialised end-organs in which they terminate, i.e. 1 for SAI and FAI, 4–7 clustered endings for SAI and 12–17 non-clustered endings for FAI [59]. When a unit ends in more than one specialised ending, the sensitivity of the receptive field remains relatively uniform across the corresponding area above the endings. The multiple endings can be densely packed or more broadly distributed. The closer the end-organ to the skin surface, the steeper the decline in sensitivity towards the periphery of the receptive field. This receptive field is usually circular or slightly oval in shape [37].

There are about 17000 mechanoreceptors in the grasping surfaces of the human hand, spacing ranges from about 0.7 mm in finger tip to 2 mm in the palm [56]. SAI units are predicted to be about 0.7–1 mm below skin surface. This depth is based on finite element models [64] and data collected on macaque monkeys [65]. The spatial density of the SA units is determined to be approximately 0.7 sensors per mm³ in the fingertips [66].

The sense of touch is quite rich and includes beside the cutaneous sensitivity, the sensitivity to an applied pressure, vibration and a variation in the temperature [67]. The vibration is used in the perception of surface texture. It is generated by displacing a finger over the explored surface [68]. Texture

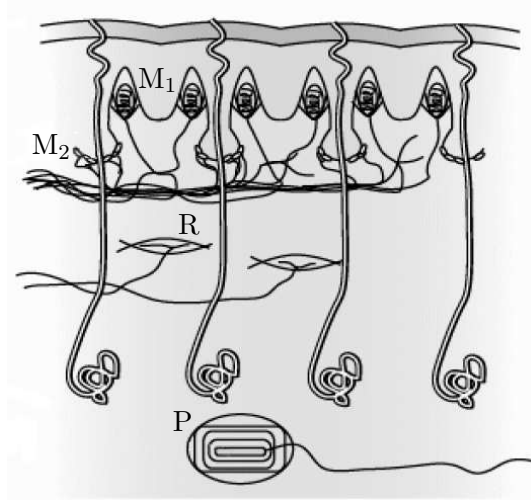


Figure 3: M_1 : Meissner Corpuscle; M_2 : Merkel Cell; R: Ruffini Corpuscle; P: Pacinian Corpuscle [60]

Receptor Type	FAI Meissner	SAI Merkel	FAII Pacinian	SAII Ruffini
Field diameter	3–4 mm	3–4 mm	> 20 mm	> 10 mm
mean receptive area	12.6 mm ²	11 mm ²	101 mm ²	59 mm ²
spatial resolution	poor	good	very poor	fair
frequency range	8–200 Hz	DC–200 Hz	50–1000 Hz	DC–200 Hz
most easily excited frequency range	8–64 Hz	2–32 Hz	> 64 Hz	< 8 Hz
sensory units	43%	25%	13%	19%
postulated sensed parameter	Skin stretch	Compressive stress (curvature)	Vibration	Directional skin stretch
density	70–140 /cm ²	70–140 /cm ²	20 /cm ²	50 /cm ²

Table 1: Characteristics of the specialised mechanoreceptor nerve endings in human finger tip skin (adapted from [42] [26] [56] [61] [62] [63])

perception is mediated primarily by spatial encoding for coarse textures and by vibrotactile encoding for fine textures [69]. The FA receptors are also important to detect contact. Pawluk and Howe [70] investigate the dynamic distributed pressure response of the human fingerpad when it first makes contact with an object.

Andersson and Lundberg [46] summarise the skin receptors as follows:

- Meissner corpuscles: Codes the movements at the surface of the skin (a held glass sliding in the hand).
- Merkel disc: Codes information on the spatial shape and texture of the stimuli (raised letters or Braille).
- Pacinian corpuscles: Codes the temporal attributes of the stimulus (such as the vibration of a tool manipulated by the hand)
- Ruffini endings: Encodes warmth

- Krause's end bulbs: Encodes cold [71]

Recently, the Ruffini endings have come under discussion. Paré et. al [72] suggest almost no Ruffini endings can be found in the human glabrous skin. The SAI signal and directional sensitivity found in electrophysiological studies may not originate from Ruffini endings after all.

In a personal discussion, Johansson gives three mechanisms for lateral inhibition. The first, and most important, is mechanical. When a square object is pressed on the skin, the stress level in the skin is highest under the edges of the object. On a lower level, different endings of a single tactile unit might interfere with one another. An activated ending dominates the nerve and even backfires to the other endings. It is not clear whether this is important. At an even lower level, the nerves interfere with each other where they meet, which can result in lateral inhibition. According to Lederman [37] all of the mechanoreceptor units synapse in the spinal cord, and there are no lateral interconnections among single units in the periphery. Hence, there is no lateral inhibition at this level. Edge enhancement may be due to mechanical rather than neural factors.

2.2 What is perceivable by humans

Humans are very good at recognising common objects by touch, within 1–2 s [37]. The skin is very sensitive to light pressure. Studies have determined that the perceived intensity of stimulation is affected by both depth of penetration and by rate of skin indentation [37]. Actual intensity judgments are more closely correlated with stimulus force than with indentation. Under ideal condition a displacement of the skin less than 0.001 mm can be perceived as a stimulation of touch, although the amount of stimuli needed to achieve such a sensation differs between body parts [73]. The absolute threshold for touch force perceived on the fingertip is 0.8 mN [74]. The minimum perceivable height of a static raised feature on a smooth surface is 0.85 μm . Small dots with 40 μm in diameter and 8 μm in height can be detected 75% of the time with active scanning [75]. 75% gap detection and grating detection are 0.87 mm and 0.5 mm [76] [77]. Johnson and Phillips [76] have shown that humans can reliably distinguish between two points that are separated by as little as 0.9 mm [78], while Sherrick and Craig [74] found this value to be 2.5 mm and Loomis [79] found 2.8 mm. This is often called the two point discrimination threshold and depends on the frequency of the applied input. There is an increased sensitivity between 1–3 Hz and between 25–40 Hz, which are the frequency ranges of SAI and FAI receptors [80]. The sensitivity can decrease after exposure of the skin to vibrations [81] [82]. There is an important difference between discrimination of spatial misalignment, spatial interval discrimination, point localisation and spatial resolution [79]. Some hyperacuity is discovered where thresholds can be much finer than the resolution acuity. Vernier acuity (two parallel lines, of which one is slightly displaced to left or right) was found between 0.37 mm and 0.70 mm. Point localisation (excitation left or right from reference) was 0.17 mm. While position localisation is within about 1 mm, a shift of 0.1 mm can be detected [37]. Spatial discriminative capacities of the skin are strongly task dependant. The just noticeable difference of pressure amplitude is 14% for static pressure and 20% at 160 Hz. Over a frequency range of 20–300 Hz it is 20–25% [83].

Tactile sensing can provide information about compliance, friction and mass [42]. People become clumsy when deprived of reliable tactile information through numbness of anesthetised or cold fingers [84]. When our arm is sleeping we can still move everything, but cannot use it because of the lack of sensory feedback. This shows that tactile sensation is essential for many exploration and manipulation tasks not only in a real environment but also in a virtual environment. While touching or feeling the surface of an object with their fingers, humans can perceive complex shapes and textures through physical quantities such as pressure distribution, vibrations from slipping and stretching, and temperature [85].

The maximum frequency of perceptible vibrations is 1000 Hz [86] with a maximum in sensitivity at 250 Hz [87], which corresponds to the FAII receptors. Bolanowski et al. [88] show a maximum sensitivity at 300 Hz, at which frequency a vibration with an amplitude of $0.1 \mu\text{m}$ can be discerned. According to Sherrick and Cholewiak [89] this is between $0.2 \mu\text{m}$ and $0.5 \mu\text{m}$ at 200 Hz to 400 Hz. At 30 Hz amplitudes of $5 \mu\text{m}$ to $20 \mu\text{m}$ can still be detected. Also [90] shows a lower threshold at 320 Hz than at 40 Hz. Van Doren et al. [91] confirm these findings and add a spatial component by using a sinusoidal wave with both temporal and spatial component. At frequencies above 64 Hz they did not find an influence of spatial component on the threshold; below, they found that a higher spatial frequency corresponds to a lower threshold. The maximum deformation of the skin at the fingertips is 3.5 mm [92]. The pain threshold is 3.2 N at a pin diameter of 1.75 mm that corresponds to a pressure of 1.3 MPa [92]. That's about 1 N for a pin diameter of 1 mm. Stiffness of the fingertip is non-linear; soft for small deformations and more rigid for larger deformations. The stiffness increases when the fingertip is tilted. For an applied total force of 7 N, deformation is between 2 mm and 3 mm [93].

Provancher [94] gives an overview on testing procedures.

2.3 Vibration

Humans have a limit in how much information they can process. That limit, we believe, can be dispersed between different perceptual systems. The use of more sensory channels can augment the coding of information without overloading any of the perceptual systems used [46]. (Interesting paper for vibrotactile displays used to convey information, for example in the MAIA project.) Humans can have difficulty detecting change between vibrotactile patterns [95]. More on the effectiveness of tactons (structured, abstract, tactile messages) can be found in [96]. These tactons can be used to replace visual progress bars [97]. MacLean and Enriquez [50] investigate the possibility to use haptic icons, represented by vibrations at different frequencies, waveforms and amplitudes, as a haptic language. The Weber factors to discriminate time duration of vibrational stimuli or to discriminate sweeping velocity of vibrational stimuli are about 0.2–0.4 [98].

Tan and Pentland [50] describe the effect of 'sensory saltation' or 'cutaneous rabbit'. For this sensation three stimulators are evenly spaced in a line and vibrating pulses are delivered in the following sequence: three pulses on the first stimulator, three on the second and one on a last. The observer is under the impression that the pulses seem to be distributed with more or less uniform

spacing from the first stimulator to the last. The sensation is characteristically discrete as if a tiny rabbit was hopping up the arm. Similar effects are experienced with an array of vibrotactile stimulators on the back.

Apart from adding artificial information, vibration also contains information about the touched objects. Vibration can enhance certain tasks, which are more difficult when vibration is absent [99]. Humans also perceive texture information from high frequency input or vibration [85] [99]. Combined with the speed of the finger, the temporal frequency is related to the perceived roughness. Konyo et al. [100] assume that the perceived roughness becomes larger when the frequency decreases. Lederman [37] on the other hand found that temporal frequency of vibrations set up in the skin by the relative motion between skin and surface is not used to perceive roughness, and friction nor groove-ridge ratio influences this perceived roughness. Without lateral motion between skin and surface, it is impossible to perform fine texture discriminations, but passive or active touch or the velocity are unimportant. 2% to 5% of variation in spatial period of patterns such as dots can be discriminated.

Vibrations is sometimes unwanted, because the sensitivity can decrease after exposure of the skin to vibrations [81] [82].

2.4 Simulation of sensation

With electrodes on the skin different mechanoreceptors can be triggered. Anodic stimulation elicits an acute vibratory sensation by stimulating the vertically oriented nerves: Meissner corpuscles. Cathodic stimulation generates a vague pressure sensation by stimulating the horizontally oriented nerves: Merkel endings [101] [102]. It is difficult to confine the general sensation to a small area. A smaller area is achieved with anodic stimulation because that stimulates vertical nerves. Because cathodic stimulation activates horizontal nerves, it gives a sensation in de nerve ending which is in a slightly different location.

The relationship between amount of current and the generated sensation was unclear and unstable. Sudden pain caused invasive impression, or even fear [103]. With electrocutaneous stimulation an electric shock can be the result because there is no relation with contact force. Use of a force sensor can compensate [103]. Experiments in single-nerve stimulation showed that Merkel cells generate a pressure sensation, while Meissner corpuscles produce a vibratory sensation [104].

An electro-static attraction can be created between the skin and an electrode surface. This results in a 'sticky' or 'buzzing' sensation [105].

Levesque and Hayward [106] state that tactile sensation can be simulated with lateral skin stretch only. They investigate the lateral skin strain patterns when passing simple geometrical features to use this as an input for a tactile display (STReSS). The results are difficult to interpret. In movement on a glass flat surface, a central region of the finger skin stays stationary and the surrounding skin moves, resulting in compression or expansion of the intermediate skin. When moving over a bump or a hole, compression is detected on the rising part en expansion on the dropping part. The tests weren't very good with a

lot of noise. The idea is put into practice for a Virtual Braille Display (VDB) and the idea seems to work [107]. At small scale the resulting sensations seem to be indifferent to the details of skin stretch/shear orientation [108]. Drewing et al. [109] investigated with which resolution humans can discriminate the direction of skin stretch and found large individual differences between 21° and 78° .

Webster et al. [110] [111] did research on slip. Subjects can notice a difference between moving angle and slip angle of 20° and detect a sinusoidal slip speed difference of 30% of nominal slip speed. For both values, 50% of the test subjects could notice the difference.

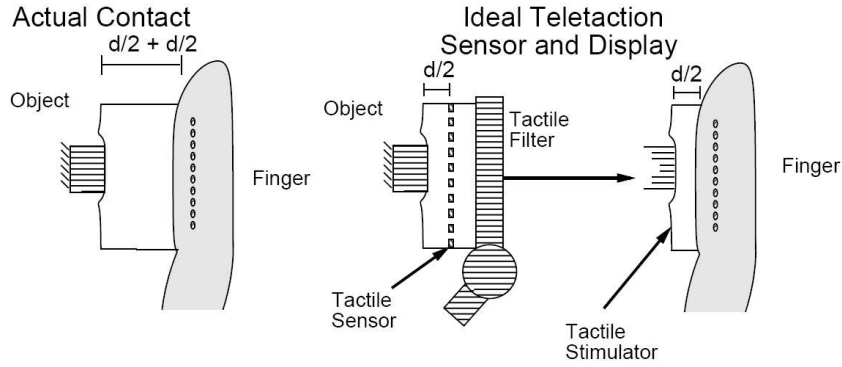


Figure 4: Real contact with finger and contact through tactile feedback [113]

3 Aim

The aim of this research is to develop a system with a tactile sensor to enter the body through a small incision, and a tactile display to convey a realistic sensation to the surgeon. The technology has to support the knowledge and skill of the surgeon as much as possible so he can focus completely on the medical aspect of the operation. The system has to be optimised in cooperation with the surgeons. There are some requirements regarding spatial resolution and frequency range, sensitivity of the sensor, force and stroke of the display. These requirements result from the psychophysical properties of the human sensory system. Apart from those, there are also other miscellaneous or application specific requirements.

Especially in industry, a lot can already be done with binary sensors in small, compact arrays [112]. In general, a system that combines a tactile display and a tactile sensor to sense remote objects is a teletaction system (Figure 4). With an ideal teletaction system, the patterns felt by the user would be indistinguishable from direct contact with the environment [26].

There's no real naming convention for the separate tactile elements; tactels (Tactile element) [26], taxels (tactile pixel) [68], texels [127] or tactors (tactile actuator) [25] are used. Taxel is the most frequently used and is adopted here.

3.1 Spatial resolution

To get a realistic feel, the spatial resolution should be close to the spatial resolution of the mechanoreceptors in the human skin. The ability to separately perceive two pointed indenters on the finger tip requires that the points be separated by 1–2 mm [25]. A spatial resolution of 1 mm in both directions is necessary [26] [114] [115] [116]. Wellman et al. [78] state that a resolution of 0.9 mm is necessary to experience shape instead of separate pins. If the problem is approached as spatial frequency, a resolution of 1 mm corresponds to a two point discrimination threshold of 2 mm or a signal with a frequency of 0.5 mm⁻¹ (Shannon). Often an elastic layer is used as a low pass filter however, so the separate pins are impossible to detect [26]. Care should be taken that the spatial resolution is not reduced by crosstalk [47].

Another approach is to state that a resolution of the size of the receptive field of the important mechanoreceptors is enough. For FAI receptors that leads to a resolution of 2–3 mm [117] or 3–4 mm [118]. The taxels must cover the entire

fingerpad area, which is typically between 1 cm^2 and 2 cm^2 [118].

In industrial applications, e.g. object recognition, the resolution is strongly application dependent. Bao and Van Brussel [119] advise a spatial resolution of 1 mm in a matrix of 20×20 cells [112] [120]. In braille displays the resolution is typically a lot coarser. In other applications where the the aim is to give other kinds of information than tactile information, there are often only a few large vibrating points [50] [46].

3.2 Frequency range

The frequency range or temporal resolution is connected to spatial resolution. Peine et al. [121] state that the average palpation speed of a surgeon is 120 mm/s. A spatial resolution of 2 mm leads with this speed to 30 Hz, a spatial resolution of 1 mm leads to 60 Hz required bandwidth. According to Howe et al. [25] a low bandwidth display may suffice in many applications. This is because the most important mechanoreceptors in small-scale shape perception are Merkel disks [58], and they only have 10 Hz bandwidth. Some others give a required bandwidth of more than 50 Hz [26] [114] [116]. Tests show that in a search task, the average time to find dots in one dimension halves when bandwidth is increased from 5 Hz to 30 Hz [78]. This shows that a frequency higher than 5 Hz is certainly desired.

The skin's sensitive bandwidth is a lot higher, about 1000 Hz [118]. Pasquero and Hayward [108] think this high rate should be matched. This depends on what you want to feel. For coarse textures and shapes, the perception is mediated primarily by spatial encoding and for fine textures by vibrotactile encoding [69]. If the perception of texture is necessary, a frequency range from 1 Hz to more than 500 Hz should be available [85]. If the approach is only to match the frequency range of FAI and FAII receptors, frequencies between 10 Hz and 300 Hz have to be excited [117].

For other applications it is hard to give a general comment on the required frequency range. In braille displays, it depends on the length of the line or the number of characters read per minute. In industrial applications such as slip detection fast response time and a frequency range up to 100 Hz can be necessary [119] [120] [47]. The response time should be as low as 1 ms [112].

3.3 Sensitivity, force and stroke

The sensitivity of the tactile sensor and the exerted force of the tactile display are closely connected. The display has to be strong enough to support the force applied by the surgeon while maintaining the desired shape [25]. 1 N of force per factor [25] [26] [114] or a maximum pressure of 0.5 N/mm^2 [116] are mentioned. This 1 N of force on a sharp wedge is needed for 1 mm skin indentation [85] [122]. The maximum pressures during grasping and manipulation are typically less than 50 kPa [118]. In soft tissue palpation a pressure of 10–40 kPa is used [123]. This can be measured with a sensor detecting the colour changing in the finger nail when you apply pressure [124]. The sensor is only usable up to 1 N. The given needed stroke isn't consistent between references. 2 mm [26] [113], 3 mm [25] and 4 mm [114] [116] are mentioned. This last value is particularly strange if you take into account that the maximum deformation of the skin is

3.5 mm at the fingertip [92]. If you want to avoid pain, a pressure of 1.3 N/mm^2 should not be exceeded [92]. Moy actually contradicts himself between 2 mm in [26] and [113] and 4 mm in [114]. Almost all other references saying 4 mm refer to [114] for this. A height resolution of 10% should suffice [116], since the human sensory system isn't accurate enough to detect smaller differences.

Peine and Howe [125] show that in soft tissue palpation –detecting a hard ball in soft tissue, the absolute pressure hardly plays a role. More important is the indentation, caused by pressure differences. The pressure distribution is useful, but the offset pressure is not. They also show that the tactile sensor needs a sensitivity of 0.5 kPa and an tactile display a resolution of 0.05 mm.

The sensitivity in sensors for industrial applications generally has a higher range from 0.5 N up to 10 N for each sensor cell [112] [119] [120] [126]. Sensitivities as low as 0.01 N are mentioned [112]. An overload protection is essential and the sensor should be able to withstand several times the largest expected force [47].

The required power density is 10 W/cm^2 [26] [114].

3.4 Other requirements

There are a lot of other requirements. The sensor has to be flexible to be shaped like a finger, biocompatible and resistant to body fluids because it enters the human body and of course inherently safe. Klein et al. [29] summarise this safety as follows:

- material selection with respect to toxicity, flammability, ageing, etc...
- no dangerous reactions with other materials (fluid, solid state or gaseous) with which the product may come into contact.
- no risk of injury (electrical hazard, explosion, fire) during usage, storage or transport
- no risk of magnetic, electric or electromagnetic interference (EMI) or electrostatic discharge
- no risk of changes in specified characteristics (through temperature, pressure, acceleration etc...) which may lead to injury or other danger.
- electrical design in respect to national and international laws and directives (e.g. low voltage directive)

The tactile display has to be light enough to avoid limiting responsiveness and inertial forces while moving the hand and small enough to fit on the finger [25]. These requirements also apply for displays to be build into a mouse or a steering wheel [108]. Of course the display has to be safe as well, but not as stringent as the sensor, because it does not have to enter the body. It does however need to be able to resist prolonged exposure to skin abrasion and be impervious to skin secretions [108]. Care should be taken that the power input per taxel is not too high, since it is multiplied by the number of taxels. An excess of dissipated power should also not heat the taxels. The price is also an important factor, especially for the tactile sensor, since surgical instruments are usually thrown away after a few uses.

Pasquero and Hayward [108] also discuss different design factors like biomechanical, neuroanatomical, psychological and behavioural, cognitive and application related factors.

Kyung et al. [85] describe the need for reversible lateral movement of the display regions for the skin slip/stretch, from 0 cm/s to more than 5 cm/s. This apart from a distributed pressure for displaying a small-scale shape. In applications in virtual reality and texture perception a combination of kinaesthetic and tactile feedback is needed.

Also according to Schuenemann and Widmann [117] lateral skin stretch is necessary. Since mainly SAII receptors detect directional skin stretch the requirements are based on their receptive properties: a resolution of 7–10 mm, a frequency range of 10–100 Hz and a force of 10 N. According to Lederman [37] lateral forces must be known to assess the coefficient of friction. Therefore, the design of tactile sensors should include measurement of lateral forces. Sensitivity to microscopic irregularities on a surface appears to involve or be mediated by shear forces.

In general the sensor should demonstrate a low hysteresis, linear behaviour, physically robust to withstand hostile environments, wear resistant and chemically inert. For commercial sensors, price, reliability, power consumption and flexibility are also important [47].

When the aim is to reproduce different textures and materials in virtual reality, two excitation modes of the skin are necessary: mechanical and thermal excitation [68]. The mechanical excitation is a vibration with 2 mm resolution, a force of several tens of mN and a frequency range of 20–300 Hz.

For industrial applications the sensor must have a high ruggedness with compliant skin, a wide operating temperature interval and low hysteresis [112] [119] [120].

4 Sensors

Designing a tactile sensor for robot assisted minimally invasive surgery proves very difficult. When a resolution and sensitivity, close to that of the human skin is required, a lot of separate elements are needed. Each of these elements has to be connected to the outside world through a small shaft and also the sensor itself has to be minimised to fit in the small available space. The sensor should also be flexible to fit around a finger-shaped probe. The possibility might be studied to curl the sensor more upon entering the body and uncurl it slightly to accomplish the same sensing area through a smaller incision. This curling accentuates the importance of structural flexibility.

Tactile sensors in general are used to collect local contact information, such as contact location, contact force, contact area, local shape, texture, and thermal properties. Tactile sensors can sense things like: presence; target shape, location, orientation; contact area pressure, pressure distribution; force magnitude, direction and location; moment magnitude, plane and direction; the targets' compliance, texture, viscoelasticity, etc... [131]. In case of a shape/pressure sensor, a choice has to be made to sense either strain or stress [26]. Studies have determined that the perceived intensity of stimulation is affected by both depth of penetration and by rate of skin indentation. Actually intensity judgments are more closely correlated with stimulus force than with indentation [37]. Also a difference has to be made between static and dynamic sensing. A static sensor can feel constant pressure and shape, while a dynamic sensor is better at feeling very small features and textures by moving over them and detecting change [132]. Dynamic tactile sensors respond to changes, in analogy with FA mechanoreceptors. They measure vibrations or changes in stress [42].

An analysis with noise in sensed tactile data, demonstrates that the relationship between the surface profile and the observed image is ill-conditioned [133]. One method of overcoming this problem is to combine several sets of data from different perspectives using spatial filtering to suppress the effect of the noise. This approach appears to be used by human touch, which relies heavily on motion for collecting tactile data. The analysis reveals that motion is not only beneficial to touch, but essential in amassing sufficient data to extract accurate surface information. In parallel with a model of the human skin [61], a continuum mechanics model of a photoelastic sensor is developed.

Surface features can also be sensed without a tactile sensor by tracing the surface and deriving the surface from the curve the robotic fingertip follows. The curvature of the fingertip is a limitation to the maximum sensed curvature of the surface [134]. For example in a robot grasper with three fingers, the tactile sensor is actually force sensor beneath the finger tip [135]. To grasp in an unstructured environment, it is necessary to know the magnitude and direction of forces and torques [136]. Four 3D pressure sensors can be used to determine the orientation of torque and force.

A lot of tactile sensors use semiconductor technology in some way. In general, semiconductors are fragile and particularly sensitive to their environment, such as heat, noise and ambient fields [112].

Elastomer layer Sensor covering is sometimes a forgotten topic in tactile sensor development [137]. A frequently adopted sensor concept which reason-

ably fits the industrial requirements is that of the elastomer-based tactile sensors [47]. These types of tactile sensors utilise a layer of elastic material which constitutes the essential transduction element. The elastic layer employs Hooke's law to transduce pressure loads into an indentation distribution, and a variety of physical principles, such as the resistive, inductive, capacitive, optical, magnetic, piezoelectric or acoustic sensitivity of the elastomer with applied load are explored. The properties of the covering material can severely influence the underlying sensor measuring properties [138]. According to Cutkosky [139], the ideal properties of a robotic skin are durability, compliance to conform to rough surfaces, texture to reduce lubricating effects of liquids and a moderate but uniform and reliable coefficient of friction.

Shimoga and Goldenberg [140] presented an interesting study on soft materials for robotic fingers. They claim that the human skin has three useful features in terms of grasping properties: it reduces impact forces, conforms to uneven surfaces and dissipates repetitive strains. The materials that appear to be good candidates for robotic fingers can be classified into three categories: solids, elastomers and rheological materials. Shimoga and Goldenberg performed experiments comparing six materials chosen as representatives of these three categories. The criteria for the experiments were the above mentioned properties of the human skin. The results show that sponge is the most suitable and plastic is the least suitable covering for robotic fingers. For practical reasons, however, the gel is a good compromise over the sponge. The material for a soft robot fingers has to be carefully chosen.

An elastic layer can also function as a spatial low-pass filter [141]. Consider the spatial impulse response of the teletaction system, i.e. the response to a pin prick. Without some superficial layer, it is impossible to localise the pin to better than one tactel, no matter how dense the sensors, and the pin may be between sensors and not sensed [26] [142].

There are of course some limitations to an elastomer based tactile sensor, like creep and hysteresis [47], which are both unwanted in any kind of sensor. This might in fact not be a very big problem because the human fingertip acts the same way. Especially in the application of tactile feedback, the human might not even be able to feel slow and/or small changes caused by creep or hysteresis. Whether or not this affects the performance of a surgeon is a possible subject for further research. The fact that an elastomer acts as a low-pass filter also results in unwanted mechanical cross-talk. And the elastomer could mechanically limit the frequency range and dynamic behaviour of the sensor, acting as frequency dependent damping. These limitations can result in loss of significant data.

Like the human skin however, tactile sensors must not only serve as a source of information regarding physical contact with the external world, they must also serve as the frontline bearer of chemical and mechanical contact [143]. In [132] this problem is dealt with a thin outer skin of relatively tough rubber to be less fragile and less easily damaged, and an inner layer of rubber foam to improve grasp stability and control of contact forces. Peine et al. [144] suggest that a rigid sensor is preferable since it will most effectively compress the artery and surrounding tissue, thus increasing the perceived pressure from blood pulses. However, some compliance in the sensor surface is useful as it permits the sensor to conform to geometric and elastic irregularities in the sensed region. The challenge of designing and building a successful tactile sensor is thus a

difficult balancing act. Strength and durability are traded against sensitivity and repeatability [143].

A last reason to use an elastomer layer is that traditional microfabricated tactile sensors are typically based on silicon, which is usually a rigid and fragile material from a mechanical point of view. Exposing the sensors presents problems if silicon is used, because silicon easily fractures upon mechanical impact and over-loading. A elastomer layer can spread the mechanical forces and protect a more fragile underlying structure. A continuous layer of rubber is better resistant against non-uniform forces than e.g. membranes. The latter deform in different ways if pressed in a different angle or distribution.

Something else to keep in mind is the surface quality. An extremely smooth surface (local roughness less than about $1\ \mu\text{m}$) can produce a very large coefficient of friction. A mat finish (local roughness of a few tens of μm) has a substantially lower coefficient of friction and can slide evenly over smooth surfaces [132]. Cutkosky et al. [139] found that a high coefficient of friction is not necessarily the hallmark of an excellent skin material. A high coefficient of friction is found to be very sensitive to contamination. From this point of view 'fingerprints' are very important because they improve the consistency of the coefficient of friction under moist conditions.

The geometry of an elastic cover can be used to enhance tactile signals [145]. Nature does it. Fingerprints increase sensitivity to the tactile receptors that lie underneath. Hemispherical bumps are used in [146] and in [145], because they are not as direction selective as ridges. They apply the technique on the 3D tactile sensor described in [147] and a commercial sensor by Xsensor. Positioning a silicon rubber hemisphere over four taxels, decreasing the number of taxels by four, but instead of only 1D pressure, 3D pressure can be measured. Both concerning the compression of the bump as the measurement of the stress below, there is no crosstalk between X and Z components of stress.

A similar strategy is used by Holweg [148] [149]. Instead of hemispheres, the rubber is shaped in blocks, each covering 4 taxels. A block that is not completely covered will, however, result in a wrong measurement. Thicker rubber results in higher sensitivity to shear forces.

Readout circuit Because of the large amount of sensitive elements, some attention should be given to selecting the readout circuit. This circuit has to take into account all the properties of the sensor, minimise the noise and preferably the number of wires coming from the sensor. One way to do this is to make an array of tactile elements and select a taxel by selecting a row and a column. This reduces the number of wires from n^2 to $2n$.

An alternative for a stretchable, flexible tactile sensor is presented in [150]. The communication is based on two-dimensional signal transmission technology. A high frequency 2.4 GHz microwave is transmitted through conductive fabric. Between two layers of the fabric are sensor elements capacitively coupled with the fabric. The sensor elements are on-off switches. The minimisation of the elements is limited by the wavelength of the waves, 6 mm by 6 mm in this case. Another method is to insert the sensor elements in a ring-type sensor network [151]. In the example structure, the sampling time for one element is 0.2 ms

and the maximum number of elements is 65536.

When the sensor probe is manually pressed against the area of interest, low frequency noise can obscure the signal. To lessen the effects of these perturbations on the signal of interest, [144] uses the large-amplitude harmonics of the fundamental frequency of the pulse. Tactile data can be processed using conventional pattern recognition techniques that have already been developed for cameras [47]. This can be useful for shape identification. Neural networks can be used to derive force vectors from a tactile image [152]. In [153] a skin-like, stretchable transistor circuit is described, to be used in e.g. a robot skin.

Previous reviews In the past already some overviews have been given on tactile sensing. Wolffenbuttel [47] gives an elaborate overview of tactile sensing technologies in 1994. Lee and Nicholls [154] gave an overview in 1999 for mechatronic applications. Tegin and Wikander [155] give a more recent overview (2005) for robotic manipulation. De Rossi et al. [156] give an overview of smart skins in general with a section about tactile sensing. Ramezanifard et al. [157] give a nice overview of tactile sensing in MIS (2008).

4.1 Piezoresistance

Piezoresistance or piezoresistivity is the general term to describe the change of electrical resistance when pressure is applied. In general, the piezoresistive effect in metals is due to the change in geometry, as is the case in strain gauges. In semiconductors, the effect several orders of magnitude larger [158].

A lot of piezoresistive tactile sensors utilise the effect that the contact resistivity between two surfaces changes according to the applied load [127]. This was first discovered by the French electrical engineer Theodore du Moncel in the late 19th century. He discovered, that an electrical current flowing between a sooted metal plate and a nail is modulated by acoustic waves. Based on this conclusion, he invented the carbon microphone which revolutionised telephony [128].

Elastoresistance or elastoresistivity on the other hand, is the effect that the resistance of a conductive elastomer or foam changes. A conductive elastomer is most often a composite of a rubber with some sort of conductive particles.

In general, the construction and readout electronics of piezoresistive tactile sensors can be quite simple [127].

4.1.1 Rigid Piezoresistance

Very small strain gauge elements can be fabricated with semiconductor techniques. A typical semiconductor sensing element consists of an N-type semiconductor material that has been etched to form a vacuum cavity. Over the top of the cavity is a very thin pressure diaphragm that deflects as pressure is applied to the sensor. Four piezoresistive elements are formed on the top, or pressure side, of the diaphragm by diffusing a P-type semiconductor material into the diaphragm, or by depositing thick-film resistors onto the diaphragm [152] [159].

The response of this kind of silicon tactile sensor is very linear, and exhibit low hysteresis and creep. Another advantage is that signal-conditioning electronics

can be built into the same piece of silicon. The planar nature of silicon integrated circuits presents a problem when curved sensors are required, since the silicon material is mechanically brittle and rigid [143].

Vásárhelyi et al. [147] present a tactile sensor using this principle. The sensor consists of a silicium membrane, 300 by 300 μm , with four perpendicular piezoresistive bridges connected in the middle, and a cavity underneath. In the centre of the membrane, where the bridges meet, there is a hole in which a beam can be placed to increase lateral sensitivity. The sensitivity is very high and can be adapted by applying a silicon rubber layer on top of the membrane and inside the cavity. The resolution is 0.5 mm. Four of these sensors can be combined to determine the orientation of torque and force [136].

A similar sensor is produced by Sugiyama et al. [160]. It comprises of full bridges of polysilicon piezoresistors, and has 32×32 elements, a resolution of 0.25 mm. An access time of 16 μs to a single element leads to 60 Hz readout for the entire sensor.

To increase the sensitivity of silicon piezoresistors a porous silicon membrane of 63% porosity can be used [161]. Increasing the porosity further decreases the sensitivity, possibly because of the percolation threshold at 66%. The element has a mostly linear region between 10 and 60 kPa or 0.01–0.06 N/mm^2 , with a sensitivity that is about three times higher than conventional silicon piezoresistors.

Flexible tactile sensors can be made with micromachined thin-film metal strain gauges, positioned on the edges of or into polyimide or polydimethylsiloxane substrates. The piezoresistive factor is smaller, because silicon is not compatible. In [143], the result is a flexible robust, monolithic polymer-based sensor with embedded thin-film metal sensors and interconnects. The gauge factor of 1.3 is lower than silicon, but the use of a thicker polymer film can counteract this a bit. The resolution is sub-mm. In [71], they use Dupont Kapton for a multimodal sensor measuring hardness, temperature and thermal conductivity. For the hardness measuring they use two structures like in [143] with different stiffness, located more than 1 mm from each other. It doesn't work on irregular surfaces. The sensing elements are 5 mm apart, and needs 10 wires.

In [146], the resolution is about 2 mm, with four strain gauges in each element and a polymer bump on top to be able to measure shear forces. The load range is 0–4 N, but overload doesn't damage the sensor.

Ellis et al. [162] measure thin plate deformation with strain gauges to determine the length and weight of a held object, not the pressure distribution. Furthermore, strain gauges configured in Wheatstone bridges are used in tactile sensors in [163] [164].

4.1.2 Elastoresistance

When elastomers show piezoresistance, it is often called elastoresistance. Most, if not all, conductive rubbers show elastoresistive behaviour. These rubbers are composites with some kind of conductive particle in an elastomer matrix. These particles are often graphite or small metal particles. Some of the conductive rubbers are sold as material in pressure switches and show on-off behaviour with a sudden change from a very high to a very low resistance. Others are

produced with the purpose of electric connection between parts to prevent static electricity buildup. Weiß and Wörn [127] studied EVA foam (Ethyl Vinyl Acetate), silicone rubber and PTFE, and concluded that different applications benefit from different materials. The conductivity is usually the result of added carbon blacks. The use of other semiconductive particles such as molybdenum, antimony, ferrous sulfide or carborundum are also described. To manufacture an adequate sensor material, different loadings of particles are mixed and measured in an experimental, iterative process.

There are two possible explanations for the change in resistance: the conductive particles come closer together (i.e. the bulk resistance changes); or the contact between rubber and electrode improves (i.e. the contact resistance with the electrodes changes). The bulk resistance depends on the dimensions of the rubber, the surface resistance depends on the force applied on the rubber. To achieve low sensitivity with conductive rubber, one has to depend on surface resistivity [112]. Holweg [148], [149] assumes that the second explanation dominates. When the sensor material is glued to the electrodes with conductive rubber, the contact resistance is eliminated [127]. The measurement of the load-resistance curve of this situation reveals no significant load dependency of the electrical resistance. This leads to the assumption of the contacting area, which changes under pressure, is the important factor of the working principle. A mathematical model of the contacting process of two nominally flat surfaces [129] allows to derive a relationship between the applied load and the surface resistance [127]. The theorem uses statistical methods to describe the contacts, based on the distribution of the roughness. The sensitivity of the sensor depends on the material of the electrodes (copper results in a higher sensitivity than tin), and the kind of conductive rubber. For hard contact, thicker rubber (2–4 mm) is better [149]. Although the image is blurred, it allows to see the shape of the object. Also the roughness of the rubber is important, since a smooth surface tends to stick to the electrodes, causing hysteresis [127].

The main disadvantages of a conductive rubber material include creep, relaxation, hysteresis, non-linear response, and a large, non-linear temperature dependence [71]. Some additional cited problems are fatigue, low sensitivity and contact noise Howe [42]. Due to the degradation and the non-linearities, elastoresistivity is not suited for accurate absolute force measurements, but it is suited for force distribution measurements, because this distribution is not affected by the non-linearities [148], [149]. A large stress concentration near each impregnated particle is mentioned as an important limitation and a cause of the large hysteresis, the noisy characteristics, the variation in junction resistance with contacting electrodes and non-reproducibility after over-pressure [47]. These features can be difficult to model. The unknown factors in pressure to resistance response, restricts the application of elastoresistive tactile sensors to binary images only. The non-linear behaviour can be an advantage e.g. in collision detection, since for lightweight contacts to its surface the sensor is more sensitive than at high loads – the measurement range is expanded [127]. The advantages are that this measurement principle can offer low cost sensors, which are thin, flexible, compliant [47] and have stable mechanical properties over a large range of temperatures [152] [159]. Due to the simple construction they are in general very robust on overpressure, shock and vibration due to its simple construction [127]. Polyimides (like Kapton) exhibit outstanding

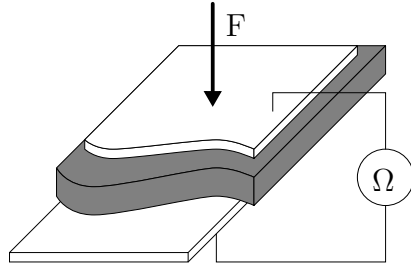


Figure 5: Double sided contact of conductive rubber (adapted from [127])

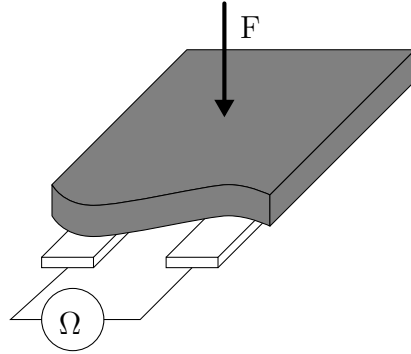


Figure 6: Single sided contact of conductive rubber (adapted from [127])

mechanical, chemical, and thermal properties as a result of their cyclic chain bonding structure [71]. For the application of surgery, the thermal behaviour might be less relevant as the temperature in the body does not change drastically. The modern conductive rubbers are also more homogeneous, which reduces the effect of the individual particles and increases reproducibility. Several empirical characteristic curves have been proposed to describe the effect. Lim and Chong [126] suggest a logarithmic characteristic curve of resistance versus force, following the empirical equation:

$$R = C_2 \exp(-C_1 F) \quad (1)$$

with R : resistance, F applied force, C_1 and C_2 positive constants. Holweg [148] [149] compares the inverse of the force-resistance characteristic with an arctangent function. Weiß and Wörn [127] shows a hyperbolic style characteristic. Non of these are entirely satisfactory for every rubber.

The common way to construct an elastoresistive tactile sensor is to mount the electrodes on both sides of the sensor material (Fig. 5). While contacting the sensor material from both sides, the load has to be applied over the upper electrode. This is unfavourable, since the sensor material is usually flexible, whereby the upper electrode is exposed to a bending stress, which reduces the life time of the sensor [127]. Better is to put the electrodes on the same side (Fig. 6). This is more robust because a single block of sensor material can be used to cover the entire sensor.

There are several ways to measure resistance. An oscillator translates the resistance to a frequency. The voltage can be measured over the resistance while a constant current is applied. The simplest method is to integrate the resistance in a voltage divider. In some configurations, there is a lot of crosstalk between the sensor elements, both mechanical and electrical in nature. [165]

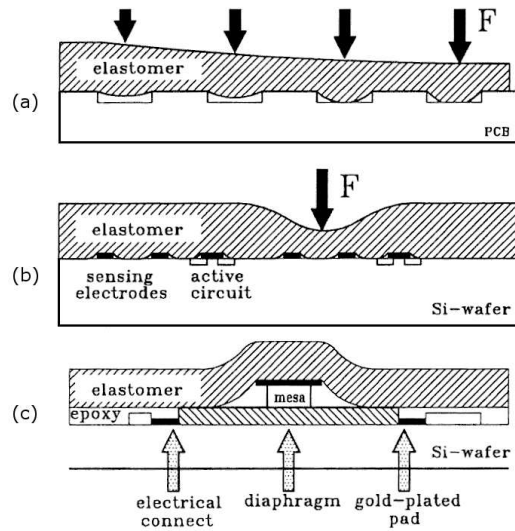


Figure 7: elastoresistive sensors [47]

proposes a solution for this by solving a lot of equations instead of avoiding the crosstalk. The electrodes might be etched immediately on the rubber. This is not possible by direct currentless deposition of copper. After sputtering of a gold layer on the rubber, the currentless deposition is possible [166]. It is important to put an isolating layer on top of the rubber, to prevent leak currents through the measured object. The effect of water absorption by the rubber on elastoresistance is not yet described.

A common way to reduce the number of wires in elastoresistive sensors is to work with a row and column configuration. A specific taxel is selected electronically by connecting the right row and the right column. This reduces the number of wires from N^2 to $2N$. This configuration, however, introduces a lot of crosstalk, since leak currents can flow between unselected rows and columns. There are several techniques to prevent this, Shimojo et al. [138] give an overview. Another way to prevent crosstalk completely is surrounding one electrode completely by the other [152] [159] [149] [130] (Figure 8).

There are several possible configurations for elastoresistive tactile sensors (Figure 7) [47] [167] [168]. A first has conducting rubber covering, but not touching electrodes. If pressure is applied, the contact area increases with the force and the resistance decreases [169]. This sensor has 16×16 elements in 100 mm^2 . D-shaped conductive rubber cords have also been used [170]. They are pressed against electrodes to increase contact surface. Instead of rubber, conductive foam can be used [171]. Another sensor using this principle has a conductive rubber sandwiched between row and column electrodes. Between the bottom electrodes are spacers to prevent contact with the rubber. The output voltage is fed back to other rows (but not columns) to prevent leakage. The tactile sensor has 3×7 elements elements with a resolution of 1.6 mm and a sensitivity of 10 g.

Holweg [148] [149] produced a sensor with 16×16 taxels, 1.375 mm apart. The force range is 0–20 N and scanning time is 4 ms. The rows are connected rings on top of the pcb and the columns are connected on the bottom side with electrodes in the middle of the rings so the elements are electrically isolated (Figure 8).

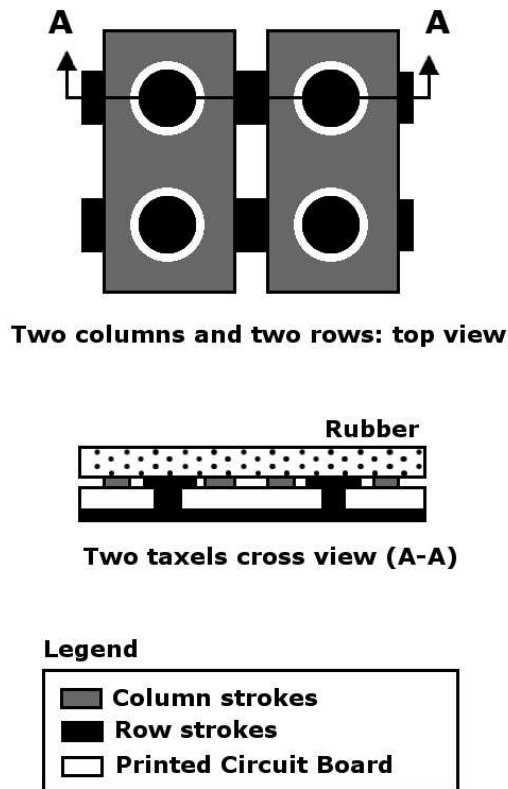


Figure 8: rows and columns of piezoresistive tactile sensor [148]

This configuration was already mentioned in [152] and [159]. The resistance is measured by putting a voltage over a row and a column and measuring the current. Capacitive effects in the cables may cause phantom points in the taxels that are read out immediately after a taxel with a high value.

To measure tangential forces, the rubber is shaped in blocks, each covering 4 taxels. When a lateral force is present, this force can be calculated from the difference between the 4 taxels under the block. A block that is not completely covered will, however, result in a wrong measurement. Thicker rubber results in higher sensitivity to shear forces. The sensor is not able to detect small shear forces.

A tactile sensor by Lim and Chong [126] has 8×8 taxels, with 3 mm resolution, and a zero-force resistance of $0.3 \text{ k}\Omega$. The sensor elements are cubes or cylinders of conductive silicon rubber, glued to electrodes with conductive glue. The transient time is 60 ms and the force range 0.5–9 N.

Shimojo et al. [138] designed a sensor with 64×64 elements with the electrodes on flexible PCBs on both sides of the rubber (Yokohama Rubber Co. Ltd.) with 1 mm resolution. The total thickness is 0.7 mm. Crosstalk is avoided by putting all unused rows and columns to zero. In another sensor [172], instead of putting the rubber on an array of electrodes, they stitched the electrodes (beryllium copper wires, coated with gold) in a woven structure through the rubber. This sensor should be more wear resistant. The resolution is 3 mm. The tension in the wires causes a preload on the rubber. They report limited hysteresis and drift, and a time response of 1 ms. The pressure range in the experiments is 0.6 MPa.

Göger et al. [130] use a flexible PCB based sensor to cover a service robot. They measure the resistance between square electrodes and one common electrode which surrounds all squares, eliminating crosstalk. To reduce the number of wires, they mount the multiplexer circuit directly underneath the sensor. Sampling rate is 12.5 kHz divided by the number of elements. The spatial resolution is 9 mm in the robot arm, 10 mm on its shoulders and 3 mm on the finger.

[173] [174] [175] [176] use two piezoresistive materials coated on fabric to detect position and movement of body parts. The first is polypyrrole (PPy), the second a solution of rubber and micro-dispersed phases of carbon (carbon-loaded rubber, CLR or carbon filled rubber, CFR). The resistance of PPy changes over time because it oxidises, and it has very long (several minutes) response time. These problems can be partially helped with decent coding. CLR also has a rather long response time and hysteresis. No real solution is offered.

Someya [177] built a conformable, flexible, large-area network of pressure and thermal sensors. The skin is bendable down to a 2 mm radius. Thanks to net-shaped structure, the E-skin (electronic artificial skin) can be extended by 25%. They use organic field-effect transistors (OFETs; manufactured on plastic films at low temperatures instead of VLSI - Very Large Scale Integrated circuits [178]). The resolution is 4 mm (with small leakage), while every element has a width of 0.3–0.5 mm. There is no influence of temperature between 30 and 80 °C. Pressure sensors are combined with thermal sensors. The pressure range is 0–3 N/cm² but there is a fairly large variation of the performance of individual transistors. In [179] they present a sensor with 32×32 elements and 2.54 mm resolution. An important downside is the long readout time of 480 ms for a 16×16 sensor. In [178] they discuss an array of sensors with the same resolution that can be cut and paste to form smaller or larger arrays, up to 512×512 sensor elements (sencels). The elements are piezoresistive, with a very slow access time of 23 ms per element, which results in 2 s for the standard 16×16 elements. The resistance of pressure-sensitive conducting rubber rapidly changes from 10 MΩ to 1 kΩ when certain pressure is given. Therefore, the pressure-sensitive rubber is not suitable for an analog circuit, but for digital use.

At PMA, throughout the years, several sensors were built using piezoresistive rubber [159] [166] [180] [39] [120] [119] [152] [181] [137] [182]. In [159], the rows and columns were attached to tape and fastened on both side of the rubber. The binary tactile sensor had a resolution of 1 mm, a sensitivity of 400–500 g, and a scan time of 2.56 ms. It was very robust and both shape recognition and slip detection were implemented.

[166] used pressoduct 105 E conductive rubber from Gummi maag. The pressure-resistance curve was measured to have a strong downward slope. The sensitivity was about 5 mN/mm² and the minimal resolution smaller than 0.5 mm. Linearisation is possible, but the output voltage was fluctuating and not very repeatable. Only three or four pressure levels could be differentiated. [39] claimed that the rubber they used was not suited for low pressures, as it could not detect an object on the tactile sensor that is only pressing with its weight. They made a larger sensor with 32×32 elements.

In this configuration, undesired leak currents flow between electrodes when no countermeasures are taken. In figure 9, it can be seen that, while measuring

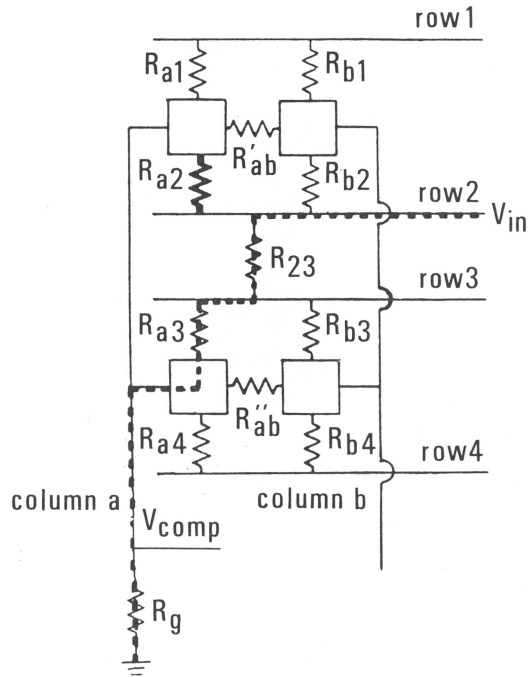


Figure 9: leak current in elastoresistive sensor [120]

the rubber resistance R_{a2} , a leaking current flows from row 2, via resistance R_{23} , the electrode of row 3 and R_{a3} . The resistances R_{23} and R_{a3} can be the same order of magnitude, or even smaller, than R_{a2} . Putting row 3 on the same voltage as column a can prevent this leakage. A similar current flow can occur via R_{b2} and R_{ab} , which can be similarly prevented by a feedback of the voltage from column a to column b. The scheme can be seen in figure 10. There are some other measures that have to be taken [159]. The maximum current through the rubber is 10 mA for 5 minutes. The current followers can give problems with low voltages and currents higher than 10 mA. The input voltage used was 190 mV and they couldn't lower it under 50 mV. Modern operational amplifiers, however, don't necessarily have this problem. The feedback resistors to the rows have to be chosen as high as possible to separate the feedback voltage from the input voltage.

In [119] [120] CS57-7RSC rubber from the Yokohama Rubber Company is used. The spatial resolution is 1.2 mm and can easily be reduced. There are 16×16 cells with 16 distinct pressure levels from 1–50 N/cm², and an acquisition time for 2 times 256 cells of 75 ms. The operating temperature is -30 – 100 °C. The rubber shows minor creep behaviour in and hysteresis. It proves difficult to fixing rigid electrodes to non-rigid rubber material, which compromises the robustness of the sensor. Pressures of more than 10 bar are allowed without damage. It satisfies the design criteria concerning robustness, reliability, compactness, lightness and cheapness.

PCR Technical reports on their CSA (formerly CS57-7RSC) rubber in [183]. The base material is poly-siloxane elastomer (silicone rubber), and the electric conductive particles are artificial graphite. Red ocher (Fe_2O_3) and amorphous silica (SiO_2) are also contained as a small amount of additives. The material is stabilised chemically, and contains neither the residual substances of antioxidants and plasticisers like common rubber products, nor curing agents,

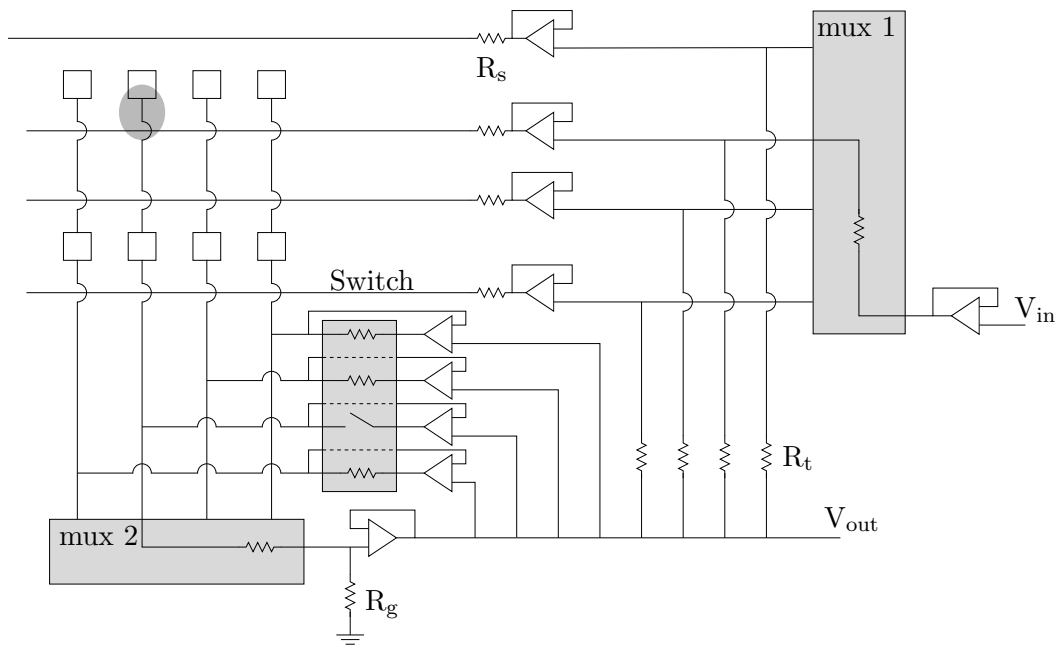


Figure 10: compensation scheme for elastoresistive sensors (adapted from [120])

etc. Moreover, the components of volatile poly-siloxane, which causes the poor contact of electric connections, are carefully removed. Neither permission nor approval has been given to CSA for application to medical treatment at present. In order to prevent oxidation, plating of the electrodes with gold is recommended. Flash plating of about $0.1 \mu\text{m}$ thickness is enough.

Conductive particles don't make contact. Under pressure they do and conduct. It is strain sensitive, rather than position sensitive. Under pressure, there are more contact points between particles, and the contact resistance between particles drops. Due to the viscoelastic behaviour and the fact that the resistance is mainly dependant on the strain, the resistance shows creep and hysteresis. They didn't perform experiments concerning the contact resistance. The fact that the behaviour is strain rather than position dependant, however, suggests that it is indeed the contact resistance which is important.

There are some alternatives to conductive rubber. The following examples aren't really elastoresistive since no elastomer is used. In [184], carbon fibres and carbon felt is sandwiched between metal electrodes. The sensor has only one element, with a sensitivity of 1 g. They withstand very high temperatures and considerable overloads. Compared to conductive elastomers, they have low hysteresis, but sensor noise is a problem at low loads. The carbon fibres have a diameter of $7\text{--}30 \mu\text{m}$. When they are pressed together, the contact surface increases and the contact resistance decreases. The fibres are arranged in felt with the fibres perpendicular. The resistance ranges from 200Ω to very low under high pressure. The carbon fibre has a negative temperature coefficient, but the influence is only a few percent.

Another possibility is pressure sensitive paint or pressistor [152] [159]. The paint is made by mixing piezoresistive semiconductor powders with an organic material. The combination produces a liquid that can be painted onto electrode arrays or used to impregnate porous foam to produce a tactile sensor.

Interlink Electronics use a kind of conductive ink as well [185]. The tactile sensor is based on a conductive polymer film called FSR. The film is deposited with a screening technique, allowing patterned features. Rows on one flexible substrate and columns on another can form a tactile sensor. They also feed the output voltage back to the other columns to eliminate a flow of current between the measured column and the others. It takes about $25 \mu\text{s}$ for the feedback loop to settle.

A disadvantage of a conductive polymer, the patterned FSR doesn't have is in-plane conduction between the rows, which reduces sensitivity. This reduction can be described by

$$\frac{dR_{eff}}{dF} = -\frac{\left(\frac{R_m}{\beta}\right)R_p^2}{(R_m + R_p)^2} \quad (2)$$

with R_m the resistance we want to measure and R_p the in-plane resistance, which is more or less the same magnitude, which leads to a reduction in sensitivity of 4.

They implemented dynamic or variable resolution. By shunting different rows or columns, the resolution can be reduced to decrease the processing time for applications where speed is more important than a detailed tactile image.

Static and dynamic sensors can be combined in one sensor [57]. The static sensor is based on semi-conductive ink and produced by Interlink Electronics. It has a force range between 50 mN and 10 N. On one element the size of the force and the position in one dimension can be measured. Two elements are combined to have a two-dimensional position, but no pressure distribution measurement is possible. The static elements are surrounded by 16 dynamic sensors. These are capacitive with fibers on one of the plates to sense contact. Hesel et al. [186] built a one dimensional tactile sensor with a conductive fluid under a membrane and an array of electrodes on the bottom. An AC voltage is put over the liquid and the voltage between each electrode is measured and thus the resistivity, which is dependent on the indentation of the membrane between the concerning electrodes. This is an example of purely geometrical piezoresistivity. The resolution is less than 1 mm.

A block of pure carbon nanotubes also exhibits piezoresistive behaviour [187] [188]. The tubes buckle, resulting in a larger interconnectivity and a decreased resistance. Some advantages are supercompressibility, resilience, and large elastic modulus of carbon nanotubes. These kind of multiwalled carbon nanotube brushes can also be embedded in a polymer like PMDS [189]. This results in a flexible skin with a pattern of aligned nanotubes. The resistance of these patterns is very sensitive to pressure and the skin can be used as a pressure sensor.

4.1.3 Percolation theory

The start of percolation theory is associated with a 1957 publication of Broadbent and Hammersley which introduced the name [190]. The term originally denotes the slow movement of a liquid through a porous substance or small holes, such as hot water through a coffee filter. A more general interpretation is the connectivity of statistically spread entities in a medium. Some examples of percolation theory include the gelation of polymers, the boiling of an egg, forest fires, the connectivity between oil patches (near the percolation threshold,

the size of clusters increases with a fractal dimension comparable to the size of the whole: 2.5), the diffusion in porous material (normal random walk: $radius = \sqrt{time}$; near the percolation threshold: $radius = \sqrt[3]{time} \rightarrow$ fractal), the spread of a disease in an orchard, resistance networks or the spontaneous magnetisation above a critical concentration in a dilute ferromagnet [190] ([191], Chapter 6).

Percolation theory is relevant to the elastoresistive behaviour of conductive rubbers, as a certain percentage of the volume of these rubbers is conductive and the rest is not. A conductive rubber is in fact a resistance network, which changes under pressure (Fig. 12). Percolation theory describes which volume of particles is needed to have a conductivity path. This volume fraction is the percolation threshold. Below the threshold, there is no conductivity. Above the threshold, conductivity rises as the number of paths increases; the resistivity network becomes denser. The theoretical value for the percolation threshold in a three-dimensional continuum is $16 \pm 2\%$ [192]. Theoretically, the location or size of the electrodes on the rubber should not influence the percolation threshold, since in a continuous medium it is fixed no matter what the geometry. The electrodes can have an effect on the magnitude of the resistance, as in any conductor.

For infinite networks the conductivity σ is zero below the percolation threshold, and proportional to $(p - p_c)^\mu$ above percolation threshold [190] [193]. μ is the conductivity exponent and p_c is the percolation threshold. In [194] the percolation threshold is studied for conductive fibres in solid plastic. Close to the percolation threshold, the resistivity can change drastically by several orders of magnitude for small variations of conductive solid content. At high loading of conductive solid, the increasing number of conducting paths forms a three dimensional network. In this range, the resistivity is low and less sensitive to small changes in volume fraction of conductive solids. At the range, where the concentration of conductive solid particles is higher than but close to the percolation threshold, these composite solids exhibit piezoresistivity.

Elastoresistive materials are composites with the following characteristics: conductive particles uniformly dispersed into an elastic matrix; the particle content is near the percolation threshold so that a small decrease of sample volume can give an abrupt increase in conductivity [195]. In ideal conditions the effect should be reversible due to the material elasticity. A problem is that rubber has a Poisson coefficient close to 0.5 and it is not the volume fraction that changes, but the configuration of the particles. Some conductive elastomer materials are very porous or even foams, and the air gaps that separate the particles can be closed under pressure.

Lanotte et al. [195] consider an elastic material (silicone) in which conductive particles (nickel) are uniformly dispersed. If d is the average particle size and the sample has cubic shape of side 1, consider the sample divided into cubic cells of side $d \ll 1$ and that each cell may be occupied or not by a particle with the probability increasing with the particles content in the sample. As $V\%$ increases the probability of a direct conduction path between opposite sample sides changes from 0 to 1. There is a threshold value at which these paths suddenly emerge. This is called the (site) percolation threshold. Lanotte expects this threshold to be between $1/8$ and $1/4$.

The percolation threshold for nickel particles in silicone is experimentally found

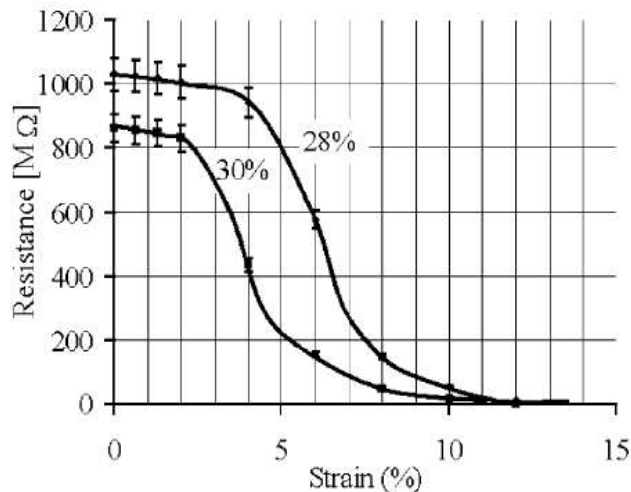


Figure 11: Piezoresistance for different V% [196]

to be 18%[195]. This hints at a simulation with hexagonal connectivity. When compressed, the effective V% increases, due to the larger stiffness of the conducting particles. The conductivity of a compressed sample is lower than of an uncompressed sample with the same effective V%. For a carbon black/polyethylene composite, the percolation threshold was also found to be between 17 and 17.5% [146], with $\mu = 2.9$. As temperature rises, conductivity decreases, and even drops below the percolation threshold. The reason is probably that the carbon black has a smaller thermal expansion coefficient than polyethylene. Beruto et al. [196] use graphite powder of micrometre size in a silicone matrix (production method included). They measured the properties of the rubber in a micrometer with a load cell and a multimeter connected to both sides of the elastomer. The percolation threshold was about 31 V%, which hints at a simulation with orthogonal connectivity. The electric resistance of the composite, charged a little beyond the percolation threshold, is also strain dependent, according to an equation of the type

$$R = R_0 \exp(\beta \epsilon) \quad (3)$$

β was found to be 51.5. This value corresponds to a very high electric sensitivity of the material to an applied strain and makes it a candidate for application as a logarithmic strain transducer. Figure 11 shows the strain-resistance characteristic for two different mixtures.

The stiffness of the composite increases up to 30 V%. after that it decreases, possibly due to an increased porosity caused by an increased viscosity and thus more difficult mixing. The stress-strain response is visco-elastic with a relaxation time of about 2s. As far as strain is concerned, the response is one-to-one, and can easily be linearised by coupling a logarithmic operational circuit in the acquisition chain.

Influence of particle shape It is difficult to determine the connectivity of the conductive particles as they generally have neither a fixed shape nor a fixed size. This makes it hard, if not impossible, to predict the percolation threshold. Even if the shape and size is controlled, a different size has a very large influence. Round particles need a high V%, and the piezoresistance

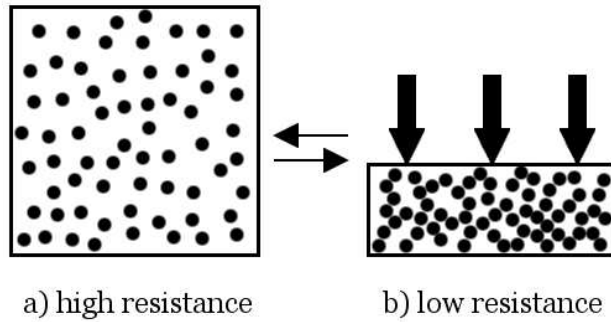


Figure 12: Principle of percolation in elastoresistance

is probably less. Very long particles require only a very small $V\%$ to form conductive paths. In nanotubes/polymer composites the percolation threshold occurs at 0.055 weight % (0.029 $V\%$), with $\mu = 1.36$ [193]. They do not mention piezoresistance. The higher the aspect ratio of the conductive particles, the lower p_c . For economic reasons, the achievement of extremely low percolation thresholds is important.

The expansion or movement of one phase with respect to the other is not equivalent to changing the volume fraction by varying the volume ratio of the two phases. Taya et al. [197] [191] show that an initially electrically conductive short fibre composite can become less conductive as straining increases, and even non-conductive above a critical strain. This is mainly due to the reorientation of the conductive fibres upon straining. Something similar was found in [194]. During compression the resistivity at first drops a little bit and then increases strongly. For tensile stress, the resistivity just increased. The sensitivity of piezoresistive effect of the composite depends on the elastic properties of the matrix material and on whether the applied loading is hydrostatic or uniaxial [194]. In any case is the volume fraction important: too high and there is always a high conductivity, too low and the resistance stays high.

Electron Tunnelling Sett [194] developed an analytical model to describe the effect by combining the principle of percolation theory and continuum mechanics. Taya et al. [197] [191] propose an analytical model with hard fibres and a tunnelling layer around those fibres in which tunnelling of electrodes is possible. In these composites any deformation related to a change of the total volume gives a variation of the average distance among the particles. This distance change can change the passage between a status of isolated particles, for which only the tunnelling of the electrons can occur as conduction mechanism, and a status of particles in reciprocal contact, so that a great change of electric conductivity is governed by deformation [195]. If there is isolating material between the conductive particles, however, it is likely to stay between the particles and is only compressed. Possibly, electron tunnelling plays an important role in elastoresistance. As particles come closer together, the tunnelling barrier decreases and the resistance drops. An example are nanotubes/polymer composites where each nanotube is probably coated with polymer which acts as a potential barrier to internanotube hopping. It is likely that electrical conductivity in this system is limited by tunnelling between conductive regions [193]. This tunnelling is temperature dependant. Due to

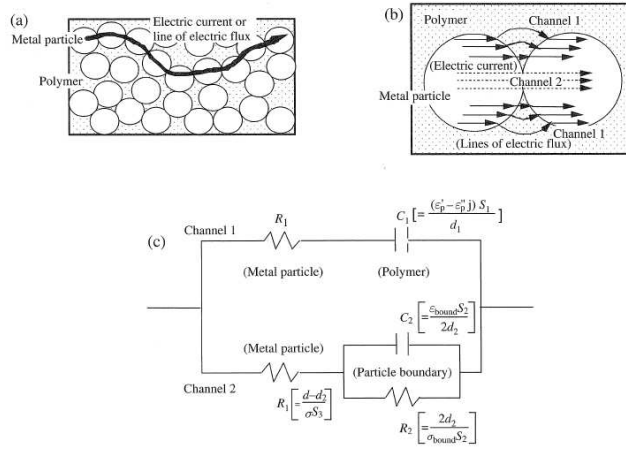


Figure 13: Electrical model for composite with metal particles in a polymer matrix [191]

tunnelling, which occurs gradually, the percolation threshold might not be infinitely hard.

It is possible to grow nanotubes in bristles directly on the electrodes. The elastomer could then be molded over the bristles.

Piezocapacitive Effect AC-current through a composite with conductive particles exposes a combination of resistances and capacitance between the particles [191] (chapter 2, Matsumoto and Miyata references). In low weight percentage materials, there is no DC conductance but there is conductance in AC, depending on the frequency and the gap between the particles. For low volume fractions (10–20%) of particles the complex permittivity of metal particle/composite matrix composites is proportional to that of the polymer matrix: $\epsilon_c = k\epsilon_p$, with k related to the volume fraction. For high volume fractions (55–60%) the experimental data is approximated by $\epsilon_c = k_1\epsilon_p + F(f)$ with $F(f)$ depending on the frequency f (Fig. 13).

Carbon microcoils in a silicone rubber matrix have a percolation threshold of 3 weight % [198]. The phase angle goes from -90° to 0° and the impedance stops being frequency dependant. Below the percolation threshold, the composite behaves as pure silicone rubber, with capacitance dominating, above, resistance dominates. The inductance of the microcoils is negligible. These rubbers enable tactile sensing, due to changing R, C or L under an applied load. Also in nanotubes/polymer composites is an increase in conductivity measured when the frequency rises [193].

This could be interesting since pressure reduces the gap between particles and thus the capacitance. Simple experiments confirm a change in the capacitance under pressure with an AC signal. Mostly the amplitude decreases under increasing load, and in some rubbers it increases again if the load increases further. Different conductive rubbers behave differently. Possibly, the capacitance rises first, because particles get closer together, and then it lowers again because more particles get close enough to conduct.

Miscellaneous Carbon black (soot), and other particles can be difficult to mix through the rubber, inhomogeneous mixtures are generally much less

interesting. The resistance of rubbers is used to measure the degree of mixture. An idea to soften the steep percolation curve, however, is to gradually change the volume fraction of the rubber over its thickness. A similar effect might be produced by building a material with different layers with different particle densities.

Switch-like behaviour due to a steep percolation threshold might be somewhat stretched by combining spherical and short fiber conductive particles.

A lot of rubber manufacturers work with experimental recipes without knowing how it really works. In Nantes in France, there is a training centre for rubber manufacturers with a lot of knowledge and literature.

4.1.4 Dynamic Behaviour of (filled) Rubber

Rubber has all kinds of annoying dynamic behaviour that changes over time such as hysteresis, relaxation and creep. Doing the same experiment twice can yield different results and doing it again the next day might give the original results again. Some of the characteristics can be described by the complex Young's modulus [199].

$$E_{dynamic} = E' + iE'' \quad (4)$$

with E' the conservative and E'' the loss component. $E'' = E' \tan \delta$ is out of phase, which results in hysteresis. The change of both components of the Young's modulus in black carbon filled rubber (e.g. car tires) are described for different frequencies, temperatures and strains.

Chapter 11 of [200] describes the mechanical properties of rubbers some more. There is a temperature dependent frequency $f(T)$, and a time scale $t(T) = 1/f(T)$, such that at frequencies higher than f the system is elastic and for lower frequencies it is viscous when one works at the time scale of the experiment.

E , B and ν are functions of both the temperature and frequency (rate) of measurement. They are often treated as complex (dynamic) properties. The real portion quantifies the energy which is reversibly stored by the 'elastic' component of the deformation. The imaginary portion quantifies the energy lost (dissipated) by the 'viscous' component of the deformation. the complex Young's modulus $E^* \equiv E' - iE''$ and $\tan \delta_E \equiv E''/E'$.

The definitive identification of these interrelationships and differences, and their embodiment in simple and reliable predictive equations, are areas of ongoing research in fundamental polymer physics.

A general theoretical model of the stress-strain curve (only for stretch, not for compression) all the way is:

$$\sigma \approx G \frac{\sqrt{n}}{3} \left[\mathcal{L}^{-1} \left(\frac{\lambda}{\sqrt{n}} \right) - \lambda^{-3/2} \mathcal{L}^{-1} \left(\frac{1}{\sqrt{n\lambda}} \right) \right] \quad (5)$$

with $n =$ the number of Kuhn segments (average number of statistical chain segments between the entanglement junctions), λ the extension or draw ratio (the length of the deformed specimen divided by the length of the initial undeformed specimen). \mathcal{L}^{-1} is the inverse Langevin function, which is transcendental and defined by

$$\mathcal{L}^{-1} = \left[\coth(x) - \frac{1}{x} \right]^{-1} \quad (6)$$

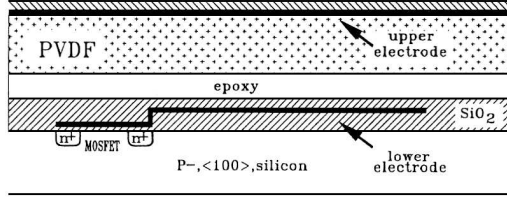


Figure 14: Piezoelectric sensor [47]

and can be estimated with a Padé approximant:

$$\mathcal{L}^{-1} \approx x \frac{3 - x^2}{1 - x^2} \quad (7)$$

which gives:

$$\sigma \approx G \left[\frac{\lambda}{3} \left(\frac{3n - \lambda^2}{n - \lambda^2} \right) - \frac{1}{3\lambda^2} \left(\frac{3n\lambda - 1}{n\lambda - 1} \right) \right] \quad (8)$$

A simpler expression for small strains is:

$$\sigma \approx G \left(\lambda - \frac{1}{\lambda^2} \right) \quad (9)$$

4.2 Piezoelectricity

Some materials, like quartz or polarised ceramics produce an electric charge when a force is applied. They are generally brittle and it is hard to give the desired shape. Piezoelectric polymers like Polyvinylidene Fluoride (PVDF or PVF2) are often used in tactile sensors (Figure 14) that are small, flexible, sensitive and have a large electrical output [152] [159] [201]. PVDF is relatively strong piezoelectric, inexpensive, commercially available in thin flexible sheets, durable and rugged. It is used in medical ultrasonic imaging systems. An important limitation is the sensitivity to temperature or pyroelectricity. Inside the human body this might not be a big problem because the temperature is more or less constant. Another limitation is that only dynamic loads can be detected, because the electric signal decays in milliseconds [47] [57] [201] [112]. The sensitivity is 13 mN/mm^2 , the output linear, and the resolution can be smaller than 0.5 mm [202]. The creep is low, but it suffers from a pyro-electric effect [201].

Because of this fast decay, Howe and Cutkosky [132] use PVDF as a stress rate sensor. They connected a PVDF film to a current to voltage amplifier to read out changes in piezoelectric charge and thus changes in the pressure applied on the film. The single point sensor has to be moved over a surface to feel small features like the free end of a roll of tape that has become reattached to the roll. It can sense ridges only $6.5 \mu\text{m}$ high.

Sedeghati et al. [203] designed a single element sensor with a hard inner cylinder and a soft outer cylinder to measure both force and elasticity. Domenici and De Rossi [204] designed a single point, multi component sensor to sense different components of the stress tensor, like the shear stress. The piezoelectric tactile sensor array of Dargahi [205] has a high force sensitivity, a large bandwidth and good linearity. It is 15 mm long, has four elements, with 3 mm spacing,

and a linear response from 0.1–2.0 N. The sensor is mounted on a laparoscopic grasper. All these sensors use PVDF as piezoelectric material. An important disadvantage of this material is the absence of DC [205]. In [157] they use seven elements with 2 mm spacing to compress tissue with hard lumps inside. They derive position and size from this small amount of data.

Krishna and Rajanna [142] developed a 15×15 element sensor with about 1 mm spacing. Electrode strips are applied perpendicular to both sides of a PZT disk. The elements consist of the intersection of these electrode strips and the PZT material in between. Applying pressure on the material changes the resonance frequency, and this change can be measured. There is a lot of hysteresis, crosstalk and low sensitivity.

[201] describes a sensor containing two force sensing layers and has the additional capacity of sensing thermal properties. The sensing sensor structure comprises a deep sensing layer, a relatively thick, intermediate compliant layer, and a superficial thin sensing layer. The dermal sensor consists of a 5×7 array of sensor elements spaced 5 mm apart and the epidermal layer contains seven elements arranged in a hexagon.

The piezoelectric strain coefficient of dry human skin is 0.02 pC/N [206].

4.3 Capacitive sensing (piezocapacitance)

Capacitive sensors are often used to measure small displacements very accurately. Combined with an elastomer between the metal plates of the condenser, you get a very simple and cheap force sensor. They can have low drift and a high reproducibility [127]. The properties of the sensor, are governed by the deformable elastic material between the capacitor plates [207]. A simple way to make an array is to put a layer of metal strips on either side of an elastomer, perpendicular to each other. One of the layers consists of the drive lines and the other consists of the sense lines. At any moment in time only one drive and one sense line is active, to read out a single element.

The changes in capacitance are in the range of femto farads which is very difficult to detect, therefore a complex signal conditioning electronic is needed [127]. Due to the required high sensitivity of the electronics, capacitive sensor systems in general are very susceptible to electromagnetic interferences [112]. An technique that integrates a capacitive tactile matrix into a single chip with the signal conditioning, greatly improves the interference robustness [127]. Capacitive sensing is also strongly materials-dependant [112]. The already small and difficult to measure capacitance is a problem for the miniaturisation of the sensor. Then the influence of crosstalk and stray capacitance increases. Stray capacity is a major problem, because it can reach the order of magnitude of the measured capacity [57]. The capacity between two plates of 1 mm² and 1 mm apart is

$$C = \varepsilon_r \varepsilon_0 \frac{A}{d} \approx 10^{-14} \quad (10)$$

with $\varepsilon_r \approx 1 - 8$ the relative permittivity or dielectrical constant, $\varepsilon_0 = 8.8510^{-12}$ the permittivity of vacuum, A the surface and d the distance. In [208] electronics for capacitance with a high accuracy, and low power consumption are described. A potential problem with capacitive air gap sensors is pull-in under DC bias, where the electrostatic force pulling together the plates is

larger than the restoring forces. With micromachined polysilicon plates, this is particularly detrimental since irreparable stiction or welding of the plates may result [209]. Some advantages of capacitive sensors are that they can easily be adapted to cylindrical and hemispherical configurations they are ease and cheap to fabricate and the scalability [26].

Silicon IC technology can be used, both for resistive and for capacitive readout circuits [47]. A resistive sensor uses integrated strain gauges on a bending site of a silicon membrane and it measures stresses in this membrane caused by an applied force. A capacitive tactile sensor is based on the detection of the alternating capacitance between a silicon membrane and the silicon substrate under an applied load. Performance of silicon sensor structures is better than rubber based structures with respect to fabrication, sensing characteristics and the possibility to integrate the sensor with a readout circuit. Also printed-circuit board (PCB) technology can be used to produce capacitive sensors [210].

Comparison of silicon based piezoresistive and capacitive sensors: piezoresistive sensors have a lower sensitivity to pressure, and a higher sensitivity to temperature. They also require an extra mask and metallisation very close to the sensing parts to interconnect the sensor. The surface-micromachining processing is simpler for capacitive sensors.

Fearing [211] gives an elaborate discussion about how to make capacitive tactile sensors and even has a construction guide on his site. The sensor has 8×12 elements around a 25.4 mm diameter cylinder with 3.3 mm spacing. With a thick layer of elastomer (3.2 mm) on top of the capacitive sensor, the impulse localisation is only 0.2 tactile. For more complicated signals this layer acts as a low-pass filter and decreases the gain. Because of the stiffness of the copper wires used, the resolution around the circumference is reduced. To reduce crosstalk, the rows and columns not scanned are put on ground potential. The nominal capacitance is about 1 pF for a dielectric constant of about 4, and the sensitivity is 5 mN/element with an accuracy of 20%. The scanning frequency is 7 Hz. Gray and Fearing [209] describe a microtactile capacitive sensor with 8×8 elements and a spatial resolution of 0.1 mm. The behaviour with a rubber layer on top is quite linear between $20 \mu\text{N}$ and 1.8 mN, but large hysteresis renders the sensor impractical for application. This design with crossed copper strips separated by strips of silicone rubber is followed by Howe et al. [25] [144] [212]. Their sensor is thin and compliant and has 8×8 force sensitive elements with 2 mm spacing. The readout time for the entire sensor is 5 ms. The force range is over 2 N/element with a noise level of 0.001 N. A thin rubber layer is used over the sensor, because a thick layer makes it difficult to interpret the signal.

Another capacitive tactile sensor, based on Fearing's design is produced to examine the human tactile sense. It has 8×8 elements [118]. The spatial resolution is 2 mm. The sensor is covered with a 2 mm layer of elastomer, and shielded from outside influences with a rigid back plane and a thin gold layer imbedded in the elastomer. A 200 kHz sine wave on the column scans the sensor. All unused rows and columns are grounded to reduce crosstalk. The noise level is 0.5 kPa (1.2 g per element), and the crosstalk less than 8%.

Another sensor with 3×16 elements on a cylinder with 16 mm diameter is described in [213]. Moy [26] designed a sensor with 4×8 elements, of which

4×6 are used. The spacing is 2.7 mm, the frequency range 100 Hz and the force range 1.1 N/sensor element. The capacitive sensor built with silicon IC technology by Wolffenbuttel [47] has a spatial resolution of 0.5–0.7 mm and can detect a surface profile down to 1 μm . Forces between 0.1–0.5 mN are detected with 6 bit resolution. The capacitance varies from 2 pF to 4 pF. The capacitive sensor described in [214] has a higher range and sensitivity because of a curved surface and good electronics to measure the capacitance.

[207] have described a tactile sensor which uses an injection-molded silicone rubber honeycomb material to form the dielectric between upper and lower electrodes. An outer conducting elastic skin physically protects the capacitors and screens them from outside electric fields. The upper column electrodes are plated on a Mylar sheet. The sensor consists of an 8×8 array of sensor points with 1.9 mm spacing formed into a cylinder. Capacitive sensor arrays can be molded to conform to curved parts and provide very accurate measurements of skin deflection.

[215] produced a tactile element with superelastic carbon microcoils. The tactile element has a size of 80×80×80 μm^3 with a sensitivity of 1 Pa, and a response time of 1 ms. The capacitance changes logarithmically with the load. Continuously applied stresses for 24 s results in a continuous and a constant strength in the output lines.

Finally, Voyles et al. [216] describe an electrorheological sensor and dual 'inside-out' display. The sensor is a combined intrinsic and extrinsic sensor. The intrinsic sensor is a strain gauge sensor to measure force/torque, based on [217] and calibrated with [218]. The extrinsic sensor uses the ERG (Electrorheological Gel) as a dielectric for capacitive sensing. Problems to this approach are that it's hard to know force from displacement since it's not a Newtonian but a Bingham fluid under excitation, the gel can move and does not return to any known state and it tends to sag in the gravity field. Another option is to measure the pressure with pressure sensors, because an ERG does not have a uniform pressure, but the exact behaviour is difficult to model. Both compressive and shear pressures might be measured.

4.4 Optics

Optical tactile sensors include a lot of different approaches, all of them using light in some way. The advantage of approaches that use fibres to connect readout and sensor is that they are very insensitive against corrosion and electromagnetic disturbances [127]. A simple opto-electronic approach employs an elastic layer with a reflective surface [219]. Light is directed through a bundle of glass fibres. A contact force deflects the elastic layer and changes the distance between the reflective surface and the fibres. Instead of a reflective surface, a white silicone rubber layer is used in [163], and deflection of the rubber changes the intensity of the reflected light. This sensor has 330 sensitive spots per cm^2 , but large optical fiber makes it heavy and bulky. Nomura et al. [220] describe a 15×15 element array with 2 mm spatial resolution that avoids needing a fibre for each element. LED's and photo detectors are arranged on different transparent layers, one for each taxel. The top layer is again reflective. The accuracy is 5% of the maximum 500 g/ cm^2 or 20 g/taxel. It takes 100 ms to scan one frame.

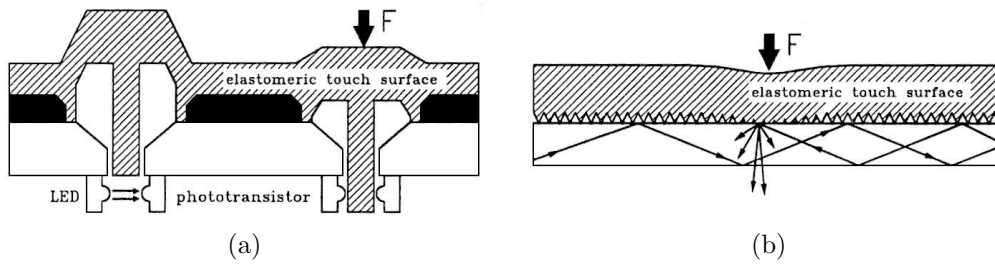


Figure 15: Optical sensors [131] [47]

Other optical tactile sensors use obstruction of light. In such a configuration, a load on a touch-sensitive surface is transduced into a displacement of an elongated pin, which extends the lower surface of the elastic structure [131] (Figure 15(a); concept from [221]). The pin blocks the beam of light between a led and a phototransistor. The Lord LTS-100 tactile sensor has 8×8 elements, with a resolution of 7.6 mm. A similar sensor has 10×16 elements with 1.8 mm spacing. In another sensor a fiber array is used and on each point a pin under pressure can block the light of one fibre [222]. The application is sound detection, which requires the switching time to be very fast because it has to be above the sampling frequency of audible sound. The spatial resolution is very coarse: 100 mm. A similar design is described by Allen [223] where the fibres are separated and pressing a metal pin causes misalignment of the fibre endings. This misalignment results in a measurable intensity decrease. The sensor has 16×16 elements, 2.54 mm resolution and a force range of 1–100 g per taxel or 0.16–16 kPa.

A third optical principle that can be used is changing the internal reflection (Figure 15(b)). In [224], light is transmitted trough the side of a glass plate. The light stays inside because there is total internal reflection. An elastomer is separated from the glass with an air gap. When forces apply on the elastomer, it makes contact with the glass plate and the high refractive index of the elastomer results in a scattering of rays and no longer total internal reflection. The scattered light can be captured on the other side of the glass. Hysteresis is caused by the rubber layer sticking to the glass after contact. The sensor has a thickness of 10 mm. In [225] a clear acrylic plate is used instead of glass. The scattered light is captured on a CCD with 64×64 elements. Begej [226] a 32×32 element tactile sensor for mounting on a parallel-jaw gripper and a sensor with the size and shape of a human fingertip for a dexterous robotic hand with 256 taxels. The same principle is used, but this time the light is conveyed to a CCD camera with optical fibres. In [151], the tactile sensing element consists of a photo-reflector covered by urethane foam. Fiber-optic cables are used to irradiate the foam. The light is scattered by the urethane foam upon deformation. The photo-reflector used has a size of 3.2 by 1.7 by 1.1 mm. It is a large-area conformable sensor. The output is nonlinear with high hysteresis. [227] uses the same principle in a finger shaped sensor to detect the contact location and the direction of the normal of the contact surface. A hemispherical shell of glass is the optical waveguide. the light stays in the glass due to total internal reflection. An elastic shell around it can be pressed against the waveguide and disturb the total internal reflection. Light is shattered and can be detected on a CCD camera. Since the shape of the

sensor is known and the object is rigid, the normal of the object depends only on the contact location. For miniaturisation a position sensitive detector is used instead of a CCD, because of its smaller size. A fibre optic plate guides the image from the waveguide to the detector. The diameter of the sensor is 32 mm, the length 60 mm. The position accuracy is 1–2 mm. Another sensor with the same principle is described in [228]. Finally in [229], silicon pyramids are pressed against an acrylic plate to achieve the same. The spatial resolution is 1 mm and the force range is 0.1 N/mm² to 0.0001 N/mm². The application here is the measurement of lip pressure of people with very long faces before surgical correction. The light is captured with single use light sensitive film. Some other sensors are based on the influence of bending on optical fibres. This is an internal effect, so these sensors have the advantage to be less sensitive to contamination or misalignment. In [230] four layers of fibres are placed perpendicular on top of each other, so that under pressure the fibres in second and third layer are bent between two layers. There are 6×5 elements with 2 mm spacing and the force range is 0–4 N with an uncertainty of 0.05 N and a resolution 0.002 N. In [231] a fibre loop is used. There is a loss of light when the loop is bent upon contact. It is however hard to miniaturise and put in an array. Also calibration is difficult. Fibre Bragg grating is another very useful technique to use [232]. A grating in the fibre ($\pm 250 \mu\text{m}$) reflects a narrow band of the wavelength. By detecting the shift in this reflected wavelength, bending or stretching of the fibre can be detected. Different gratings reflect different wavelengths and can thus be applied to the same fibre. This results in a large reduction of fibres needed. The sensor is flexible and has 3×3 elements with 5 mm spacing. The force resolution is 0.001 N and the accuracy 99.9%. The sensor array in [233] is based on a matrix of optical fibres in perpendicular rows and columns, separated by an elastomeric pad. The magnitude of the force applied is measured by a change in transmitted light coupling across the elastomer between the fibres. Eghtedari and Morgan [234] use a photoelastic layer in a binary sensor with 256×128 elements. The layer changes the polarity of the polarised light when put under pressure and causes a phase shift. The outgoing light goes again through a polariser and is captured by DRAM. A similar principle is used by [133]. Some other optical principles that might one day be used are Laser interference and thin plate interference (Newtonian rings).

4.5 Electromagnetic induction

Inductive sensors are large, more suited for force/torque sensors [57]. A tactile sensor based on magnetic induction detects either changes in the magnitude or in the orientation of a magnetic field [47]. One example is a rather bulky magnetic sensor that detects the change in orientation of magnetic flux under applied load. The spatial resolution is 2–3 mm and thickness is typically 8 mm [235]. [236] describes some needle based tactile sensors, where an array of rods slide through a guide. The position of those rods is then measured in several ways, e.g. LVDTs.

Similarly to elastoresistance, instead of conductive particles, magnetic particles could be embedded in rubber/foam. Small hall-sensors under the rubber can detect pressure on the rubber.

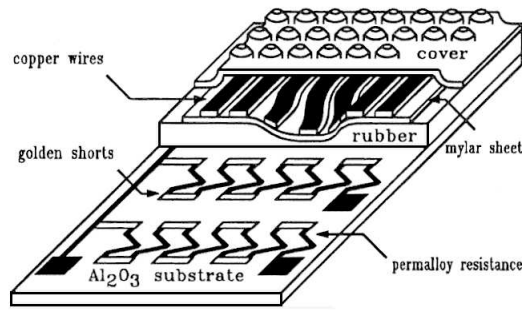


Figure 16: Magneto-resistive sensor [47]

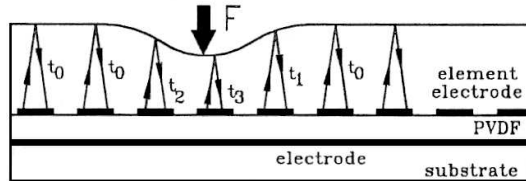


Figure 17: Ultrasonic sensor [47]

4.6 Magneto-resistance

Vranish [237] uses the sensitivity of permalloy resistors to changes in the magnitude of magnetic fields under an applied load (Figure 16). Copper strips provide the magnetic field, which increases at the permalloy resistors when the copper strips are pressed down. The tactile sensor has 8×8 elements with 2.5 mm spacing. Another sensor using this technique is a single point sensor sensitive to lateral displacement [238]. Because a DC magnetic field causes hysteresis, an AC magnetic field is used. The waveform is still polluted, but the amplitude is not affected.

Magnetic dipoles (vicalloy:Co,V,Fe; chromidur:Cr,Fe,Co) can be embedded in an elastic layer [159]. Under this layer are magneto-resistive sensors, that transduce the change in the electric field into a change in resistance. The magnetic layer suffers from interference from external fields. The tactile sensor has 7×7 elements, a small force range, a brittle layer, small hysteresis, low cost, and is easy to fabricate. The sensitivity is 2.5 g and the resolution 1–2 mm. In [239], this principle is used to built a 2×2 element prototype of a shear-sensitive tactile sensor.

4.7 Ultrasound:

There are different ways of using ultrasound to measure tactile stimuli. The first is the only one really measuring the surface, while the others measure deeper tissue. In general PVDF is used for both transmitters and receivers of ultrasound.

In a first sensor consists mainly of an elastomer layer that is deformed under a pressure distribution. The local thickness of this layer is evaluated from the time span of an ultrasonic pulse that is needed to cross an elastomer layer and to return to the transmitter [240] (Figure 17).

Böse et al. [241] want to use ultrasonic elastography as a means to get tactile

information. Instead of direct tactile information, the stiffness information of the tissue is measured and translated into tactile information for the display. They have not accomplished it yet.

Elastography is an imaging technique based on strain estimation in soft tissues under quasi-static compression. The stress is usually created by a compression plate, and the target is imaged by an ultrasonic linear array. This configuration is used for breast elastography, and has been investigated both theoretically and experimentally. Phenomena such as strain decay with tissue depth and strain concentrations have been reported. In vivo plates cannot be used, but inflated balloons in e.g. the rectal cavity are possible [242]. From the strain image a model of the Young modulus can iteratively be built [243] [244] [245] [246] [247].

4.8 Electro-optical:

In the tactile sensor described by Maheshwari and Saraf [123], a dielectric barrier separates conductive nanolayers. By pressing the layers together, electrons can tunnel through the barrier and this current causes localised electroluminescent light. This light is then captured on a CCD. The resolution is about 20–40 μm and the sensitivity about 10 kPa or 0.01 N/mm². No load above 90 kPa is mentioned. The described sensor is flat and rigid, but authors suggest complex shapes are possible because of easy fabrication.

5 Displays

The design of a tactile display for robot assisted surgery is a big challenge. Different requirements are hard to be met simultaneously. Conflicting requirements are resolution, frequency and force. Another problem is the actuator size [26]. A lot of physical principles have been used already in attempts to accomplish this, but none have really succeeded. Most existing systems are cumbersome, bulky, expensive, and often focused on the optimisation of one single feature [108].

The difference between information for sensory substitution or information during surgery is important. A blind person for example, is trained to interpret the information given by a braille display. The aim of these displays is to give some kind of information, not necessarily realistic tactile information. The same is the case for tactile displays in steering wheels of cars, in military clothing... even in robot manipulation or virtual reality, the aim is to get information. In [48] direct sensory substitution is defined as opposed to symbolic sensory substitution. The former gives the same input as a real system, the later gives a symbolic input that can be understood when trained.

For some applications, a vibrotactile display can give a lot of tactile information, without the need for an array. It can convey e.g. the moment of touching a hard object. In a lot of inspection tasks, like searching for loose parts or texture inspection, one point of vibration information may suffice [99]. In some applications where frequency information is important, a uniform vibration of the entire display can very easily be added to a shape display.

A surgeon doesn't want information he has to interpret. He has to be able to do what he would do in open surgery, without having to worry about interpreting information. Most surgeons won't use a system if he has to train to use it. If it feels natural, the surgeon will trust it and be able to fully concentrate on the medical aspects of the operation. For the same reason it's not advised to scale the tactile image. Though this may provide a better spatial and/or force resolution [117]. It's also important that the passive sensation of pins pressing in the skin is the same as the active sensation of the vinger pressing on the pins. According to research conducted by Lamotte [257] softness discrimination is the same in both situations.

There are different possible approaches to display tactile information. The display may control displacement, to match the strain experienced by the sensor, or the forces, to match the sensed stress [26]. Another approach is to use lateral skin stretch or electrical stimulation to simulate the tactile sensation. When displaying shape, it is not always necessary to display the absolute measured shape. Kinaesthetic feedback can take care of the spatial 'DC' signal. A reference position can be subtracted from all the pins in the display [212]. The same is of course true for displaying force.

To feel a smooth contact instead of pins an elastic layer, acting as a low pass filter is essential [26]. If high-density high-stress actuators were available for a display, a low-pass filter would then be necessary to prevent skin damage when touching sharp objects. Thus, the best teletaction system feels like touching the real world through an elastic layer or glove. The elastic layer also acts as antialiasing filter. A 3:2 thickness ratio of anti-aliasing layer to sensor and

display resolution reduces the energy of the sampling effects to undetectable levels [258].

There has been a lot of research on this subject. Eltaib and Hewit [259] give an overview of the technology before the year 2000. The existing displays were then large, expensive, not user friendly and not sufficiently accurate but that barely changed. Monkman et al. [260] give an overview of technologies, viable for commercialisation in 2003. A more recent overview is given by Benali Khoudja et al. [261] in 2004. Pasquero [52] summarises the state of the art in a table. They conclude the following: electromagnetic actuation is used a lot, but bulky; SMA is also widely used, but has a low bandwidth and poor performance; because of high bandwidth and forces, piezoelectricity is used in most commercial displays; other solutions are rare and mostly not far enough in development. In general mechanical actuation gives fast and stiff responses and has good control characteristics, but is very bulky [26].

This section divides a selection of tactile displays according to their actuator technology. Braille displays and haptic devices are mentioned, and finally McKibben actuators are discussed as a viable candidate to design a tactile display.

5.1 Electromagnetic

Although they are generally cheap and easy to control, electromagnetic actuators don't scale down well. As a result, only a low force can be reached, except with a large, heavy device. This is because

$$F = \frac{AB^2}{2\mu} \quad (11)$$

with F the force, A the surface, B the magnetic induction and μ the permittivity. A large magnetic field is required, which is hard to generate in a small volume [262].

Examples of use are solenoids [263], servomotors [116] and voice coils [264] [265]. Wagner et al. [116] made a cheap, bulky display with RC servomotors and 6×6 pins, 2 mm stroke, 2 mm resolution and 7.5 Hz bandwidth. Drewing et al. [109] also use servomotors for a display with 4 pins which can move laterally in both horizontal directions. The resolution is 3 mm and the maximum lateral movement 2 mm.

More recently, smaller and lightweight, portable displays are developed. Sarakoglou et al. [266] constructed a 4×4 display in which the pins are controlled by nylon wires connected to a separate block with light electric motors and a spring to push them back. The display has a stroke of 2.5 mm, a resolution of 2 mm, a force of 1 N per tactor and a frequency range of 15 Hz. Ottermo et al. [267] use very small motors to drive a screw to move each pin up and down. They built a 4×8 display with a stroke of 3 mm, a force of 1.7 N and a resolution of 2.7 mm. The frequency range is only 2 Hz. Tabli et al. [268] developed a 4×4 vibrotactile array. At the actuation frequency (250 Hz), the amplitude is $200 \mu\text{m}$ and the static force is 1.2 mN. In [269], an electromotor simulates touching objects by tightening a fabric strip against the fingertip.

Because vibration demand a lower force, electromagnetism can be used for a

vibrotactile display. An example of this is VITAL [68]. It has 8×8 elements, is actuated with micro-coils, resolution is 4 mm, force 13 mN, pin deflection $100 \mu\text{m}$ and frequencies up to 800 Hz are possible. It's combined with thermal feedback to make a distinction between different materials like wood or glass. Kontarinis and Howe [99] used a display based on a modified loudspeaker. The vibration is measured with an accelerometer on the inside of the rubber skin of the slave fingertip and transferred to a single vibrating element.

A special case is a two-dimensional tactile slip display designed by Murphy et al. [110] [111]. A ball is positioned under the user's fingertip and is driven in both directions by electric motors with friction wheels. It allows users to use less force in a virtual paper manipulation task in combination with force feedback. Another two-dimensional tactile slip display is described in [270].

5.2 Electrostatic - Electrostrictive

In Electrostatic actuators, Coulomb forces in the electric field E between two charged parallel plates are used. The size of this force F is

$$F = \epsilon_r \epsilon_0 A E^2 = \epsilon_r \epsilon_0 A \frac{U^2}{d^2} \quad (12)$$

with $\epsilon_r \approx 1 - 8$ the relative permittivity or dielectrical constant, $\epsilon_0 = 8.8510^{-12} \text{ C}^2/\text{Nm}^2$ the permittivity of vacuum, A the surface, d the distance between the plates and U the applied voltage [271]. Very high voltages have to be applied and force and displacement remain low [271].

Jungmann and Schlaak [271] conceived an electrostatic display that is low cost, lightweight and flexible. A polymeric elastic dielectric is sandwiched between compliant electrodes and contracts when a voltage is applied. This concept is not yet tested in [271]. A single 100-layer actuator is able to drive the maximum deflection of 0.5 mm at 1200 V [272]. This electro-active polymer (EAP) is electrostrictive. Electrostrictive polymers change shape under the influence of an electric voltage, much like a piezoelectric crystal or an electrostatic actuator, but force and stroke are in between both [273]. There are recently new developments on the field of electro-active polymers. <http://www.artificialmuscle.com/>

A very light tactile display is developed by Koo et al. [274]. It is based on membranes of electroactive polymers that buckle under high voltages. They realised a thin display with 4×5 elements. The taxels have a maximum displacement of 0.9 mm at 3 kV, and a force of 14 mN, while weighing only 2 g.

5.3 Piezoelectric

The piezoelectric effect is the deformation of certain materials under the influence of an electric field E . The displacement Δl is very small, a few μm , but the force is very large. The effect is described by:

$$\frac{\Delta l}{l} = \frac{\sigma}{E_Y} + d_p E \quad (13)$$

With d_p the piezoelectric coefficient, E_Y Young's modulus and σ the mechanical tension [262].

To achieve larger displacements, multi-layer or bimorph actuators are used. A multi-layer actuator consists of about 100 piezo elements on top of each other. The advantages are large forces, fast response and relatively low activation voltage compared to bimorphs. A bimorph consists of two long piezo elements. When a Voltage is applied, one element shrinks and the other grows, resulting in the bending of the bimorph. Displacement is in the order of $10\ \mu\text{m}$, while bimorphs go up to a few $100\ \mu\text{m}$. These bimorphs have a lower response time and force [275].

Some displays use piezoelectric beams [91] [276]. Van Doren et al. designed a one dimensional display with 88 plates $0.38\ \text{mm}$ apart, a frequency range of $0\text{--}1000\ \text{Hz}$ and a peak-to-peak of $11\ \mu\text{m}$. Debus et al. [276] designed a handle with four piezoelectric bimorphs to convey vibration in four directions. The advantages of piezoelectric actuators are a high bandwidth and a high force. On the other hand, the required voltage is high and the stroke is very small. For this last reason, the actuators use a large levering system, bimorphs or vibration.

STReSS (Stimulator for Tactile Receptors by Skin Stretch) [108] is a piezoelectric tactile display developed at McGill university. It uses piezoceramic bimorphs to stretch the skin laterally. The resolution is $1\ \text{mm}$ and the frequency range $700\ \text{Hz}$. The display uses an array of one hundred laterally moving skin contactors designed to create a time-varying programmable strain field at the skin surface. The actuator movement is only 5% or $25\ \mu\text{m}$. These piezoceramic actuators can be operated over a large bandwidth and easy to form in a desired miniature structure. The next generation of this device [277] is more robust, has a modular design, and reaches a deflection of $0.1\ \text{mm}$. The spatial resolution of the new device is $1.2\times 1.8\ \text{mm}$, with 6×10 teeth. The bandwidth is about $250\ \text{Hz}$.

Kyung et al. [85] also use piezoelectric bimorphs, but with a displacement larger than $1\ \text{mm}$ and lower operating input voltage ($60\ \text{V}$). The display has 8 bimorphs with each 6 pins moving together. Each bimorph can exert a force of $1\ \text{N}$, has $2\ \text{mm}$ indentation and a frequency range up to $1\ \text{kHz}$. It combines normal with lateral movement. In [278] they made a 5×6 display with 30 bimorphs with a resolution of $1.8\ \text{mm}$, $0.7\ \text{mm}$ stroke and a frequency response up to $500\ \text{Hz}$. Tests show a performance in recognition of simple geometric shapes between 50% and 95% .

Summers et al [90] built a 10×10 display with $1\ \text{mm}$ resolution using bimorphs. The bandwidth is $20\text{--}400\ \text{Hz}$ with an amplitude of $50\ \mu\text{m}$ at $40\ \text{Hz}$ and $6\ \mu\text{m}$ at $320\ \text{Hz}$. It was designed and used for psychophysical experiments.

Because of the low stroke and high frequency range, piezoelectricity is suited for vibrotactile displays [279]. Schuenemann and Widmann [117] combine piezoelectricity and hydraulics in their display. 4×2 actuators have both lateral and normal movement, with a resolution of $2\text{--}3\ \text{mm}$. Vibration is used to generate sensations like hardness, touch and itch, but very fast adaptation of fingerpad skin to the stimulus is recorded. (not much care has been put in this paper)

Biet et al. [280] describe a display based on Lamb waves generated in a piezoelectric motor. It generates a variable shear force, resulting in a smooth or braking sensation. In lower frequencies roughness can be simulated.

5.4 Shape Memory Alloy (SMA)

Shape memory alloys change shape when heated, because of a phase transition. Their most common shape is a wire, which can contract typically 2% for millions of times, but 4.5% strain is considered safe by some [78]. They are used in a lot of displays [78] [25] [212] [281] [282]. This is because their high power-to-volume, power-to-weight and force-to-weight ratio's, their high intrinsic stiffness and despite their nonlinear behaviour, hysteresis, directional asymmetry and slow response time. This can be overcome by appropriate control schemes. A display by Howe et al. [25] [212] reaches almost 10 Hz, by using a large derivative term in the control and using forced air cooling. It uses SMA wires of 30 mm long pulling at a lever, raising and lowering individual tactors to approximate the desired surface shape on the skin, with a maximum excursion of 3 mm. It has optical emitter-detector position sensors for each element. This display, with 4×6 elements (first 3×3) and a resolution of 2.1 mm was designed and tested for surgical applications. In a test a hard object, 4 mm in diameter, was located beneath 5 mm of foam with an error of less than 3 mm 95% of the time. Without tactile feedback, mean error was 13 mm. In [78], they even reached 40 Hz bandwidth with liquid cooling in a display with 10 pins in a row. 150 Hz can still be felt. For high frequencies, a high phase transition temperature is chosen, because the rate of cooling is linearly related to the temperature difference. They used a proportional controller with constant current feed-forward.

Nakatani et al. [283] built a large 3D form display with Coil-type SMA (C-SMA). It uses a 16×16 array of pin-rods with 30 mm stroke (resolution 0.4 mm) at 5 mm intervals. C-SMA is SMA material, shaped as a coil to create a very large strain, at the expense of force. It can be extended up to twice its original length, while producing a force of 0.4–0.6 N. The C-SMA is fan cooled. This low force (relative to the size of each pin), makes the display malleable. This property is proposed to be useful as a form of 3D CAD, in which modelers can sculpt directly by their own hands. It takes a long time to actuate every pin to present one shape (5–10 s). A faster linear programming method for actuating the pins is proposed.

5.5 Active fluids

Several researchers have tried to make tactile displays with active fluids. Most are electrorheological (ERF) or magnetorheological (MRF) in nature, which means the viscosity of the fluid changes when an electric or a magnetic field is applied. Because it is only a viscosity change, all of these displays are passive. Klein et al. [29] [241] [284] made a system where the downward force of maximum 0.5 N/tactel is resisted by increasing the viscosity of an electrorheological fluid. The use of a return spring is briefly mentioned. The display of Taylor et al. [285] has no moving components and extra accessories. The electrorheological fluid is trapped between a flexible conductive rubber sheet and an 5×5 array of tactels with a resolution of 13 mm. High voltage is required (maximum 10 kV per 20 mA) and fabric is needed between the layers to prevent short circuit and to increase the force output. The fabric also smoothes the signal. ([285] doesn't give a very good or useful impression) They tried a similar configuration with MRFs instead of ERFs [286]. Voyles et al. [216]

have developed an electrorheological sensor and 'inside-out' symmetric display. It suffers from all the disadvantages of MRFs: it's a passive system requiring a high voltage with no possibility to display edges and very rigid surfaces. It's shaped like a thimble around the finger, with the ERF between a hard outer shell and rubber inner shell.

Bicchi et al. [287] use magnetorheological fluids in their display. It has 4×4 elements with 45 mm resolution. The test persons have to insert a gloved hand in a box with fluid. It's a proof of concept but far from any application. A new and improved version of this Haptic Black Box (HBB II) is presented in [288]. It is very big and most of a gloved arm can be inserted.

MRFs and ERFs have a common problem of sedimentation: they degrade over time. Ferrofluids don't have this problem and might be an option for an active display, but have not yet been used. To accomplish the necessary pressure difference of 0.5 N/mm^2 in a ferrofluid, the local difference in magnetic flux density has to be 10 T. This is the case for a fairly strong ferrofluid with a saturation magnetisation of 50 kA/m [289] [290]. It seems unlikely the requirements can be met in this kind of display. MRFs have the same viscoelastic behaviour as biological tissue, ferrofluids not (personal communication with author of [287]). Another configuration is to use electrolysis to increase or decrease the pressure of the resulting hydrogen and oxygen mixture inside a tactile display element [291]. Ionic Conducting Polymer Gel Film (ICPF) actuators pressing against the fingertip are used to present fine texture, such as in cloth [292] [100] [293].

Another possibility is hydraulic actuators with active fluids which push a membrane and are controlled with electric or magnetic fields.

5.6 Pneumatic

Pneumatics have the advantage of a good power density and the possibility to use light and non-metal materials. Pneumatically actuated displays control the flow or pressure of air to drive pins [294] [92] [295] or inflate air chambers [113]. They are suited to combine with kinaesthetic feedback, because they have a very simple structure at the point of contact [49]. On the other hand it has difficult and nonlinear control of either pressure or flow, low power efficiency and large valves [296]. A disadvantage of this mechanical simplicity is that the length and diameter of the tubing clearly affects the time between the initial display of a stimulus and the actual tactile sensation of the user. In some situations this kind of latency may be simply unacceptable [297].

Cohn et al. [294] made a display with 5×5 pneumatically-actuated pins, controlled by pulse-width modulated solenoid valves. Mounting on surgical instruments is difficult due to the large number of valves and tubes connected to its elements. Moy [26] [113] made a compliant tactile display with air chambers which allow ease of construction, low cost, no pin friction, no extraneous information from air leakage, and response linearity. It uses strain matching, has a 5-4-5 configuration with 2 mm resolution and 35–50 Hz bandwidth. However, the pneumatic valves make noise, but in experiments, the skin of the index finger soon gets numb. This is possibly caused by higher frequencies introduced by the opening and closing of the valves (Gudrun De Gersem). The sensitivity can decrease after exposure of the skin to vibrations [81] [82].

A special display is the CASR display developed by Bicchi et al. [44], based on their Contact Area Spread Rate hypothesis. This hypothesis states that stiffness can be simulated by adapting the rate at which the contact area of the display increases, and thus that softness discrimination can be done using the display. Several experiments show that the results are indeed better than with only kinaesthetic feedback.

Makino and Shinoda [298] propose a suction based tactile display for the palm, with 5 mm resolution. The system uses the illusion that the human can not distinguish a compression by a pinlike object from a suction pressure stimulation through a hole. How much suction gives the sensation of a certain pin is not discussed, but the pain level can be reached. They can separately trigger SAI and RAI receptors by adding DC and 40 Hz signals; the deeper receptors are not reached.

Asamura et al. [299] designed a air pressure based display for psychophysical experiments. It has three elements, spaced 2.5 mm, with a small voice coil driven air pressure controller. The bandwidth is 300 Hz and the pressure 2.8 kPa/V. The maximum Voltage mentioned is 6 V.

The display of Caldwell et al. [92] has 4×4 elements, with a resolution of 3.5 mm. Pneumatic muscle actuators supply a shear force element by moving the entire display sideways. The total display weighs only 20 g and has a bandwidth of 11 Hz. A frequency signal of 20 Hz to 300 Hz is superimposed on the pressure signal by a solenoid valve. The stroke of the pins is 5 mm, with a maximum force of 3 N.

Another display makes use of air jets [297] [49]. The finger has to be pressed against tubes with an internal diameter of 1.5 mm, and these tubes are pressurised to produce a tactile sensation. If the skin is not pressed tightly enough, some air will escape, altering the sensation. It is currently unclear what the effect of an air jet is compared to a pin. The display has 5×5 elements with 3.2 mm resolution in one direction, 2.4 mm in the other. It is a binary display and the pressure is 1.034 bar. The used valves are binary with a 20 ms latency and a pressure range up to 8 bar. Three versions of the display were constructed [49]. One with 5×5 taxels with 1.0 and 1.8 mm spacing, one with 5×5 taxels with 2.4 and 3.2 mm spacing and one with 3×3 taxels with 4.5 and 5.3 mm spacing. Psychophysical experiments show that smaller jets result in better spatial performance. In a simple virtual button pressing task, the combination of kinaesthetic and cutaneous cues is better than kinaesthetic cues only. This might be explained by a higher confidence level upon touching the buttons.

5.7 Acoustic

Iwamoto et al. [300] made a tactile display based on acoustic radiation pressure. The tactile sensation is produced with PZT-generated ultrasound through an ultrasound conducting gel. The sound has a frequency of 3 MHz which leads to a wave length of 0.5 mm. A focus of 1 mm is achieved and a scanning frequency of 1 kHz is possible (100 mm², 50 periods of ultrasound at each point). The force is very low, 6.4 mN, and can barely be felt. More recently they reached 20 mN [301]. A prototype in free space resulted in 3 mN force with a focus of 20 mm at 250 mm above the display [302].

5.8 Photostrictive

Hecker et al. [303] suggest photostriction as actuation principle, but have made no efforts in that direction. This is the mechanical expansion of special materials like PLZT when illuminated. With a strain of 0.1% it's probably not very useful.

5.9 Electrocutaneous

Instead of a straightforward display that indents the skin, a tactile sensation can be simulated by passing electric current through the skin [87] [304]. Kajimoto et al. [60] [103] designed an electrocutaneous display. Electrodes with an inner and an outer circle are placed on the skin. Anodic stimulation (current from central to outer electrode) elicit an acute vibratory sensation because it stimulates the vertically oriented nerves: Meissner corpuscles; cathodic stimulation generates a vague pressure sensation because it stimulates the horizontally oriented nerves: Merkel endings [101] [102]. The static resolution of the display is 2–4 mm with discrimination between lines with 0.5 mm difference around 4 mm. The 4×4 electrodes are spaced 2 mm apart. It is not a natural sensation because only part of the mechanoreceptors are triggered: vibration is felt.

Another way to represent a tactile texture sensation is electrostatic tactile stimulation. When the finger touches and scans an insulated metal surface, the metal surface and the layer of conductive substance under the skin form a condenser. By applying cyclic voltage to the metal plate, an electrostatic attraction and, thus, friction force, is generated periodically, inducing a mechanical vibration on the moving finger [305]. Strong and Troxel [306] built a braille display with this method with a resolution of 2.54 mm. The advantage is a simple structure that can be very thin. On the other hand, only texture can be displayed and it only works on dry skin [307]. When the finger is wet, a superficial water layer forms a condenser together with the electrode. In this case, all of the electrostatic force acts on the water layer and not on the finger. Humidity can make the perception unstable [308]. This problem is solved in [305] with a very thin conductive slider. Another problem is that when the taxels are made to small, the electrostatic force is too small to stimulate the finger [305]. A polyimide-on-silicon electrostatic fingertip tactile display creates an electro-static attraction between the skin and electrode surface which presents a 'sticky' or 'buzzing' sensation [105]. A reason not to use electrostatic displays or electrocutaneous stimulation is the chance of electrochemical or thermal burns [26].

5.10 Conjugated polymers

Conjugated polymers consist of electrolyte between conductive polymers [309]. They have a powerful actuator with up to 15% strain and 49 MPa and a stretchable actuator with 34% strain and up to 10 MPa. This might be useful for a tactile display, but not yet tried... The response time is rather slow and the stability is a severe shortcoming. An overview of electroactive polymers can be found in [309] and [310].

5.11 Braille displays

Printed information in Braille is not abundant, so a display to make digital information available for blind people is very useful. Braille displays are related to tactile displays, but generally easier to build. The reason for that is that the requirements are lower: lower force, larger spatial resolution, very low frequency and more available space for less elements. Another important difference is that braille dots only have two states: up or down. The International Building Standard for Braille cells are a dot interval of 2.5 mm, a dot base diameter 1.5–1.6 mm and a dot height of 0.6–0.9 mm. (see http://www.tiresias.org/reports/braille_cell.htm). The most frequently adopted technology for Braille displays are piezoelectric bimorphs. Nobels [262] gives a nice overview of Braille displays, and defines the requirements. The minimal force is 0.1 N and the minimal displacement 0.8 mm.

The binary working allows for less actuators than there are dots. An example of this is developed by NIST [311]. A single actuator on an X–Y table pushes the passive pins up. There are 71×51 elements with 2.54 mm in between. In a Braille mouse [262] four electromagnetic actuators push up the dots to generate 10 characters per second to glide under the finger. A problem is that blind people want to move their hands while reading.

Some of the first displays were Optacon and Optacon II (OPTical-to-TACTile CONversion). It has 144 vibrating pins (6×24 in a concave surface that fits the finger) to represent the intensity pattern as a camera is manually scanned across a printed page [312]. It was produced by Telesensory Corp. in the 1960's and with some practice a reading speed of 10–100 words per minute [313] (from [50]) is possible. Optacon [314] had a matrix of vibrating pins [103]. There is a long learning curve. Some other displays are TVSS (Tactile Vision Substitution System) [315] and Kinotact (Kinesthetic, optical and tactile display) [316]. And more can be found on <http://www.humanware.ca/web/index.html> or <http://www.sighted.com/english/elba2003.html>. Babbage sells Braille cells with sensors to detect finger position and take reading speed into account. They probably work with piezoelectric actuators.

Lee [317] presents a braille display based on paraffine expanding when heated. It has a cyclus time of 50 s, consuming 0.6 W per dot to reach a dot height of 0.6 mm, with a minimum of 0.3 W per dot. Silicon rubber is used to provide flexibility in volume change. Nakashige et al. [318] use low melting point metals. When the metal is melted, pins are pushed up or down with compressed air. It has 10×10 pins with 2 mm resolution. Matysek et al. [262] designed a single sell Braille display using dielectric polymer actuators (electrostatic). The deflection is 0.5 mm and the actuation is active in the off position, when the pin disappears in the hole. The driving voltage is 1000 V. They want to use vibration because they only have one cell and static touch is not very sensitive.

6 Applications

There are two main applications for a tactile feedback system: minimally invasive surgery [259] and robot manipulation [155]. These are both kinds of teleoperation or telepresence systems. A tactile sensor or a tactile display on their own are also applicable in those areas, and in a few others.

6.1 Minimally invasive surgery

Surgery is mentioned as a possible, but difficult, application long before there was actual research in this area [112]. As discussed in the section about minimally invasive surgery, palpation is an important tool for the surgeon to make decisions. The lack of feedback is one of the most important drawbacks of minimally invasive surgery. While De Gerssem [21] already solved the problem of kinaesthetic feedback, tactile feedback is not yet accomplished.

Tactile feedback can be useful for hidden artery localisation beneath opaque tissue [25] or hidden nerves. The pulsatile pressure variation can be detected (Kaniusas et al. [332] present a model to estimate blood pressure from skin deformation). The localisation of lesions [34] and tumours [25] [78] [32], which often appear as hard lumps embedded in soft tissues, such as the lung and the liver. Another area where it can prove its usefulness is breast lump detection [333]. Different temporal states of the same organ can even be compared by saving the tactile data [241]. The sensor can measure the distribution of reactive pressure from palpated tissues in many diseases, like muscular-skeleton disorders, nerve ending disorders, spinal cord injury, arthritis, and skin lesions. When the camera is blocked, the finger can guide the instrument.

To train surgeons the tactile display could be connected with a virtual model of the human body [108] [334] [68]. This way rare tumours can be simulated so young doctors get a chance to experience them [29]. The display on its own can also be used as an elastographic visualisation method for ultrasound or magnetic resonance imaging techniques (MRI). Mechanical properties such as elasticity can't be visualised directly with conventional diagnostic imaging [29]. In other medical applications larger area tactile sensors can be very useful to measure pressure maps of the foot, the back or the buttocks. For the design of prostheses and wheelchairs, it can be utilised for reducing the discomfort and to assist in the patient's movements. For the limb disabled patients, load cells can measure the force changes, assess the functions, and assist in the rehabilitations of the patient's limbs [335].

Laboratory prototypes can be used to study the different tactile parameters (study of psychophysics) of the human sensory system [261] [109] [90]. Test with a larger spatial or temporal resolution will be possible. For functional MRI tests, the tactile display cannot contain metal, like the compliant tactile display Moy [26] developed.

6.2 Robot manipulation

Robots are needed when objects have to be manipulated in hazardous environments, such as space or underwater [26] [241], on the battlefield [15] or the remains of an exploded chemical or nuclear plant. Humans can quickly perceive complex shapes and textures while touching or feeling the surface of an object

with their fingers [85] [47]. If they can do the same during telemanipulation, their actions will be much faster.

Tactile sensors can also give a greater autonomy to robots, e.g. in assembly [112]. A tactile sense can detect contact and the location and extent thereof. The magnitude and distribution of contact forces can be determined [185]. Several possibilities are slip detection (detection of shift in gravity centre, or detecting a high frequency component caused by stick-slip between rubber and object [148]) [234], detection of surface roughness and burs, object localisation, orientation and weight detection, material and object recognition [251] [212] [148] and picking up fragile or compliant objects [119] [120] [238] [160]. This information can be used to predict frictional behaviour and rolling motions [212]. Compared to computer vision, in tactile sensing less data is required, the measurements are direct, location and recognition are combined with a grasping function and the sensors don't have the disadvantages of vision like occlusion or lighting influence. Pressure distribution is important in detecting sliding and curvature. A tactile sensory system makes automatic grasping, edge tracking and rolling manipulation possible [42]. Tactile or force feedback is necessary to prevent a robot from crushing an object or let it slip [47].

Distributed pressure sensors are also applicable in a robotic skin [151] as developed by Someya et al. [177]. If robots have to interact with humans it is important that they can immediately detect contact or collision and respond to it. Tactile sensors can also serve as a sensitive skin for an arm prosthesis [336]. Another application is measuring the ground reaction force on the soles of a walking robot [162].

6.3 Other applications

Other applications use the tactile sensor or the tactile display separately. In most applications however, the requirements aren't as high as for teleoperation. The reason for this is the difference in what kind of information you need. It's a lot easier to display coded information than realistic tactile information. The sensor can be used in all applications where pressure distribution is important, e.g. mouse pads (cfr. Interlink Electronics), ergonomic tests (cfr. Tekscan) in the design of wheelchairs and saddles [47], lip pressure of people with very long faces before plastic surgery [229] ...

The most important application for the tactile display is sensory substitution for blind computer users [337] [50] [261] [68]. These are mainly braille displays to translate written text, such as a braille mouse developed by Nobels [262]. Other systems display an image directly from the screen, or in the case of the Optacon system, from a camera moved with the hand [314]. A display can also be used to convey schematic information such as figures to the blind [318].

Sensory substitutions for the deaf is also possible [50]. This system is based on the cochlea model of speech: positional encoding of frequency information. By vibrating different fingerpads for different frequency ranges, frequency information is conveyed to the deaf.

Next to sensory substitution for the blind and the deaf, a tactile display can also be used for Augmented Reality (AR), or in this case: augmented haptics. According to Kajimoto et al. [103] it is possible to feel more than normal with a sensor and a display connected to the skin. They want to make it possible

to experience colours in the finger by simulating the primary colours with the stimulation of different tactile receptors.

Tactual displays and in particular vibrotactile displays can serve as supplementary displays in wearable computers. Tactual displays are effective in conveying information in an intuitive and attention-grabbing way [50]. Different vibrational signals constituting a haptic language can even replace or enrich spoken or written language, without the need of more visual or auditory information [52] [338]. This can be used in the automotive industry [68] or in the army. Vibrotactile interfaces can be very valuable for communication between soldiers on the battlefield, when gunfire and explosions impair hearing and camouflage and cover prevent visual contact [46], and in general when auditory and visual stimuli are already rich or not desired [276].

Some other applications are Virtual Reality [337] [339] [340], interfaces for an internet shopping mall (remotely touching materials like clothes via the internet [108] [334] [292] [68]), CAD or other tangible spaces [85], haptic feedback to aid design of MEMS [38]. The entertainment industry could implement tactile displays in games [261], e.g. integrated in the amBX technology of Philips, which aims at a multi-sensory experience [341]. For these applications the display can be build in in a computer mouse or steering wheel [108]. Tactile sensors are also used in intelligent robot toys like Pleo of UGOBE, which react to their environment [342].

References

- [1] M.J. Riezenman. Haptics takes hold. *the institute*, 32(1):6, 2008.
- [2] F. Robicsek. Robotic cardiac surgery: time told! *Journal of Thoracic and Cardiovascular Surgery*, 135(2):343–246, 2008.
- [3] Minimally invasive surgery and the challenges in medical training. *GMV News*, (36):4–7, 2007.
- [4] M.H. Shiu. A surgeon’s look at the treatment of cancer. *Annals of The College of Surgeons Hong Kong*, 7:B7–B17, 2003.
- [5] J. Rosen and B. Hannaford. Doc at a distance. *IEEE Spectrum*, 43(10):34–39, 2006.
- [6] Z. Cui, M. Ogawa, S. Kono, K. Matsunaga, and K. Shidoji. Effects of tactile feedback on simulated telesurgery work in network delay environment. In *Proceedings of the Virtual Reality Society of Japan Annual Conference*, volume 9, pages 575–578, 2004.
- [7] P.P. Pott, H.P. Scharf, and M.L.R. Schwarz. Today’s state of the art in surgical robotics. *Computer Aided Surgery*, 10(2):101–132, 2005.
- [8] S. Misra and A.M. Okamura. Environment parameter estimation during bilateral telemanipulation. In *14th Symposium on Haptic Interfaces for Virtual Environments and Teleoperator Systems*, pages 301–307, 2006.
- [9] J. Peirs, J. Clijnen, D. Reynaerts, H. Van Brussel, P. Herijgers, B. Corteville, and S. Boone. A micro optical force sensor for force feedback during minimally invasive robotic surgery. *Sensors and Actuators A*, 115:447–455, 2004.
- [10] G. Tholey, J.P. Desai, and A.E. Castellanos. Force feedback plays a significant role in minimally invasive surgery. *Annals of Surgery*, 241(1):102–109, 2005.
- [11] C.R. Wagner, N. Stylopoulos, P.G. Jackson, and R.D. Howe. The benefit of force feedback in surgery: examination of blunt dissection. *Presence-Teleoperators and Virtual Environments*, 16(3):252–262, 2007.
- [12] A.M. Okamura. Methods for haptic feedback in teleoperated robot-assisted surgery. *Industrial Robot*, 31(6):499–508, 2004.
- [13] A.P. Miller, W.J. Peine, J.S. Son, and Z.T. Hammoud. Tactile imaging system for localizing lung nodules during video assisted thoracoscopic surgery. In *IEEE International Conference on Robotics and Automation*, pages 2996–3001, 2007.
- [14] M. MacFarlane, J. Rosen, B. Hannaford, C. Pellegrini, and M. Sinanan. Force-feedback grasper helps restore sense of touch in minimally invasive surgery. *Journal of Gastrointestinal Surgery*, 3(3):278–285, 1999.

- [15] S.S. Sastry, M.B. Cohn, and F. Tendick. Milli-robotics for remote, minimally invasive surgery. *Robotic and Autonomous Systems*, 21:305–316, 1997.
- [16] D.M. Ota. Laparoscopic colectomy for cancer: a favorable opinion. *Annals of Surgical Oncology*, 2(1):3–5, 1995.
- [17] J.P. Ruurda and I.A.M.J. Broeders. Feasibility of robot assisted laparoscopic cholecystectomy. In *CARS*, pages 159–164, 2001.
- [18] J. Rassweiler, J. Binder, and T. Frede. Robotic and telesurgery: will they change our future? *Current Opinion in Urology*, 11:309–320, 2001.
- [19] D.H. Boehm, M.B. Arnold, C. Detter, and H. Reichenspurner. Incorporating robotics into an open-heart program. *Surgical Clinics of North America*, 83(6):1369–1380, 2003.
- [20] H.W. Tang, H. Van Brussel, J. Vander Sloten, D. Reynaerts, and P.R. Koninckx. Implementation of an intuitive writing interface and a laparoscopic robot for gynaecological laser assisted surgery. *Proceedings of the I MECH E Part H Journal of Engineering in Medicine*, 219(4):293–302, 2005.
- [21] G. De Gerssem. *Kinaesthetic feedback and enhanced sensitivity in robotic endoscopic telesurgery*. PhD thesis, 2005.
- [22] F. Farhat, F. Depuydt, F. Van Praet, J. Coddens, and H. Vanermen. Hybrid cardiac revascularization using a totally closed-chest robotic technology and a percutaneous transluminal coronary dilatation. *The Heart Surgery Forum*, 3(2):119–122, 2000.
- [23] H. Reichenspurner, R.J. Damiano, M. Mack, D.H. Boehm, H. Gulbins, C. Detter, B. Meiser, R. Ellgass, and B. Reichart. Use of the voice-controlled and computer-assisted surgical system zeus for endoscopic coronary artery bypass grafting. *Journal of Thoracic and Cardiovascular Surgery*, 118(1):11–16, 1999.
- [24] W.R. Chitwood. Endoscopic robotic coronary surgery - is this reality or fantasy. *Journal of Thoracic and Cardiovascular Surgery*, 118(1):1–3, 1999.
- [25] R.D. Howe, W.J. Peine, D.A. Kontarinis, and J.S. Son. Remote palpation technology for surgical applications. *IEEE Engineering in Medicine and Biology Magazine*, 14(3):318–323, 1995.
- [26] G. Moy. *Bidigital teletaction system design and performance*. PhD thesis, 2002.
- [27] G. De Gerssem, H. Van Brussel, and F. Tendick. Reliable and enhanced stiffness perception in soft-tissue telemanipulation. *The International Journal of Robotics Research*, 24(10):805–822, 2005.

- [28] W.A. Bemelman, J. Ringers, D.W. Meijer, C.W.M. de Wit, and J.J.G. Bannenberg. Laparoscopic-assisted colectomy with the dexterity pneumo sleeve. *Diseases of the Colon and Rectum*, 39(10):S59–S61, 1996.
- [29] D. Klein, H. Freimuth, G.J. Monkman, S. Egersdörfer, A. Meier, and H. Böse. Electrorheological tactel elements. *Mechatronics*, 15:883–897, 2005.
- [30] O.S. Bholat, R.S. Haluck, W.B. Murray, P.J. Gorman, and T.M. Krummel. Tactile feedback is present during minimally invasive surgery. *Journal of the American College of Surgeons*, 189(4):349–355, 1999.
- [31] J.A. Norton, T.H. Shawker, J.L. Doppman, D.L. Miller, D.L. Fraker, D.T. Cromack, P. Gorden, and R.T. Jensen. Localization and surgical treatment of occult insulinomas. *Annals of Surgery*, 212(5):615–620, 1990.
- [32] T.S. Ravikumar, S. Buenaventura, R.R. Salem, and B. D’Andrea. Intra-operative ultrasonography of liver: detection of occult liver tumors and treatment by cryosurgery. *Cancer Detection and Prevention*, 18(2):131–138, 1994.
- [33] C. Nies, R. Leppek, H. Sitter, H.J. Klotter, J. Riera, K.J. Klose, W.B. Schwerk, and M. Rothmund. Prospective evaluation of different diagnostic techniques for the detection of liver metastases at the time of primary resection of colorectal carcinoma. *European Journal of Surgery*, 162:811–816, 1996.
- [34] R. Carter, F.W. Poon, D. Hemingway, J.A. McKillop, T.G. Cooke, C.S. McArdle, and R. Pickard. A prospective study of six methods for detection of hepatic colorectal metastases. *Annals of the Royal College of Surgeons of England*, 78:27–30, 1996.
- [35] R.D. Howe and D.A. Kontarinis. Task performance with a dextrous teleoperated hand system. In *Proc. Telemanipulator Technology*, volume 1833, pages 199–207, 1992.
- [36] R.D. Howe and D.A. Kontarinis. High-frequency force information in teleoperated manipulation. In *Proc. Experimental Robotics III: The Third International Symposium*, 1993.
- [37] S.J. Lederman and R.A. Browse. The physiology and psychophysics of touch. In *NATO ASI series Sensors and Sensory Systems for Advanced Robots*, volume F43, pages 71–91, 1988.
- [38] M. Calis and M.P.Y. Desmulliez. Haptic sensing technologies for a novel design methodology in micro/nanotechnology. *Nanotechnology Perceptions*, 1:89–97, 2005.
- [39] L. Demonie and R. Verbrugghe. Ontwikkeling van een tactiel krachtplatform ter identificatie van onderdelen. Master’s thesis, 1987.
- [40] J.M. Loomis and S.J. Lederman. *Handbook of human perception and performance*, chapter Tactual perception. 1986.

- [41] S. Lee. Proprioception: how and why? <http://serendip.brynmawr.edu/bb/neuro/neuro02/web2/slee.html>, 2002.
- [42] R.D. Howe. Tactile sensing and control of robotic manipulation. *Advanced Robotics*, 8(3):245–261, 1994.
- [43] M.A. Srinivasan and R.H. LaMotte. Tactual discrimination of softness. *Journal of Neurophysiology*, 73(1):88–101, 1995.
- [44] A. Bicchi, E.P. Scilingo, and D. De Rossi. Haptic discrimination of softness in teleoperation: the role of the contact area spread rate. *IEEE Transactions on Robotics and Automation*, 16(5):496–504, 2000.
- [45] F.W. Mott and C.S. Sherrington. Experiments upon the influence of sensory nerves upon movement and nutrition of the limbs. preliminary communication. *Proceedings of the Royal Society of London*, 57:481–488, 1895.
- [46] J. Andersson and A. Lundberg. Multimodal machines makes military move - a visiotactile artefact for augmented soldier communication. Technical Report 2004:42, IT University of Göteborg, 2004.
- [47] M.R. Wolffenbuttel. *Surface micromachined capacitive tactile image sensor*. PhD thesis, 1994.
- [48] P. Kammermeier, M. Buss, and G. Schmidt. A systems theoretical model for human perception in multimodal presence systems. *IEEE/ASME Transactions on Mechatronics*, 6(3):234–243, 2001.
- [49] Y. Kim, I. Oakley, and J. Ryu. Human perception of pneumatic tactile cues. *Advanced Robotics*, 22:807–828, 2008.
- [50] H.Z. Tan and A. Pentland. Tactual displays for wearable computing. *Personal Technologies*, 1:225–230, 1997.
- [51] C.M. Reed. The implications of the tadoma method of speechreading for spoken language processing. In *Fourth International Conference on Spoken Language Processing*, volume 3, pages 1489–1492, 1996.
- [52] J. Pasquero. Survey on communication through touch. Technical Report TR-CIM 06.04, Center for Intelligent Machines, McGill University, 2006.
- [53] R.S. Johansson and Å.B. Vallbo. Tactile sensory coding in the glabrous skin of the human hand. *Trends in Neurosciences*, 6(1):27–32, 1983.
- [54] I. Birznieks, P. Jenmalm, R.S. Johansson, and A.W. Goodwin. Encoding of direction of fingertip forces by human tactile afferents. *Journal of Neuroscience*, 21:8222–8237, 2001.
- [55] I. Birznieks, P. Jenmalm, R.S. Johansson, and A.W. Goodwin. Responses in humans tactile afferents to fingertip forces with tangential force components in distal and proximal directions. *Acta Universitatis Latviensis*, 631:7–23, 2001.

- [56] Å.B. Vallbo and R.S. Johansson. Properties of cutaneous mechanoreceptors in the human hand related to touch sensation. *Human Neurobiology*, 3:3–14, 1984.
- [57] P.A. Schmidt, E. Maël, and R.P. Würtz. A sensor for dynamic tactile information with applications in human-robot interaction and object exploration. *Robotics and Autonomous Systems*, 54:1005–1014, 2006.
- [58] R.H. LaMotte and M.A. Srinivasan. Tactile discrimination of shape: responses of slowly adapting mechanoreceptive afferents to a step stroked across the monkey fingerpad. *Journal of Neuroscience*, 7(6):1655–1697, 1987.
- [59] R.S. Johansson. Tactile sensibility in the human hand: receptive field characteristics of mechanoreceptive units in the glabrous skin area. *Journal of Physiology*, 281:101–123, 1978.
- [60] H. Kajimoto, M. Inami, N. Kawakami, and S. Tachi. Smarttouch: electric skin to touch the untouchable. *IEEE Transactions on Computer Graphics and Applications*, Jan-Feb:36–43, 2004.
- [61] J.R. Phillips and K.O. Johnson. Tactile spatial resolution iii: a continuum mechanics model of skin predicting mechanoreceptor responses to bars, edges and gratings. *Journal of Neurophysiology*, 46(6):1204–1225, 1981.
- [62] R.S. Johansson, U. Landström, and R. Lundström. Responses of mechanoreceptive afferent units in the glabrous skin of the human hand to sinusoidal skin displacements. *Brain Research*, 244:17–25, 1982.
- [63] K.B. Shimoga. Finger force and touch feedback issues in dextrous telemanipulation. In *NASA-CIRSSE Int. Conf. on Intelligent Robotic Systems for Space Exploration*, 1992.
- [64] T. Maeno, K. Kobayashi, and N. Yamazaki. Relationship between the structure of human finger tissue and the location of tactile receptors. *JSME International Journal, Series C*, 41(1):94–100, 1998.
- [65] J.R. Phillips and K.O. Johnson. Tactile spatial resolution ii: neural representation of bars, edges and gratings in monkey primary afferents. *Journal of Neurophysiology*, 46(6):1192–1203, 1981.
- [66] Å.B. Vallbo and R.S. Johansson. Detection of tactile stimuli. thresholds of afferent units related to psychophysical thresholds in the human hand. *J.Physiology*, 297:405–422, 1979.
- [67] D.G. Caldwell and C. Gosney. Multi-modal tactile sensing and feedback (tele-taction) for enhanced tele-manipulator control. In *Proceedings of the IEEE/RSJ*, pages 955–960, 1993.
- [68] M. Benali Khoudja and M. Hafez. Vital: a vibrotactile interface with thermal feedback. In *Journée Scientifique Internationale IRCICA*, 2004.
- [69] M. Hollins, S.J. Bensmaïa, and E.A. Roy. Vibrotaction and texture perception. *Behavioural Brain Research*, 135:51–56, 2002.

- [70] D.T.V. Pawluk and R.D. Howe. Dynamic contact of the human fingerpad against a flat surface. *Journal of Biomechanical Engineering-Transactions of the Asme*, 121(6):605–611, 1999.
- [71] J. Engel, J. Chen, Z. Fan, and C. Liu. Polymer micromachined multimodal tactile sensors. *Sensors and Actuators A*, 117:50–61, 2005.
- [72] M. Paré, C. Behets, and O. Cornu. Paucity of presumptive ruffini corpuscles in the index finger pad of humans. *The Journal of Comparative Neurology*, 456(3):260–266, 2003.
- [73] H.R. Schiffman. *Sensation and Perception*, chapter The skin, body and chemical senses. 1995.
- [74] C.E. Sherrick and J.C. Craig. *Tactual Perception: A Sourcebook*, chapter The Psychophysics of Touch, pages 55–81. 1982.
- [75] R.S. Johansson and R.H. LaMotte. Tactile detection thresholds for a single asperity on an otherwise smooth surface. *Somatosensory Research*, 1(1):21–31, 1983.
- [76] K.O. Johnson and J.R. Phillips. Tactile and spatial resolution i: two point discrimination, gap detection, grating resolution, and letter recognition. *Journal of Neurophysiology*, 46(6):1177–1191, 1981.
- [77] R.B. Van Boven and K.O. Johnson. The limit of tactile spatial resolution in humans: grating orientation discrimination at the lip, tongue and finger. *Neurology*, 44:2361–2366, 1994.
- [78] P.S. Wellman, W.J. Peine, G. Favalora, and R.D. Howe. Mechanical design and control of a high-bandwidth shape memory alloy tactile display. *Experimental Robotics V*, 232:56–66, 1998.
- [79] J.M. Loomis. An investigation of tactile hyperacuity. *Sensory Processes*, 3(289):302, 1979.
- [80] K.U. Kyung, M. Ahn, D.S. Kwon, and M.A. Srinivasan. Perceptual and biomechanical frequency response of human skin: implication for design of tactile displays. In *World Haptics*, pages 96–101, 2005.
- [81] R. Lundström and R.S. Johansson. Acute impairment of the sensitivity of skin mechanoreceptive units caused by vibration exposure of the hand. *Ergonomics*, 29:687–698, 1986.
- [82] S.J. Bensmaïa, Y.Y. Leung, S.S. Hsiao, and K.O. Johnson. Vibratory adaptation of cutaneous mechanoreceptive afferents. *Journal of Neurophysiology*, 94:3023–3036, 2005.
- [83] S.J. Lederman. *Encyclopedia of human biology*, chapter Skin and touch, pages 51–63. 1991.
- [84] R.S. Johansson and G. Westling. Roles of glabrous skin receptors and sensorimotor memory in automatic control of precision grip when lifting rougher or more slippery objects. *Experimental Brain Research*, 56:550–564, 1984.

- [85] K.U. Kyung, S.W. Son, D.S. Kwon, and M.S. Kim. Design of an integrated tactile display system. In *Proceedings of the 2004 IEEE International Conference on Robotics and Automation*, pages 776–781, 2004.
- [86] H.Z. Tan, M.A. Srinivasan, B. Ebermann, and B. Cheng. Human factors for the design of force-reflecting haptic interfaces. *Dynamic Systems and Control*, 55(1):353–359, 1994.
- [87] K.A. Kaczmarek, J.G. Webster, P. Bach-y Rita, and W.J. Tompkins. Electrotactile and vibrotactile displays for sensory substitution systems. *IEEE Transactions on Biomedical Engineering*, 38(1):1–16, 1991.
- [88] S. Bolanowski, G. Gescheider, R. Verrillo, and C. Checkosky. Four channels mediate the mechanical aspects of touch. *The Journal of the Acoustical Society of America*, 84(4):1680–1694, 1988.
- [89] C.E. Sherrick and R. Cholewiak. *Handbook of Perception an Human Performance - Sensory Processes and Perception*, chapter Cutaneous sensitivity, pages 12–30. 1986.
- [90] I.R. Summers and C.M. Chanter. A broadband tactile array on the fingertip. *Journal of the Acoustical Society of America*, 112(5):2118–2126, 2002.
- [91] C.L. Van Doren, D.G. Pelli, and R.T. Verrilo. A device for measuring tactile spatiotemporal sensitivity. *Journal of the Acoustical Society of America*, 81(6):1906–1916, 1987.
- [92] D.G. Caldwell, N. Tsagarakis, and C. Giesler. An integrated tactile/shear feedback array for stimulation of finger mechanoreceptor. In *Proceedings IEEE International Conference on Robotics and Automation*, volume 1, pages 287–292, 1999.
- [93] H.Y. Han and S. Kawamura. Analysis of stiffness of human fingertip and comparison with artificial fingers. In *Proc. IEEE Int. Conf. on Systems, Man, and Cybernetics*, pages 800–805, 1999.
- [94] W.R. Provancher. *On tactile sensing and display*. PhD thesis, 2003.
- [95] A. Gallace, H.Z. Tan, and C. Spence. Tactile change detection. In *World Haptics*, pages 12–16, 2005.
- [96] L.M. Brown, S.A. Brewster, and H.C. Purchase. A first investigation into the effectiveness of tactons. In *World Haptics*, pages 167–176, 2005.
- [97] S.A. Brewster and A.A. King. The design and evaluation of a vibrotactile progress bar. In *World Haptics*, pages 499–500, 2005.
- [98] T. Homma, S. Ino, H. Kuroki, T. Izumi, T. Tanabe, and T. Ifukube. Transmitted information using a fingerpad-sized tactile display. In *Proceedings of the Virtual Reality Society of Japan Annual Conference*, volume 8, pages 229–232, 2003.

- [99] D.A. Kontarinis and R.D. Howe. Tactile display of vibratory information in teleoperation and virtual environments. *Presence -Teleoperators and Virtual Environments*, 4(4):387–402, 1995.
- [100] M. Konyo, T. Maeno, A. Yoshida, and S. Tadokoro. Roughness sense display representing temporal frequency changes of tactile information in response to hand movements. In *World Haptics*, pages 609–610, 2005.
- [101] F. Rattay. *Electrical nerve stimulation*. Springer-Verlag, 1990.
- [102] K.A. Kaczmarek, M.E. Tyler, and P.B. y Rita. Electrotactile haptic display on the fingertips: preliminary results. In *Proc. 16th Int. Conf. IEEE Eng. Med. Biol. Soc.*, pages 940–941, 1994.
- [103] H. Kajimoto, N. Kawakami, T. Maeda, and S. Tachi. Electro-tactile display with force feedback. In *Proc. World Multiconference on Systemics, Cybernetics and Informatics*, pages 95–99, 2001.
- [104] Å.B. Vallbo. Sensations evoked from the glabrous skin of the human hand by electrical stimulation of unitary mechanosensitive afferents. *Brain Research*, 215:359–363, 1981.
- [105] D.J. Beebe, C.M. Hymel, K.A. Kaczmarek, and M.E. Tyler. A polyimide-on-silicon electrostatic fingertip tactile display. In *1995 IEEE Engineering in Medicine and Biology*, volume 2, pages 1545–1546, 1995.
- [106] V. Levesque and V. Hayward. Experimental evidence of lateral skin strain during tactile exploration. In *Proceedings of Eurohaptics*, pages 261–275, 2003.
- [107] H. Park and J. Lee. Adaptive impedance control of a haptic interface. *Mechatronics*, 14:237–253, 2004.
- [108] J. Pasquero and V. Hayward. Stress: a practical tactile display system with one millimeter spatial resolution and 700 hz refresh rate. In *Proceedings of Eurohaptics*, pages 94–110, 2003.
- [109] K. Drewing, M. Fritschi, R. Zopf, M.O. Ernst, and M. Buss. First evaluation of a novel tactile display exerting shear force via lateral displacement. *ACM Transactions on Applied Perception*, 2(2):118–131, 2005.
- [110] T.E. Murphy, R.J. Webster, and A.M. Okamura. Design and performance of a two-dimensional tactile slip display. In *Proceedings of EuroHaptics*, pages 130–137, 2004.
- [111] R.J. Webster, T.E. Murphy, L.N. Verner, and A.M. Okamura. A novel two-dimensional tactile slip display: design, kinematics and perceptual experiment. *ACM Transactions on Applied Perception*, 2(2):150–165, 2005.
- [112] L.D. Harmon. Automated tactile sensing. *International Journal of Robotics Research*, 2(1):3–32, 1982.

- [113] G. Moy, P.S. Wellman, and R.S. Fearing. A compliant tactile display for teletaction. In *Proc.ICRA*, volume 4, pages 3409–3415, 2000.
- [114] G. Moy, U. Singh, E. Tan, and R.S. Fearing. Human psychophysics for teletaction system design. *Haptics-e*, 1(3), 2000.
- [115] N. Asamura, T. Shinohara, Y. Toyo, N. Koshida, and H. Shinoda. Necessary spatial resolution for realistic tactile feeling display. In *Proceedings of IEEE International Conference on Robotics and Automation*, volume 2, pages 1851–1856, 2001.
- [116] C.R. Wagner, S.J. Lederman, and R.D. Howe. Design and performance of a tactile display using rc servomotors. *Haptics-e*, 3(4), 2004.
- [117] M. Schuenemann and H. Widmann. Tactile actuators for tactile feedback systems. In *Proceedings of the 6th International Conference on New Actuators*, pages 333–336, 1998.
- [118] D.T.V. Pawluk, J.S. Son, P.S. Wellman, W.J. Peine, and R.D. Howe. A distributed pressure sensor for biomechanical measurements. *ASME Journal of Biomechanical Engineering*, 102(2):302–305, 1998.
- [119] C. Bao and H. Van Brussel. A sensory controlled gripper system. *Robotics and Autonomous Systems*, 6(3):283–295, 1990.
- [120] H. Van Brussel and H. Belien. A high resolution tactile sensor for part recognition. In *Proc. RoViSeC6*, pages 49–60, 1986.
- [121] W.J. Peine, P.S. Wellman, and R.D. Howe. Temporal bandwidth requirements for tactile shape displays. In *Sixth Annual Symposium on Haptic Interfaces for Virtual Environment and Teleoperator Systems, ASME International Mechanical Engineering Congress and Exposition*, pages 107–113, 1997.
- [122] M.A. Srinivasan. Surface deflection of primate fingertip under line load. *Journal of Biomechanics*, 22(4):343–349, 1989.
- [123] V. Maheshwari and R.F. Saraf. High-resolution thin-film device to sense texture by touch. *Science*, 312:1501–1504, 2006.
- [124] S.A. Mascaro and H.H. Asada. Photoplethysmograph fingernail sensors for measuring finger forces without haptic obstruction. *IEEE Transactions on Robotics and Automation*, 17(5):698–708, 2001.
- [125] W.J. Peine and R.D. Howe. Do humans sense finger deformation or distributed pressure to detect lumps in soft tissue. In *Proceedings of the ASME Dynamic Systems and Control Division*, volume 64, pages 273–278, 1998.
- [126] K.B. Lim and Y.S. Chong. Low cost tactile gripper using silicone rubber sensor array. *Robotica*, 6:23–30, 1988.
- [127] K. Weiß and H. Wörn. The working principle of resistive tactile sensor cells. In *Proceedings of the IEEE International Conference on Mechatronics & Automation*, pages 471–476, 2005.

- [128] T. du Moncel. *Le téléphone, le microphone et le phonographe*. Hachette, 1878.
- [129] J.A. Greenwood and J.B.P. Williamson. Contact of nominally flat surfaces. *Proceedings of the Royal Society of London, Series A, Mathematical and Physical Sciences*, 295(1442):300–319, 1966.
- [130] D. Göger, K. Wei, C. Burghart, and H. Wörn. Sensitive skin for a humanoid robot. In *Human-Centered Robotic Systems*, 2006.
- [131] J. Rebman and K.A. Morris. A tactile sensor with electrooptical transduction. In *Proceedings of the 3rd International Conference on Robot Vision and Sensory Controls*, pages 210–216, 1983.
- [132] R.D. Howe and M.R. Cutkosky. Dynamic tactile sensing - perception of fine surface-features with stress rate sensing. *IEEE Transactions on Robotics and Automation*, 9(2):140–151, 1993.
- [133] A. Cameron, R. Daniel, and H. Durrant-Whyte. Touch and motion. In *Proceedings of the IEEE International Conference on Robotics and Automation*, volume 2, pages 1062–1067, 1988.
- [134] A.M. Okamura and M.R. Cutkosky. Haptic exploration of fine surface features. In *Proceedings of the 1999 IEEE International Conference on Robotics and Automation*, volume 4, pages 2930–2936, 1999.
- [135] B. Santoso. *Design and control of a multi-fingered robot hand with tactile feedback*. PhD thesis, 1987.
- [136] A. Kis, F. Kovács, and P. Szolgay. Grasp planning based on fingertip contact forces and torques. In *Proceedings of Eurohaptics*, pages 455–458, 2006.
- [137] D. Reynaerts. *Control methods and actuation technology for whole-hand dexterous manipulation*. PhD thesis, 1995.
- [138] M. Shimojo, M. Ishikawa, and K. Kanaya. A flexible high resolution tactile imager with video signal output. In *Proceedings of the IEEE International Conference on Robotics and Automation*, volume 1, pages 384–391, 1991.
- [139] M.R. Cutkosky, J.M. Jourdain, and P.K. Wright. Skin materials for robotic fingers. In *Proceedings of the IEEE International Conference on Robotics and Automation*, volume 4, pages 1649–1654, 1987.
- [140] K.B. Shimoga and A.A. Goldenberg. Soft materials for robotic fingers. In *Proceedings of the IEEE International Conference on Robotics and Automation*, volume 2, pages 1300–1305, 1992.
- [141] M. Shimojo. Spatial filtering characteristic of elastic cover for tactile sensor. In *Proceedings of the IEEE International Conference on Robotics and Automation*, volume 1, pages 287–292, 1994.

- [142] G.M. Krishna and K. Rajanna. Tactile sensor based on piezoelectric resonance. *IEEE Sensors Journal*, 4(5):691–697, 2004.
- [143] J. Engel, J. Chen, and L. Chang. Development of polyimide flexible tactile sensor skin. *Journal of Micromechanics and Microengineering*, 13:359–366, 2003.
- [144] W.J. Peine, J.S. Son, and R.D. Howe. A palpation system for artery localization in laparoscopic surgery. In *Proceedings of the First International Symposium on Medical Robotics and Computer Assisted Surgery*, pages 250–253, 1994.
- [145] G. Vásárhelyi and B. Fodor. Enhancing tactile capabilities with elastic hemispheres. In *Proceedings of Eurohaptics*, pages 491–494, 2006.
- [146] D.S. McLachlan and M.B. Heaney. Complex ac conductivity of a carbon black composite as a function of frequency, composition, and temperature. *Physical Review B*, 60(18):12746–12751, 1999.
- [147] G. Vásárhelyi, M. dam, . Vazsonyi, Z. Vızvary, A. Kis, I. Barsony, and C. Ducso. Characterization of an integrable single-crystalline 3-d tactile sensor. *IEEE Sensors Journal*, 6(4):928–934, 2006.
- [148] E. Holweg. Tactiele sensoren. *Mikroniek*, 37(1):6–14, 1997.
- [149] F. Zee, E.G.M. Holweg, W. Jongkind, and G. Honderd. Shear force measurement using a rubber based tactile matrix sensor. In *ICAR*, pages 733–738, 1997.
- [150] H. Chigusa, Y. Makino, and H. Shinoda. Large area sensor skin based on two-dimensional signal transmission technology. In *World Haptics Conference 2007*, pages 151–156, 2007.
- [151] Y. Ohmura, Y. Kuniyoshi, and A. Nagakubo. Conformable and scalable tactile sensor skin for curved surfaces. In *Proceedings of the 2006 IEEE International Conference on Robotics and Automation*, pages 1348–1353, 2006.
- [152] A.S. Soembagijo. Application of neural networks to derive manipulation force vectors from tactile sensing images. Master’s thesis, 1992.
- [153] S.P. Lacour, C. Tsay, and S. Wagner. An elastically stretchable tft circuit. *IEEE Electron Device Letters*, 25(12):792–794, 2004.
- [154] M.H. Lee and H.R. Nicholls. Tactile sensing for mechatronics - a state of the art survey. *Mechatronics*, 9:1–31, 1999.
- [155] J. Tegin and J. Wikander. Tactile sensing in intelligent robotic manipulation - a review. *Industrial Robot*, 32(1):64–70, 2005.
- [156] D. De Rossi, F. Carpi, and E.P. Scilingo. Polymer based interfaces as bioinspired ’smart skins’. *Advances in Colloid and Interface Science*, 116:165–178, 2005.

- [157] M. Ramezanifard, S. Sokhanvar, J. Dargahi, W.F. Xie, and M. Packirisamy. Graphical reproduction of tactile information of embedded lumps for mis applications. In *Symposium on Haptic Interfaces for Virtual Environments and Teleoperator Systems*, pages 247–252, 2008.
- [158] C.S. Smith. Piezoresistance effect in germanium and silicon. *Physical Review*, 94(1):42–49, 1954.
- [159] E. Verrijssen and E. Taeymans. Kunsthuid voor robotvingers. Master’s thesis, 1984.
- [160] K. Kawahata, M. Yoneda, and I. Igarashi. Tactile image detection using a 1k-element silicon pressure sensor array. *Sensors and Actuators A*, 22:239–248, 1990.
- [161] C. Pramanik and H. Saha. Piezoresistive pressure sensing by porous silicon membrane. *IEEE Sensors Journal*, 6(2):301–308, 2006.
- [162] R.E. Ellis, S.R. Ganeshan, and S.J. Lederman. A tactile sensor based on thin-plate deformation. *Robotica*, 12:343–351, 1994.
- [163] P. Dario and D. De Rossi. Tactile sensors and the gripping challenge. *IEEE Spectrum*, pages 46–52, 1985.
- [164] K.E. Pennywitt. Robotic tactile sensing. *Byte*, pages 177–200, 1986.
- [165] J. Tima. Tactile sensor array signal and data processing. In *Workshop Metrological aspects of the quality assurance*, pages 137–145, 2001.
- [166] J. Mertens and P. Eeckelers. Ontwikkeling van een kunsthuid voor robots. Master’s thesis, 1985.
- [167] B.E. Robertson and A.J. Walkden. Tactile sensor system for robotics. In *Proceedings of the 3rd International Conference on Robot Vision and Sensory Controls*, pages 572–577, 1983.
- [168] M.H. Raibert and J.E. Tanner. Design and implementation of a vlsi tactile sensing computer. *International Journal of Robotics Research*, 1(3):3–17, 1982.
- [169] W.D. Hillis. A high-resolution imaging touch sensor. *The International Journal of Robotics Research*, 1(2):33–44, 1982.
- [170] J.A. Purbrick. A force transducer employing conductive silicone rubber. In *Proceedings of the 1st International Conference on Robot Vision and Sensory Controls*, pages 73–80, 1981.
- [171] J. Mallin. A simple sense of touch for robotic fingers. *Robotics age*, 1983.
- [172] M. Shimojo, A. Namiki, M. Ishikawa, R. Makino, and K. Mabuchi. A tactile sensor sheet using pressure conductive rubber with electrical-wires stitched method. *IEEE Sensors Journal*, 4(5):589–596, 2004.
- [173] D. De Rossi, A. Della Santa, and A. Mazzoldi. Dressware: wearable hardware. *Material Science and Engineering C*, 7:31–35, 1999.

- [174] A. Mazzoldi, D. De Rossi, F. Lorussi, E.P. Scilingo, and R. Paradiso. Smart textiles for wearable motion capture systems. *AUTEX Research Journal*, 2(4):199–203, 2002.
- [175] D. De Rossi, F. Capri, F. Lorussi, A. Mazzoldi, R. Paradiso, E.P. Scilingo, and A. Tognetti. Electroactive fabrics and wearable biomonitring devices. *AUTEX Research Journal*, 3(4):180–185, 2003.
- [176] F. Lorussi, W. Rocchia, E.P. Scilingo, A. Tognetti, and D. De Rossi. Wearable, redundant fabric-based sensor arrays for reconstruction of body segment posture. *IEEE Sensors Journal*, 4(6):807–818, 2004.
- [177] T. Someya, Y. Kato, T. Sekitani, S. Iba, Y. Noguchi, Y. Murase, H. Kawaguchi, and T. Sakurai. Conformable, flexible, large-area networks of pressure and thermal sensors with organic transistor active matrixes. *PNAS*, 102(35):12321–12325, 2005.
- [178] S. Sugiyama, H. Kawaguchi, T. Someya, T. Sekitani, and T. Sakurai. Cut-and-paste customization of organic fet integrated circuit and its application to electronic artificial skin. *IEEE Journal of Solid-State Circuits*, 40(1):177–185, 2005.
- [179] T. Someya, T. Sekitani, S. Iba, Y. Kato, H. Kawaguchi, and T. Sakurai. A large-area, flexible pressure sensor matrix with organic field-effect transistors for artificial skin applications. *PNAS*, 101(27):9966–9970, 2004.
- [180] G. Wierdsma. Krachtsturing van een pneumatische grijper met taktiele sensoren. Master’s thesis, 1986.
- [181] P. Gonçalves. Integratie van taktiele sensoren in een robothand. Master’s thesis, 1994.
- [182] P. Goethals, B. Willaert, M.M. Sette, D. Reynaerts, and H. Van Brussel. Tactile sensing technology for robot assisted minimally invasive surgery. *Journal of Biomechanics*, 40(S2):S647, 2007.
- [183] PCR Technical. How to use analog type pressure-conductive rubber csa. Technical report, 2002.
- [184] H.E. Larcombe. Carbon fiber tactile sensors. In *Proceedings of the 1st International Conference on Robot Vision and Sensory Control*, pages 273–277, 1981.
- [185] T.H. Speeter. Tactile sensing system for robotic manipulation. Technical report, 1988.
- [186] M. Helsel, J.N. Zemel, and V. Dominko. An impedance tomographic tactile sensor. *Sensors and Actuators*, 14(1):93–98, 1988.
- [187] The sensitive side of carbon nanotubes: creating powerful pressure sensors. *Rensselaer Research Review*, (Winter 2007), 2007.

- [188] V.L. Pushparaj, L. Ci, S. Sreekala, A. Kumar, S. Kesapragada, D. Gall, O. Nalamasu, and A.M. Pulickel. Effects of compressive strains on electrical conductivities of a macroscale carbon nanotube block. *Applied Physics Letters*, 91(153116), 2007.
- [189] Y.J. Jung, S. Kar, S. Talapatra, C. Soldano, G. Viswanathan, X. Li, Z. Yao, F.S. Ou, A. Avadhanula, R. Vajtai, S. Curran, O. Nalamasu, and P.M. Ajayan. Aligned carbon nanotube-polymer hybrid architectures for diverse flexible electronic applications. *Nano Letters*, 6(3):413–418, 2006.
- [190] D. Stauffer and A. Aharony. *Introduction to percolation theory*. Taylor and Francis, 1994.
- [191] M. Taya. *Electronic Composites*. Cambridge University Press, 2005.
- [192] J. Wu. Introduction to percolation theory. <http://www.people.fas.harvard.edu/~wu2/paper1/paper1.html>, 1997.
- [193] B.E. Kilbride, J.N. Coleman, J. Fraysse, P. Fournet, M. Cadek, A. Drury, S. Hutzler, S. Roth, and W.J. Blau. Experimental observation of scaling laws for alternating current and direct current conductivity in polymer-carbon nanotube composite thin films. *Journal of Applied Physics*, 92(7):4024–4030, 2002.
- [194] K. Sett and C. Vipulanandan. Modeling and verification of the behavior of piezoresistive material under uniaxial loading. *ASCE Journal of Engineering Mechanics*, In review, 2007.
- [195] L. Lanotte, G. Ausanio, C. Hison, V. Iannotti, C. Luponio, and C.Jr. Luponio. State of the art and development trends of novel nanostructured elastomagnetic composites. *Journal of Optoelectronics and Advanced Materials*, 6(2):523–532, 2004.
- [196] D.T. Beruto, M. Capurro, and G. Marro. Piezoresistance behavior of silicone-graphite composites in the proximity of the electric percolation threshold. *Sensors and Actuators A*, 117:301–308, 2005.
- [197] M. Taya, W.J. Kim, and K. Ono. Piezoresistivity of a short fiber/elastomer matrix composite. *Mechanics of Materials*, 28:53–59, 1998.
- [198] T. Katsuno, X. Chen, S. Yang, and S. Motojima. Observation and analysis of percolation behavior in carbon microcoils/silicone-rubber composite sheets. *Applied Physics Letters*, 88(23):232115–1–232115–3, 2006.
- [199] T. Riccò and A. Pegoretti. Nonlinear dynamic behavior of rubber compounds: construction of dynamic moduli generalized master curves. *Polymer Engineering and Science*, 40(10):2227–2231, 2000.
- [200] J. Bicerano. *Prediction of Polymer Properties*. Marcel Dekker, 2002.

- [201] P. Dario and G. Buttazzo. An anthropomorphic robot finger for investigating artificial tactile perception. *The International Journal of Robotics Research*, 6(3):25–48, 1987.
- [202] J. Severwright. Tactile sensor arrays: the other option. *Sensor Review*, pages 27–29, 1983.
- [203] R. Sedaghati, J. Dargahi, and H. Singh. Design and modeling of an endoscopic piezoelectric tactile sensor. *International Journal of Solids and Structures*, 42:5872–5886, 2005.
- [204] C. Domenici, D. De Rossi, A. Bacci, and S. Bennati. Shear-stress detection in an elastic layer by a piezoelectric polymer tactile sensor. *IEEE Transactions on Electrical Insulation*, 24(6):1077–1081, 1989.
- [205] J. Dargahi, S. Payandeh, and M. Parameswaran. A micromachined piezoelectric teeth-like laparoscopic tactile sensor: theory, fabrication and experiments. In *Proceedings of IEEE International Conference on Robotics and Automation*, volume 1, pages 299–304, 1999.
- [206] D. De Rossi, P. Dario, and C. Domenici. The electret nature of human skin: a model for artificial tactile sensor. *Journal of Biomechanics*, 18(7):549, 1985.
- [207] D. Siegel, S. Drucker, and I. Garabieta. Performance analysis of a tactile sensor. In *Proceedings of the IEEE International Conference on Robotics and Automation*, volume 4, pages 1493–1499, 1987.
- [208] P.D. Dimitropoulos, D.P. Karampatzakis, G.D. Panagopoulos, and G.I. Stamoulis. A low-power/low-noise readout circuit for integrated capacitive sensors. *IEEE Sensors Journal*, 6(3):755–769, 2006.
- [209] B.L. Gray and R.S. Fearing. A surface-micromachined microtactile sensor array. In *Proceedings of IEEE International Conference on Robotics and Automation*, volume 1, pages 1–6, 1996.
- [210] J.N. Palasagaram and R. Ramadoss. Mems-capacitive pressure sensor fabricated using printed-circuit-processing techniques. *IEEE Sensors Journal*, 6(6):1374–1375, 2006.
- [211] R.S. Fearing. Tactile sensing mechanisms. *International Journal of Robotics Research*, 9(3):3–23, 1990.
- [212] D.A. Kontarinis, J.S. Son, W.J. Peine, and R.D. Howe. A tactile shape sensing and display system for teleoperated manipulation. In *Proceedings of IEEE International Conference on Robotics and Automation*, volume 1, pages 641–646, 1995.
- [213] E.J. Nicolson and R.S. Fearing. Sensing capabilities of linear elastic cylindrical fingers. In *IEEE/RSJ Int. Conf. on Intelligent Robots and Systems*, volume 1, pages 178–185, 1993.
- [214] R.B. McIntosh, P.E. Mauger, and S.R. Patterson. Capacitive transducers with curved electrodes. *IEEE Sensors Journal*, 6(1):125–138, 2006.

- [215] X. Chen, S. Yang, M. Hasegawa, K. Kawabe, and S. Motojima. Tactile microsensor elements prepared from arrayed superelastic carbon micro-coils. *Applied Physics Letters*, 87(5):054101/1–054101/3, 2005.
- [216] R.M. Voyles, G. Fedder, and P.K. Khosla. Design of a modular tactile sensor and actuator based on an electrorheological gel. In *Proceedings of the IEEE International Conference on Robotics and Automation*, pages 13–17, 1996.
- [217] A. Bicchi and P. Dario. Intrinsic tactile sensing for artificial hands. In *Proceedings of the International Symposium on Robotics Research*, pages 83–90, 1988.
- [218] R.M. Voyles, J.D. Morrow, and P.K. Khosla. Shape from motion approach to rapid and precise force/torque sensor calibration. In *Proceedings of the ASME Dynamic Systems and Control Division*, pages 67–73, 1995.
- [219] J.L. Schneiter and T.B. Sheridan. An optical tactile sensor for manipulators. *Computer Integrated Manufacturing*, 1(1):65–72, 1984.
- [220] A. Nomura, I. Abiko, I. Shibata, T. Watanabe, and K. Nihei. Two-dimensional tactile sensor using optical method. *IEEE Transactions on Components, Hybrids and Manufacturing Technology*, 8(2):264–268, 1985.
- [221] J.W. Hill and A.J. Sword. Manipulation based on sensor directed control: an integrated end effector and touch sensing system. In *Annual Human Factors Society Convention*, 1973.
- [222] K. Nakamura, S. Toda, and M. Yamanouchi. A two-dimensional optical fibre microphone array with matrix-style data readout. *Measurement Science and Technology*, 12:859–864, 2001.
- [223] R. Allen. Tactile sensor tucks a 256-point array into a robots palm. *Electronic Design*, 33(11):45–46, 1985.
- [224] D.H. Mott. An experimental very-high-resolution tactile sensor array. *Robot Sensors*, 2:179–188, 1986.
- [225] M. Beedie. Tactile sensor hits high-resolution mark of robotic vision systems. *Electronic Design*, 33(3):69–70, 1985.
- [226] S. Begej. Planar and finger-shaped optical tactile sensors for robotic applications. *IEEE Journal of Robotics and Automation*, 4:472–484, 1988.
- [227] H. Maekawa, K. Tanie, K. Komoriya, M. Kaneko, C. Horiguchi, and T. Sugawara. Development of a finger-shaped tactile sensor and its evaluation by active touch. In *Proceedings of the 1992 IEEE International Conference on Robotics and Automation*, pages 1327–1334, 1992.
- [228] A.A. King and R.M. White. Tactile sensing array based on forming and detecting an optical image. *Sensors and Actuators*, 8:49–63, 1985.

- [229] M. Umemori, J. Sugawara, M. Kawauchi, and H. Mitani. A pressure-distribution sensor (pds) for evaluation of lip functions. *American Journal of Orthodontics and Dental Orthopedics*, 109(5):473–480, 1996.
- [230] D.T. Jenstrom and C.L. Chen. A fiber optic microbend tactile sensor array. *Sensors and Actuators*, 20(3):239–248, 1989.
- [231] D.J.F. Toal, C. Flanagan, W.B. Lyons, S. Nolan, and E. Lewis. Proximal object and hazard detection for autonomous underwater vehicle with optical fibre sensors. *Robotics and Autonomous Systems*, 53:214–229, 2005.
- [232] J.S. Heo, J.H. Chung, and J.J. Lee. Tactile sensor arrays using fiber bragg grating sensors. *Sensors and Actuators A*, 126:312–327, 2006.
- [233] J.S. Schoenwald, A.W. Thiele, and D.E. Gjellum. A novel fiber optic tactile array sensor. In *Proceedings of the IEEE International Conference on Robotics and Automation*, pages 1792–1797, 1987.
- [234] F. Eghtedari and C. Morgan. A novel tactile sensor for robot applications. *Robotica*, 7(4):289–295, 1989.
- [235] R.C. Luo, F. Wang, and Y.X. Liu. A piezoelectric film sensor for robotic end-effectors. In *Proceedings of SPIE conference on Intelligent Robots and Computer Vision*, volume 521, pages 264–270, 1984.
- [236] P. Coiffet. *Robot Technology 2: Interaction with the environment*, chapter Interactions involving physical contact between robot and environment: tactile detection, pages 75–89. 1983.
- [237] J.M. Vranish. Magneto-resistive skin for robots. *Robot Sensors*, 2:99–111, 1986.
- [238] P. Adl, Z.A. Memon, D.J. Mapps, and R.T. Rakowski. Serpentine magneto-resistive elements for tactile sensor applications. *IEEE Transactions on Magnetism*, 26(5):2047–2049, 1990.
- [239] T.J. Nelson, R.B. van Dover, S. Jin, S. Hackwood, and G. Beni. Shear-sensitive magneto-resistive robotic tactile sensor. *IEEE Transactions on Magnetism*, 22(5):394–396, 1986.
- [240] A. Grahn and L. Astle. Robotic ultrasonic force sensor array. In *8th Robots Conference Proceedings*, volume 2, pages 21.1–21.18, 1984.
- [241] H. Böse, G.J. Monkman, H. Freimuth, D. Klein, H. Ermert, M. Baumann, S. Egersdörfer, and O.T. Bruhns. Er fluid based haptic system for virtual reality. In *Proceedings of the 8th International Conference on New Actuators*, pages 351–354, 2002.
- [242] R. Souchon, L. Soualmi, M. Bertrand, J.Y. Chapelon, F. Kallel, and J. Ophir. Ultrasonic elastography using sector scan imaging and a radial compression. *Ultrasonics*, 40:867–871, 2002.

- [243] J. Camino, M.M. Sette, and M. Diehl. Young's modulus reconstruction using a constrained gauss-newton method. In *26th Benelux Meeting on Systems and Control*, 2007.
- [244] M.M. Sette, H. Van Brussel, and J. Vander Sloten. *New technology frontiers in minimally invasive therapies*, chapter Estimation of tactile data using an elastography-based approach, pages 80–88. 2006.
- [245] M.M. Sette, J. Camino, J. D'Hooge, H. Van Brussel, and J. Vander Sloten. Comparing optimization algorithms for the young's modulus reconstruction in ultrasound elastography. In *IEEE International Ultrasonics Symposium*, page 445, 2007.
- [246] M.M. Sette, J. D'Hooge, S. Langeland, P. Goethals, H. Van Brussel, and J. Vander Sloten. Tactile feedback in minimally invasive procedures using an elastography-based method. *International Journal of Computer Assisted Radiology and Surgery*, 2(Suppl. 1):S504, 2007.
- [247] M.M. Sette, P. Goethals, J. Vander Sloten, and H. Van Brussel. Tactile sense in minimally invasive surgery. In *Aris*er Summer School: Minimally Invasive Therapies & Novel Embedded Technology Systems*, pages 159–171, 2006.
- [248] M.A. Helvie, P.L. Carson, A. Sarvazyan, N. Thorson, V. Egorov, and M.A. Roubidoux. Mechanical imaging of the breast: a pilot trial. *Ultrasound in Medicine and Biology*, 29(5S):S112, 2003.
- [249] T.J. Kearney, S. Airapetian, and A. Sarvazyan. Tactile breast imaging to increase the sensitivity of breast examination. *Journal of Clinical Oncology*, 22(14S):1037, 2004.
- [250] C.S. Kaufman. Palpation imaging: current status. Technical report, Mecical Tactile inc., 2005.
- [251] J.W. Roach, P.K. Paripati, and M. Wade. Model-based object recognition using a large-field passive tactile sensor. *IEEE Transactions on Systems, Man and Cybernetics*, 19(4):846–853, 1989.
- [252] R. Cork. Xsensor technology: a pressure imaging overview. *Sensor Review*, 27(1):24–28, 2007.
- [253] L. Yobas, M.A. Huff, F.J. Lisy, and D.M. Durand. A novel bulk micro-machined electrostatic microvalve with a curved-compliant structure applicable for a pneumatic tactile display. *Journal of Microelectromechanical Systems*, 10(2):187–196, 2001.
- [254] L. Yobas, D.M. Durand, G.G. Skebe, F.J. Lisy, and M.A. Huff. A novel integrable microvalve for refreshable braille display system. *Journal of Microelectromechanical Systems*, 12(3):252–263, 2003.
- [255] C. Lee, E.H. Yang, S.M. Saeidi, and J.M. Khodadadi. Fabrication, characterization, and computational modeling of a piezoelectrically actuated microvalve for liquid flow control. *Journal of Microelectromechanical Systems*, 15(3):686–696, 2006.

- [256] B. Nouri. *Modelling and control of pneumatic servo positioning systems*. PhD thesis, 2001.
- [257] R.H. LaMotte. Softness discrimination with a tool. *Journal of Neurophysiology*, 83:1777–1786, 2000.
- [258] R.S. Fearing, G. Moy, and E. Tan. Some basic issues in teletaction. In *Proceedings of IEEE International Conference on Robotics and Automation*, volume 4, pages 3093–3099, 1997.
- [259] M.E.H. Eltaib and J.R. Hewit. Tactile sensing technology for minimal access surgery - a review. *Mechatronics*, 13:1163–1177, 2003.
- [260] G.J. Monkman, S. Egersdörfer, A. Meier, H. Böse, M. Baumann, H. Ermert, W. Khaled, and H. Freimuth. Technologies for haptic displays in teleoperation. *Industrial Robot*, 30(6):525–530, 2003.
- [261] M. Benali Khoudja, M. Hafez, J.M. Alexandre, and A. Kheddar. Tactile interfaces: a state-of-the-art survey. In *35th International Symposium on Robotics*, pages 721–726, 2004.
- [262] T. Nobels. *Ontwerp en realisatie van een braillecomputermuis*. PhD thesis, 2005.
- [263] H. Fischer, B. Neisius, and R. Trapp. Tactile feedback for endoscopic surgery. *Interactive Technology and New Paradigm for Healthcare*, pages 114–117, 1995.
- [264] A.M. Murray, R.L. Klatzky, and P.K. Khosla. Enhancing subjective sensitivity to vibrotactile stimuli. In *Proceedings of the ASME Dynamic Systems and Control Division*, pages 157–162, 1998.
- [265] D.T.V. Pawluk, C.P. van Buskirk, J.H. Killebrew, S.S. Hsiao, and K.O. Johnson. Control and pattern specification for a high density tactile array. In *Proceedings of the ASME Dynamic Systems and Control Division*, pages 97–102, 1998.
- [266] I. Sarakoglou, N. Tsagarakis, and D.G. Caldwell. A portable fingertip tactile feedback array - transmission system reliability and modelling. In *World Haptics*, pages 547–548, 2005.
- [267] M.V. Ottermo, Ø. Stavadahl, and R.A. Johansen. Electromechanical design of a miniature tactile shape display for minimally invasive surgery. In *World Haptics*, pages 561–562, 2005.
- [268] A. Talbi, O. Ducloux, N. Tiercelin, Y. Deblock, P. Pernod, and V. Preobrazhensky. Vibrotactile using micromachined electromagnetic actuators array. In *Actuator 2006*, pages 120–123, 2006.
- [269] G. Inaba and K. Fujita. A pseudo-force-feedback device by fingertip tightening for multi-finger object manipulation. In *Proceedings of Eurohaptics*, pages 475–478, 2006.

- [270] N. Tsagarakis, T. Horne, and D.G. Caldwell. Slip aestheasis: a portable 2d slip/skin stretch display for the fingertip. In *World Haptics*, pages 214–219, 2005.
- [271] M. Jungmann and H.F. Schlaak. Miniaturised electrostatic tactile display with high structural compliance. In *Proceedings of Eurohaptics*, pages 12–17, 2002.
- [272] M. Matysek, P. Lotz, and H.F. Schlaak. Braille display with dielectric polymer actuator. In *Actuator 2006*, pages 997–1000, 2006.
- [273] R.E. Pelrine, R. Kornbluh, and J.P. Joseph. Electrostriction of polymer dielectrics with compliant electrodes as a means of actuation. *Sensors and Actuators A*, 64(1):77–85, 1998.
- [274] I.M. Koo, K. Jung, J.C. Koo, J.D. Nam, Y.K. Lee, and H.R. Choi. Development of soft-actuator-based wearable tactile display. *IEEE Transactions on Robotics*, 24(3):549–558, 2008.
- [275] M. Märtens and H. Waller. Vibration control of a mechanical structure with piezoelectric actuators - a comparison of bimorph and stack actuators. In *Actuator 1998*, pages 269–272, 1998.
- [276] T. Debus, T.J. Jang, P. Dupont, and R.D. Howe. Multi-channel vibrotactile display for teleoperated assembly. *International Journal of Control, Automation, and Systems*, 2(3):390–397, 2004.
- [277] Q. Wang and V. Hayward. Compact, portable, modular, high-performance, distributed tactile display device based on lateral skin deformation. In *14th Symposium on Haptic Interfaces For Virtual Environment And Teleoperator Systems IEEE VR 2006*, pages 67–72, 2006.
- [278] K.U. Kyung, M. Ahn, D.S. Kwon, and M.A. Srinivasan. A compact broadband tactile display and its effectiveness in the display of tactile form. In *World Haptics*, pages 600–601, 2005.
- [279] Y. Ikei, M. Yamada, and S. Fukuda. A new design of haptic texture display - texture display2 - and its preliminary evaluation. In *Proc. of IEEE Virtual Reality 2001 Conference*, pages 21–22, 2001.
- [280] M. Biet, F. Giraud, and B. Semail. New tactile devices using piezoelectric actuators. In *Actuator 2006*, pages 989–992, 2006.
- [281] C.J. Hasser and M.W. Daniels. Tactile feedback with adaptive controller for a force-reflecting haptic display. In *15th Southern Biomedical Engineering Conference*, pages 526–533, 1996.
- [282] P.M. Taylor, A. Moser, and A. Creed. A sixty-four element tactile display using shape memory alloy wires. *Displays*, 18(3):163–168, 1998.
- [283] M. Nakatani, H. Kajimoto, K. Vlack, D. Sekiguchi, N. Kawakami, and S. Tachi. Control method for a 3d shape display with coil-type shape memory alloy. In *Proceedings of IEEE ICRA*, pages 1344–1349, 2005.

- [284] W. Khaled, S. Reichling, O.T. Bruhns, H. Böse, M. Baumann, G.J. Monkman, S. Egersdörfer, D. Klein, A. Tunayar, H. Freimuth, A. Lorenz, A. Pessavento, and H. Ermert. Palpation imaging using a haptic system for virtual reality applications in medicine. In *Proceedings of the 12th Annual Medicine Meets Virtual Reality Conference*, pages 147–153, 2004.
- [285] P.M. Taylor, D.M. Pollet, A. Hosseini-Sianaki, and C.J. Varley. Advances in an electrorheological fluid based tactile array. *Displays*, 18(3):135–141, 1998.
- [286] Y. Liu, R.I. Davidson, P.M. Taylor, J.D. Ngu, and J.M.C. Zarraga. Single cell magnetorheological fluid based tactile display. *Displays*, 26:29–35, 2005.
- [287] A. Bicchi, E.P. Scilingo, N. Sgambelluri, and D. De Rossi. Haptic interfaces based on magnetorheological fluids. In *Proceedings of Eurohaptics*, pages 6–11, 2002.
- [288] N. Sgambelluri, E.P. Scilingo, A. Bicchi, R. Rizzo, and M. Raugi. Advanced modelling and preliminary psychophysical experiments for a free-hand haptic device. In *Proceedings of the 2006 IEEE/RSJ International Conference on Intelligent Robots and Systems*, pages 1558–1563, 2006.
- [289] S. Eeckhoudt and P. Goethals. Ontwikkeling van een ferrofluidische afdichting voor een lineaire, hydraulische microactuator. Master’s thesis, 2005.
- [290] M. De Volder, P. Goethals, S. Eeckhoudt, J. Peirs, and D. Reynaerts. A ferrofluid seal technology for hydraulic microactuators. In *Actuator 2006*, pages 693–696, 2006.
- [291] R. Kowalik and I. Postawka. The concept of a full screen tactile display (fstd) driven by electrochemical reactions. In *Proceedings of 4th International Conference, Computers for Handicapped Persons*, pages 455–460, 1994.
- [292] M. Konyo, S. Tadokoro, and T. Takamori. Artificial tactile feel display using soft gel actuators. In *Proceedings of IEEE International Conference of Robotics and Automation*, volume 4, pages 3416–3421, 2000.
- [293] K. Akazawa, M. Konyo, S. Tadokoro, and T. Takamori. Softness display for touch feel using high polymer gel actuators. In *Proceeding of the Virtual Reality Society of Japan Annual Conference*, volume 8, pages 221–224, 2003.
- [294] M.B. Cohn, M. Lam, and R.S. Fearing. Tactile feedback for teleoperation. In *Proc. Telemanipulator Technology*, volume 1833, pages 240–254, 1992.
- [295] J.C. Bliss. A relatively high-resolution reading aid for the blind. *IEEE Transactions on Man-Machine Systems*, 10:1–9, 1969.
- [296] K.H. Chiang. *Limits of microvalve design*. PhD thesis, 2000.

- [297] Y. Kim, I. Oakley, and J. Ryu. Combining point force haptic and pneumatic tactile displays. In *Proceedings of Eurohaptics*, pages 309–316, 2006.
- [298] Y. Makino and H. Shinoda. Selective stimulation to superficial mechanoreceptors by temporal control of suction pressure. In *World Haptics*, pages 229–234, 2005.
- [299] N. Asamura, N. Yokoyama, and H. Shinoda. Selectively stimulating skin receptors for tactile display. *IEEE Computer Graphics and Applications*, 18(6):32–37, 1998.
- [300] T. Iwamoto, D. Akaho, and H. Shinoda. High resolution tactile display using acoustic radiation pressure. In *Proc. SICE*, pages 1239–1244, 2004.
- [301] T. Iwamoto and H. Shinoda. Ultrasound tactile display for stress field reproduction -examination of non-vibratory tactile apparent movement-. In *World Haptics*, pages 220–228, 2005.
- [302] T. Iwamoto, M. Tatzono, and H. Shinoda. Non-contact method for producing tactile sensation using airborne ultrasound. In *EuroHaptics*, pages 504–513, 2008.
- [303] T. Heckner, C. Kessler, S. Egersdörfer, and G.J. Monkman. Computer based platform for tactile actuator analysis. In *Actuator 2006*, pages 993–996, 2006.
- [304] N.P. Ostrom, K.A. Kaczmarek, and D.J. Beebe. A microfabricated electrocutaneous tactile display. In *Proceedings of the First Joint BMES/EMBS Conference*, volume 2, page 838, 1999.
- [305] A. Yamamoto, S. Nagasawa, H. Yamamoto, and T. Higuchi. Electrostatic tactile display with thin film slider and its application to tactile telepresentation systems. *IEEE Transactions on Visualization and Computer Graphics*, 12(2):168–177, 2006.
- [306] R.M. Strong and D.E. Troxel. An electrotactile display. *IEEE Transactions on Man-Machine Systems*, 11(1):72–79, 1970.
- [307] E. Mallinckrodt, A.L. Hughes, and J.W. Sleator. Perception by the skin of electrically induced vibrations. *Science*, 118:277–278, 1953.
- [308] H. Tang and D.J. Beebe. A microfabricated electrostatic haptic display for persons with visual impairments. *IEEE Transactions on Rehabilitation Engineering*, 6(3):241–248, 1998.
- [309] P. Sommer-Larsen and R. Kornbluh. Overview and recent advances in polymer actuators. In *Actuator 2006*, pages 86–96, 2006.
- [310] H. Herr and R. Kornbluh. New horizons for orthototic and prosthetic technology: artificial muscle for ambulation. In *Smart Structures and Materials: Electroactive Polymer Actuators and Devices*, 2004.

- [311] J. Roberts. Nist refreshable tactile graphic display: a new low-cost technology. In *Technology and Persons with Disabilities Conference*, 2004.
- [312] J.C. Bliss, M.H. Catcher, C.H. Rogers, and R.P. Shepard. Optical-to-tactile image conversion for the blind. *IEEE Transactions on Man-Machine Systems*, 11(1):58–65, 1970.
- [313] J.G. Linvill and J.C. Bliss. A direct translation reading aid for the blind. In *Proceedings of the Institute of Electrical and Electronics Engineers*, volume 54, pages 40–51, 1966.
- [314] D.K. Stein. The optacon: past, present and future. <http://www.nfb.org/bm/bm98/bm980506.htm>, 1998.
- [315] P. Bach-y Rita. *Brain Mechanisms in Sensory Substitution*. Academic Press, 1972.
- [316] J.C. Craig. Pictorial and abstract cutaneous displays. *Cutaneous Communication Systems and Devices*, pages 78–83, 1973.
- [317] J.S. Lee and S. Lucyszyn. A micromachined refreshable braille cell. *Journal of Microelectromechanical Systems*, 14(4):673–682, 2005.
- [318] M. Nakashige, K. Hirota, and M. Hirose. High resolution tactile display. In *Proceeding of the Virtual Reality Society of Japan Annual Conference*, volume 8, pages 253–254, 2003.
- [319] B. Unger, R.L. Klatzky, and R. Hollis. Teleoperation mediated through magnetic levitation: recent results. In *IEEE Conference on Mechatronics and Robotics*, pages 1453–1457, 2004.
- [320] B. Unger and R. Hollis. Design and operation of a force-reflecting magnetic levitation coarse-fine teleoperation system. In *Proceedings of the 2004 IEEE International Conference on Robotics and Automation*, pages 4147–4152, 2004.
- [321] H.Y. Yao, V. Hayward, and R.E. Ellis. A tactile enhancement instrument for minimally invasive surgery. *Computer Aided Surgery*, 10(4):233–239, 2005.
- [322] E.L. Faulring, J.E. Colgate, and M.A. Peshkin. The cobotic hand controller: design, control and performance of a novel haptic display. *International Journal of Robotics Research*, 25(11):1099–1119, 2006.
- [323] R. Calbrunn. Design and control of a robotic leg with braided pneumatic actuators. Master’s thesis, 2005.
- [324] R.W. Colbrunn, G.M. Nelson, and R.D. Quinn. Modeling of braided pneumatic actuators for robotic control. In *International Conference on Intelligent Robots and Systems*, volume 4, pages 1964–1970, 2001.

- [325] M.C. Birch, R.D. Quinn, G. Hahm, S.M. Phillips, B.T. Drennan, A. Fife, R.D. Beer, X. Yu, S.L. Garverick, S. Laksanacharoen, A.J. Pollack, and R.E. Ritzmann. A miniature hybrid robot propelled by legs. In *International Conference on Intelligent Robots and Systems*, volume 2, pages 845–851, 2001.
- [326] S. Wakimoto, K. Suzumori, and T. Kanda. Development of intelligent mckibben actuator with built-in soft conductive rubber sensor. In *The 13th International Conference on Solid-State Sensors, Actuators and Microsystems*, pages 745–748, 2005.
- [327] Y.K. Lee and I. Shimoyama. A micro rubber artificial muscle driven by a micro compressor for artificial limbs. In *ACTUATOR 2000, 7th International Conference on New Actuators*, pages 272–275, 2000.
- [328] C.P. Chou and B. Hannaford. Measurement and modeling of mckibben pneumatic artificial muscles. *IEEE Transactions on Robotics and Automation*, 12:90–102, 1996.
- [329] G.K. Klute, J.M. Czerniecki, and B. Hannaford. Mckibben artificial muscles: pneumatic actuators with biomechanical intelligence. In *IEEE/ASME International Conference on Advanced Intelligent Mechatronics*, 1999.
- [330] C. Santulli, S.I. Patel, G. Jeronimidis, F.J. Davis, and G.R. Mitchell. Development of smart variable stiffness actuators using polymer hydrogels. *Smart Materials and Structures*, 14:434–440, 2005.
- [331] G.K. Klute and B. Hannaford. Accounting for elastic energy storage in mckibben artificial muscle actuators. *ASME Journal of Dynamic Systems, Measurement, and Control*, 122(2):386–388, 2000.
- [332] E. Kaniusas, H. Pfützner, L. Mehnen, J. Kosel, J.C. Téllez-Blanco, G. Varoneckas, A. Alonderis, T. Meydan, M. Vázquez, M. Rohn, A.M. Merlo, and B. Marquardt. Method for continuous nondisturbing monitoring of blood pressure by magnetoelastic skin curvature sensor and ecg. *IEEE Sensors Journal*, 6(3):819–828, 2006.
- [333] P.S. Wellman, R.D. Howe, N. Dewagan, M.A. Cundari, E.P. Dalton, and K.A. Kern. Tactile imaging: a method for documenting breast masses. In *Proceedings of the First Joint BMES/EMBS Conference*, page 1131, 1999.
- [334] J. Pasquero. Stress: a tactile display using lateral skin stretch. Master’s thesis, 2003.
- [335] D.J. Beebe, D.D. Denton, R.G. Radwin, and J.G. Webster. A silicon-based tactile sensor for finger-mounted applications. *IEEE Transactions on Biomedical Engineering*, 45(2):151–159, 1998.
- [336] P. Patel-Predd. Sensitive synthetic skin in the works for prosthetic arms. *IEEE Spectrum*, 2008.

- [337] A. Hardwick, S. Furner, and J. Rush. Tactile display of virtual reality from the world wide web - a potential access method for blind people. *Displays*, 18(3):153–161, 1998.
- [338] K. MacLean and M. Enriquez. Perceptual design of haptic icons. In *Proceedings of Eurohaptics*, pages 351–363, 2003.
- [339] T.P. Way and K.E. Barner. Automatic visual to tactile translation - part i: human factors, access methods, and image manipulation. *IEEE Transactions on Rehabilitation Engineering*, 5(1):81–94, 1997.
- [340] T.P. Way and K.E. Barner. Automatic visual to tactile translation - part ii: evaluation of the tactile image creation system. *IEEE Transactions on Rehabilitation Engineering*, 5(1):95–105, 1997.
- [341] A. Woolls-King and S. Keeping. Living the game. *Password - Philips Research technology magazine*, 27:16–1, 2006.
- [342] D. Stern. Revival of an extinct species. *mst news*, (3), 2006.